X-RAY MASS ABSORPTION COEFFICIENTS AND QUANTITATIVE MICROANALYSIS OF METALLURGICAL SYSTEMS, INCLUDING REFRACTORY METAL-INTERSTITIAL COMPOUNDS

Lawrence John Gray
Department of Mining, Metallurgy, and Petroleum Engineering
and
Materials Research Laboratory
University of Illinois, Urbana, Illinois 61801

February 1969

This technical information document is based on a thesis submitted in partial fulfillment of the requirements for the degree of Doctor of Philosophy in Mining, Metallurgy, and Petroleum Engineering in the Graduate College of the University of Illinois, 1969. This research was supported in part by the U. S. Atomic Energy Commission under Contract AT(11-1)-1198.

DISCLAIMER

X-RAY MASS ABSORPTION COEFFICIENTS AND QUANTITATIVE MICROANALYSIS OF METALLURGICAL SYSTEMS, INCLUDING REFRACTORY METAL-INTERSTITIAL COMPOUNDS

Lawrence John Gray, Ph. D.
Department of Mining, Metallurgy and Petroleum Engineering
University of Illinois, 1969

A method, based on consideration of atomic potentials, for the estimation of mass absorption coefficients is described. Mass absorption coefficients for wavelengths up to 80 Å can be estimated. Numerical values are given for several elements, including the refractory metals, for the characteristic emission lines of carbon, nitrogen, and oxygen. The method of calculation permits the estimation, to better than 5% in most cases, of mass absorption coefficients.

A correction procedure for the conversion of microprobe x-ray intensity data to composition is presented. The method, implemented by a described computer program, was tested in the analysis of eight metallurgical systems containing elements from carbon to gold in various combinations. The data reduction computation has been shown to be generally applicable to this variety of elements. The greatest difficulties were encountered in the analysis of carbon containing samples. Consideration of the principles on which the correction relations rest leads to the definition of a set of analytical conditions which minimize the theoretical errors.

ACKNOWLEDGEMENT

The author wishes to express his appreciation to his advisor, Professor C. A. Wert, who suggested the direction of this work and whose influence and encouragement insured its completion. The author's knowledge of many aspects of electron optics was significantly increased by discussion with Mr. F. Luehrs, presently of the Materials Analysis Company, Palo Alto, California. Several areas of electron probe microanalysis were clarified during conversations with Mr. Luehrs and Mr. J. Colby of the Bell Telephone Laboratories, Allentown, Pennsylvania. Mr. Colby generously made available his computational scheme, MAGIC I, prior to publication. The author is further indebted to numerous members of the staff of the Materials Research Laboratory, where this work was carried out, who either assisted in obtaining the necessary equipment or offered suggestions during enlightening discussions.

The author wishes, above all, to thank his wife Marjo for her understanding, patience, and encouragement.

It is a pleasure to acknowledge the support in part of the U. S. Naval Undersea Warfare Center, Pasadena, California, through a Naval Fellowship, and the U. S. Atomic Energy Commission through Contract AT(11-1)1198.

TABLE OF CONTENTS

LIST OF TABLES

LIST OF FIGURES

I. INTRODUCTION

The great advance in the analysis of metallurgical samples occasioned by the development of a practical electron probe x-ray microanalyzer*[1,2] is that elemental characteristic x-ray intensity is used to determine the composition of a very small volume. The uniqueness of this analytical method is easily seen. The volume of material analyzed is of the order of one cubic micrometer (μm^3). The analysis is non-destructive. Quantitative information is generally obtained without resorting to a series of compound "standards" for intensity comparison purposes. Point-to-point analysis yields elemental distributions on a micrometer (μm) scale. All errors of an instrumental nature, but two, have no influence on the data.

Electron probe x-ray microanalysis depends on the excitation of the sample to be analyzed by a small (10^{-8} cm^2) electron beam. X-rays generated in the excited volume are emitted by the sample. The same excitation and detection systems are used for both standards and unknowns. Intensity of the same x-ray line is measured from both standards and unknowns. It must be pointed out, however, that the directness of the method is complicated by other pheonmena which occur when an electron beam is incident on a target. These

*Also called: electron microprobe; electron probe X-ray microanalyzer; microprobe; probe; electron probe; microanalyzer a sonde electronique; Elektronenmikrosonde.

phenomena, some of which must be taken into account in microprobe analysis, are illustrated in Figure 1.

Although, in a very broad sense, there is some similarity between electron probe microanalysis and fluorescent x-ray emission spectrography, it is well to point out some of the significant differences. These are summarized in Table I.

Since the electron microprobe does utilize electron bombardment as the means of excitation of the sample, several methods of analysis, some only qualitative, are possible. These approaches are illustrated in Figure 2.

It becomes clear that characterization of micro-volumes lies well within the realm of microprobe capabilities. Likewise, it is clear that the microprobe will not necessarily yield a highly reliable total composition analysis of a specimen. Rather, variations in composition from one region to another within a specimen are the significant results of electron probe x-ray microanalysis.

Relative variations in composition can be shown rapidly by raw x-ray intensity, backscattered electron intensity or sample current measurements. Figure 3 illustrates the backscattered electron intensity distribution and the elemental characteristic x-ray intensity distributions from the sample shown in the optical photograph. The x-ray intensity distributions also show intensity vs. position traces taken across the middle of the sample. Such qualitative informa-

Figure 1. Interactions of an electron probe with a specimen.

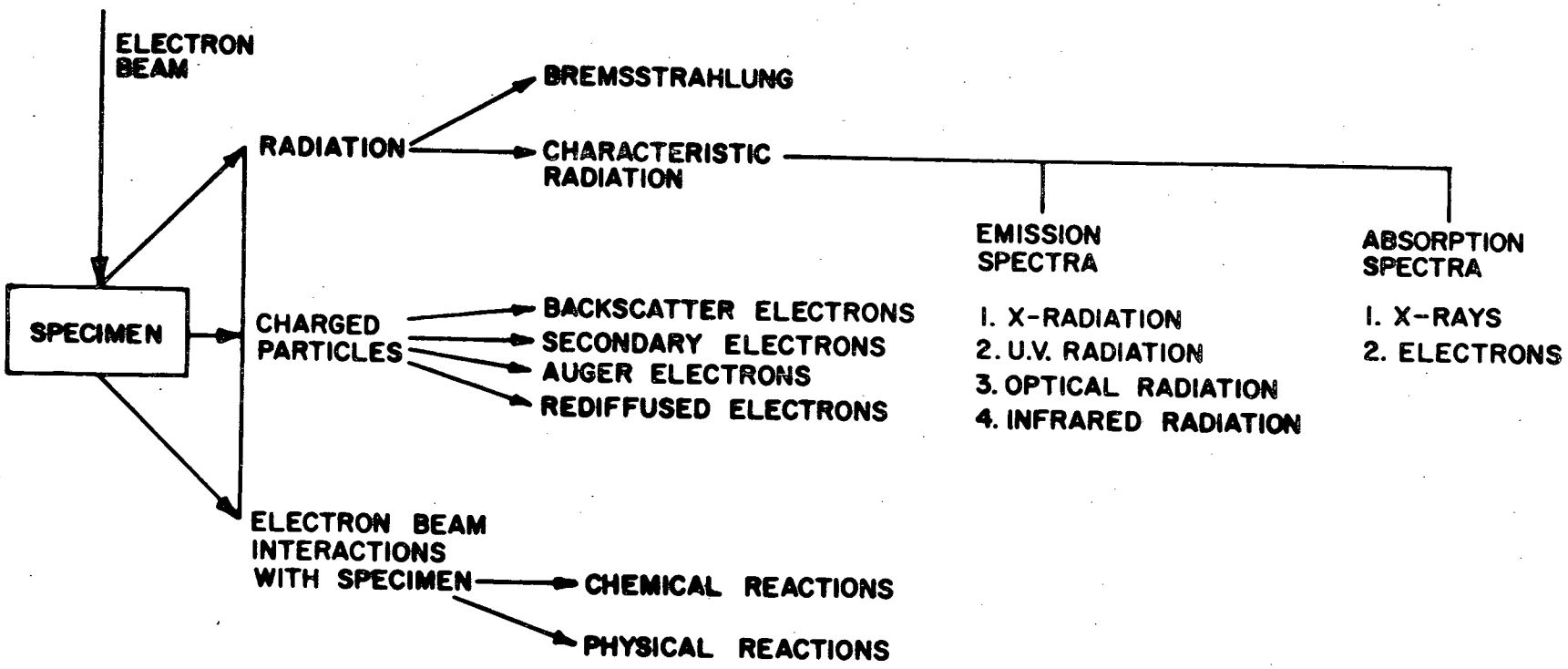
ELECTRON BEAM
SPECIMEN
RADIATION
BREMSSTRAHLUNG
CHARACTERISTIC RADIATION
EMISSION SPECTRA
1. X-RADIATION
2. U.V. RADIATION
3. OPTICAL RADIATION
4. INFRARED RADIATION
ABSORPTION SPECTRA
1. X-RAYS
2. ELECTRONS
CHARGED PARTICLES
BACKSCATTER ELECTRONS
SECONDARY ELECTRONS
AUGER ELECTRONS
REDIFFUSED ELECTRONS
ELECTRON BEAM INTERACTIONS WITH SPECIMEN
CHEMICAL REACTIONS
PHYSICAL REACTIONS

Table I. Characteristics of Electron Probe Microanalyzers and Fluorescent X-ray Emission Spectrography.

	Microprobe	Analytical[3] Spectrograph
Specimen excitation	Electrons	X-rays
Power input, watts	$(5)(10^{-3})$	$(2)(10^{3})$
Specimen area, cm^2	10^{-4} to 10^{-8}	10^{-2} to 1
X-ray intensity per cm^2 from specimen, watts	$(2)(10^{3})$	$(5)(10^{-2})$
X-ray intensity from specimen, watts	$(2)(10^{-5})$	$(5)(10^{-2})$
X-ray intensity to detector, watts	$(5)(10^{-9})$	$(5)(10^{-7})$
Counting rate, cps	$(2)(10^{4})$	$(6)(10^{5})$
Signal peak-to-background ratio	200 to 1 (white radiation)	10,000 to 1 (scattered x-rays)
Detectable mass, grams	10^{-14}	10^{-9}
Minimum detectable concentration, ppm	500	10

Figure 2. Electron microprobe analytical techniques.

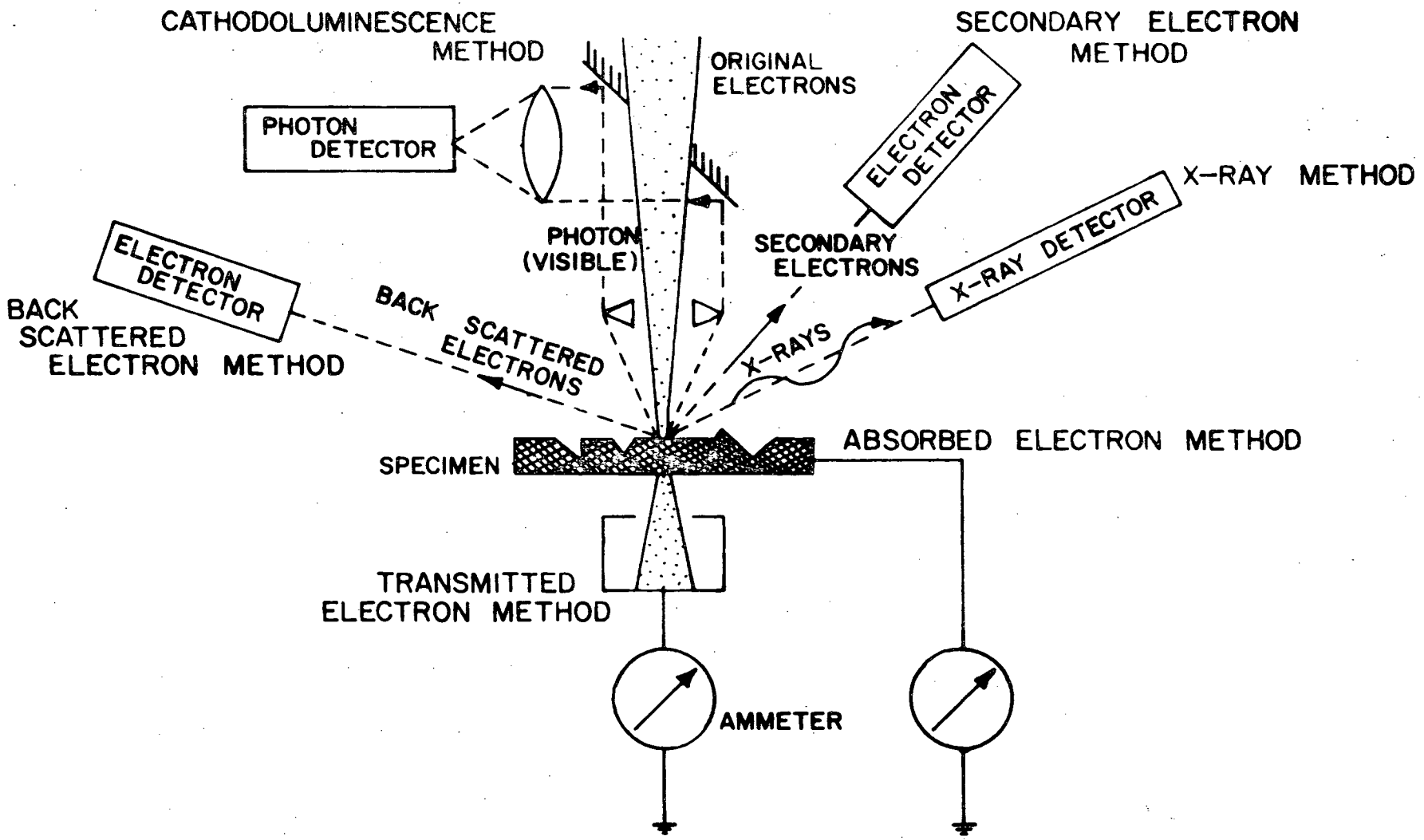
CATHODOLUMINESCENCE METHOD
ORIGINAL ELECTRONS
SECONDARY ELECTRON METHOD
PHOTON DETECTOR
ELECTRON DETECTOR
X-RAY METHOD
PHOTON (VISIBLE)
SECONDARY ELECTRONS
X-RAY DETECTOR
ELECTRON DETECTOR
BACK SCATTERED ELECTRON METHOD
BACK SCATTERED ELECTRONS
X-RAYS
SPECIMEN
ABSORBED ELECTRON METHOD
TRANSMITTED ELECTRON METHOD
AMMETER

Figure 3. Examples of backscattered electron and x-ray sweeps and line profiles.

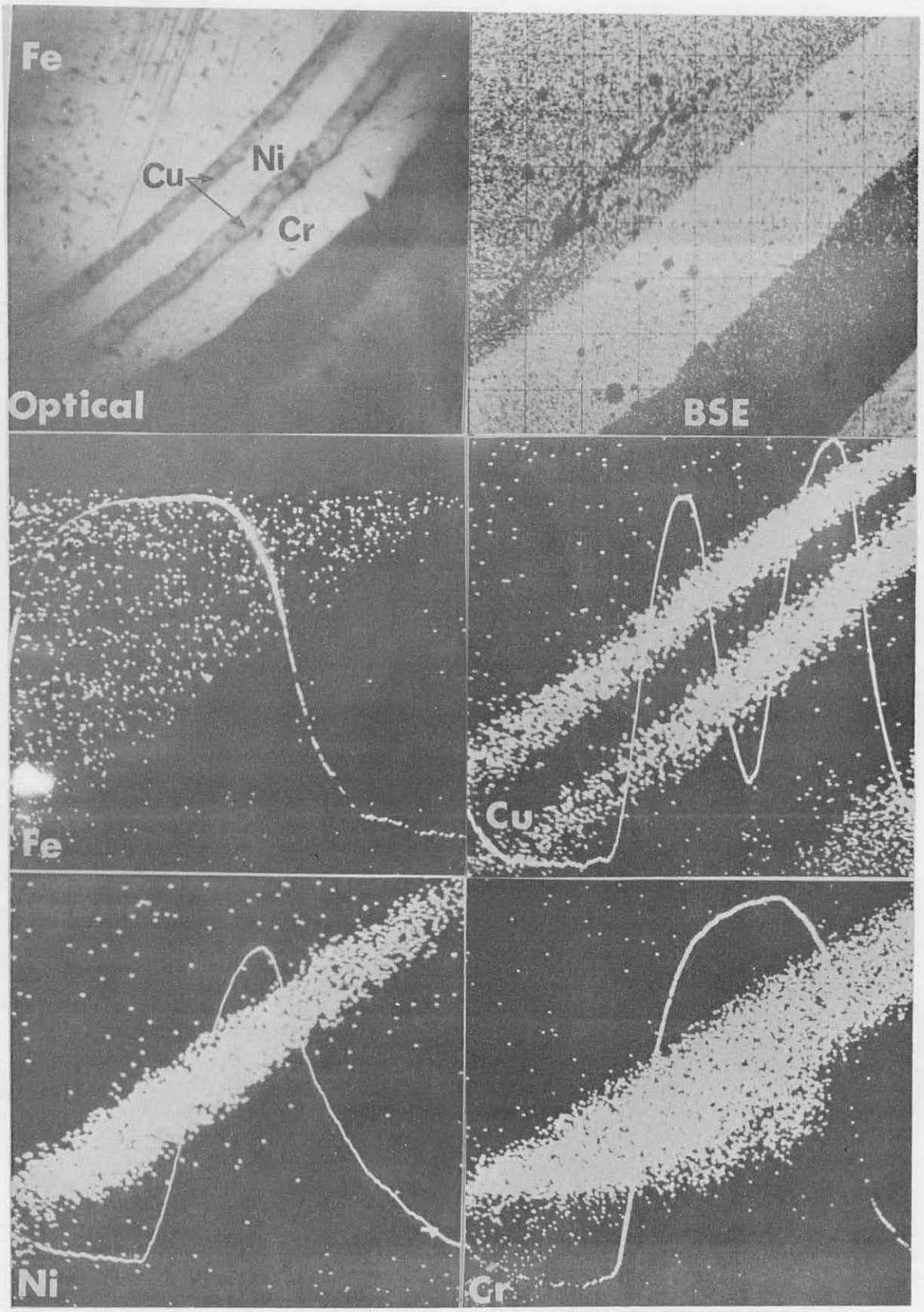
Fe
Cu
Ni
Cr
Optical
BSE
Fe
Cu
Ni
Cr

tion is obtained fairly easily. However, it is in the quantitative determination of absolute concentrations that most problems are encountered. The general foundation for the determination of concentration from characteristic x-ray line intensity was outlined by Castaing.[1] Additional contributions to the general principles of microanalysis were made by Philibert,[4] Wittry[2,5] and Poole and Thomas.[6] Many other authors have added to the information required for determination of composition. Some of these authors will be referred to in later sections of this thesis. In fact, it is necessary to do so in the running text simply because of the diversity of terminology and notation. Several reviews and bibliographies are available in the literature.[7-11] In addition, at least four books on microprobe analysis have appeared.[12-15] Each of these "overviews" has its good points, but of necessity reflects the incompleteness of theory and application which casts its shadow over the field.

One might easily follow the suggestion of Campbell and Brown[11] in evaluating the advances made in x-ray microanalysis: divide x-ray wavelengths into long and short wavelength regions with the division falling roughly at 3 Å. Such a division is motivated by both theoretical and experimental considerations. Simply stated, for analytical wavelengths less than three Angstroms, less precise theory with

many approximations and simplifications will yield relations that provide reasonably accurate concentrations from measured x-ray intensities. For analytical wavelengths greater than about three Angstroms, additional physical phenomena must be carefully considered in order to obtain a relation between measured x-ray intensity and composition. It is the consideration of the extension of the general principles of x-ray microanalysis to light elements, including carbon, that forms the subject of this thesis.

II. GENERAL CONCEPTS

The principle behind quantitative x-ray microanalysis is the irradiation with a finely focused electron beam of a selected point on a specimen surface and the detection and measurement of a characteristic x-ray line emission from a given element in the specimen. Selection of the x-ray line to be measured is made with a curved and ground diffracting crystal spectrometer. A schematic diagram of the electron probe microanalyzer is given in Figure 4. Calibration of the apparatus is accomplished by replacing the specimen by a standard containing a known amount of the element of interest. Since the measurements on the specimen and on the standard are made with x-rays of the same wavelength, there is no need to know the absolute efficiency of the spectrometer and detector. The simplicity of the analytical method appears when the calibration is made with a sample containing the pure element. In essence, this implies that a calibration curve of x-ray intensity versus concentration can be made with only two points, 100% and 0%.

The absolute nature of electron probe x-ray microanalysis has been emphasized by Castaing.[16] He has shown that such a calibration curve is to a first approximation linear. For accurate analyses, the non-linearity of such

Figure 4. Schematic diagram of the arrangement of the basic components of an electron microprobe analyzer.

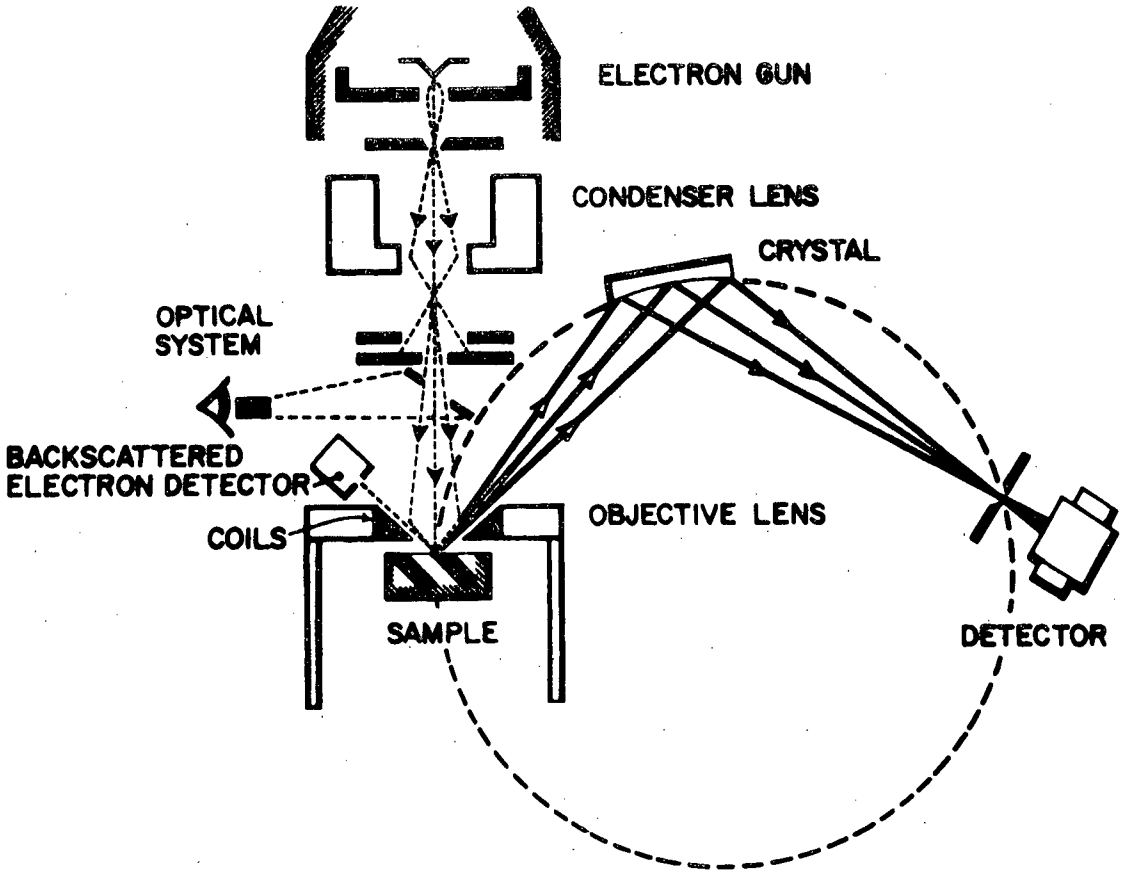
ELECTRON GUN
CONDENSER LENS
CRYSTAL
OPTICAL SYSTEM
BACKSCATTERED ELECTRON DETECTOR
COILS
OBJECTIVE LENS
SAMPLE
DETECTOR

a two point calibration can be calculated, at least in principle.

A. Instrument Effects

The non-proportionality between concentration and detected x-ray intensity arises from several general effects. The intensity (counts per second) registered by the electronic counting circuitry is not equal to the x-ray intensity emitted by the sample within the solid angle intercepted by the spectrometer.

It is an effect of the measurement procedure which causes the lack of equality between emitted and evaluated intensities. The first complication arises because the detector, usually a proportional counter, has a finite resolving time. Under the heading of "deadtime" many authors have listed two phenomena, coincidence losses and detector output pulse shrinkage.

Coincidence losses occur because x-ray emission statistics are those of radioactive decay, Poisson statistics. Two photons very closely spaced in time generate "electron clouds" in the detector, which "overlap" and then appear as a single output pulse. A count loss by coincidence has occurred. Pulse shrinkage arises because of the finite transit time to the cathode of the ions generated within the detector. At high count rates, before the ion cloud

resulting from one incident photon arrives at the cathode, a second photon enters the detector. The residual ion cloud reduces the net gas gain of the detector and a smaller output pulse is generated.

The second instrument problem has been taken as the summation of instrument drift and contamination effects. "Drift" is usually due to electron gun filament warpage and gun and lens power supply variations. Contamination is generated on the sample surface by the interaction at the sample surface of the electron probe with organic vapors. An x-ray attenuating carbon deposit is thus built up under the probe.

B. Sample Effects

Because the characteristic x-rays are generated some distance below the sample surface, absorption occurs as these x-rays leave the sample on their way to the spectrometer. This absorption is only one of the several phenomena which remove the equality between the probe generated characteristic line intensity and the detected intensity.

The spectrometer, in addition to characteristic line intensity, admits to the detector some background radiation due in general to the x-ray continuum and to secondary characteristic lines from other elements in the sample. Further, intensity at the analytical characteristic line

wavelength other than probe generated intensity arises from indirect excitation. Such secondary fluorescence radiation is generated by the absorption of primary x-rays from other elements in the sample. This necessitates a characteristic fluorescence correction. Secondary fluorescence radiation is also caused by absorption of the continuum, giving rise to a continuum fluorescence correction.

C. Effects of Electron-Target Interactions

The x-ray intensity generated by the electron probe is not strictly proportional to concentration when the sample contains elements greatly different in atomic number. As the electrons from the probe enter the specimen and cause ionizations, they do not move in straight lines. Rather, the electron motion would seem to be a series of angled paths caused by collisions. In heavy elements, these paths approach random directionality (diffusion) very rapidly. Electrons from the probe could also undergo large angle scattering. These electrons leave the sample surface while still possessing energy greater than that necessary to produce characteristic x-rays. It is this variation of electron scattering and penetration with atomic number which causes the non-proportionality between concentration and generated intensity.

Each of the above-mentioned corrections will be treated

in some detail in the following sections of this thesis. The emphasis then is on the form of the corrections to be used when one of the elements in the specimen is a light element, and on the numerical values of the various constants used in these corrections.

The approach to be used will begin with a consideration of the instrumental effects, including a discussion of certain experimental difficulties. We then consider the nature of the sample effects on the generated intensity. A discussion of the "generation" effect follows. The mathematical relations for correction of the various effects are then applied to several systems of metallurgical interest, and the results are discussed.

III. INSTRUMENTAL EFFECTS

A. Pulse Shrinkage and Coincidence Losses

The use of an x-ray detection-counting system composed of a proportional counter detector and associated pre-amplifier, linear amplifier, pulse height analyzer and scalar introduces several limitations into the measurement of the x-ray intensity incident on the detector window. Assuming that the entire energy of a photon is lost only through the ionization of detector gas atoms, the number, N, of ion pairs produced by one photon is equal to the photon energy divided by the ionization energy of the gas. (We assume zero initial kinetic energy of the ejected electron.) As these primary electrons are accelerated toward the anode, they accumulate kinetic energy. Assuming that on their way to the anode these primary electrons also lose energy only through (n) secondary ionization collisions, secondary ion pairs are generated. If the mean number of secondary collisions, $\bar{n}$, is constant for a given detector voltage, the charge collected at the anode for each incident photon of a given energy, $\bar{N}2^{\bar{n}}q$, is proportional to the energy of the incident photons. The positive ions generated by the incident photon and by the avalanche are accelerated toward the cathode. Their influence on the internal field of the detector is not removed until they arrive at the detector wall.

As the x-ray intensity, i.e., photon rate, increases, it is possible for a second photon to enter the detector while the positive ion space charge from a previous photon still exists. This space charge reduces the effective detector voltage and the gas gain ($2^{\bar{n}}$) decreases. The resultant reduction in detector output pulse amplitude causes a non-linearity in the behavior of proportional counters. Detector preamp output pulses are shown in Figure 5a, b. The two pulses in Figure 5a are widely separated in time, and thus their amplitude differences are due only to variations in the energy of the incoming photons. In Figure 5b, the third pulse is reduced in amplitude by at least 20% from the amplitude of the second pulse. This reduction of output amplitude is due to a reduced gas gain caused by the presence of the positive charge cloud from the second photon when the third photon entered the detector.

The dependence of pulse shrinkage on counting rate, detector voltage, incident wavelength, detector geometry and detector gas flow rate has been studied extensively by Bender and Rapperport,[17] with additional contributions by Burkhalter, Brown and Myklebust,[18] Birks,[13] Spielberg,[19] and Heinrich, Vieth and Yakowitz.[20] It is obvious that detector pulse shrinkage will have an effect on counting rate when a pulse height analyzer with closely set upper

Figure 5. Detector pre-amplifier output pulses; a) pulses widely separated in time; b) pulse shrinkage effect.

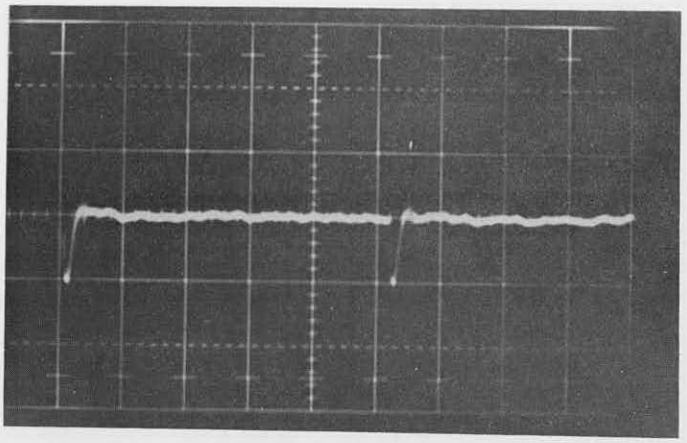

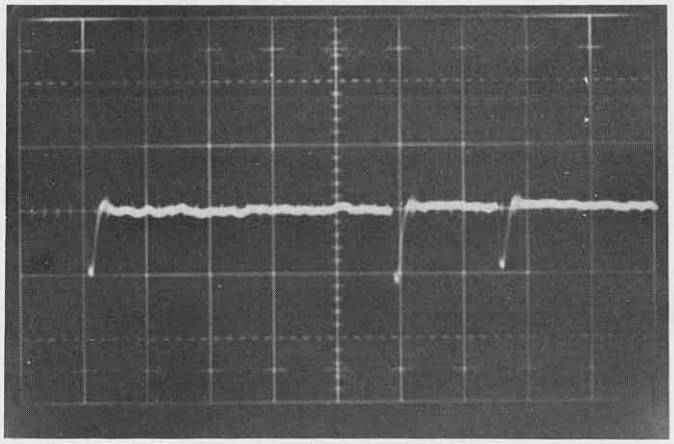

and lower level discriminators is used to eliminate noise and high and low energy background.

A separate, but not entirely distinct, problem arises when a second photon enters the detector before the electron avalanche from a preceding photon has been collected by the anode. In this case, there is the possibility that the two electron avalanche "clouds" could overlap in their arrival at the anode. The detector then outputs a single charge pulse of approximately double amplitude and a coincidence loss occurs.

Experimentally, coincidence losses can never be eliminated. In fact, the problem may be aggravated if the pulse pair resolution of the scalar, pulse height analyzer or linear amplifier is worse than the detector-preamplifier combination. For the case of losses controlled by detector response time, Schiff[21] suggested a correction of the form:

$$N = N' \exp (N \tau) \qquad (1)$$

where N = true counting rate

N' = observed counting rate

τ = deadtime

For the case where coincidence losses are controlled by a large non-extendable deadtime in the electronic pulse circuitry, Ruark and Brummer[22] derived the relation:

$$N = N'/(1 - N' \tau) \qquad (2)$$

It will be noted that if Equation (1) is expanded in

a power series:

$$N = N'(1 + N\tau + N^2\tau^2/2! + \ldots) \quad (3)$$

If $N\tau << 1$, we can terminate the series. Thus:

$$N = N'(1 + N\tau), \quad (4)$$

or:

$$N = N'/(1 - N'\tau) \quad (5)$$

The limit of the validity of such an approximation, which is of the same form as the relation of Ruark and Brummer, would be established by an experimental deviation from linearity between N and N'. Heinrich et al.[20] have shown that for counting rates up to 3×10^4 cps and deadtimes up to 3 microseconds the approximation holds for their detection system to within 5%. The point to be made is that since a precise and accurate measurement of intensity is required, deviations from linearity between N' and N must be taken into account. If one sets an arbitrary limit upon this deviation, and this limit is exceeded, higher order terms in the expansion (3) must be considered.

Various methods for determining detection system deadtime have been suggested by Beers,[23] Lonsdale,[24] Short,[25] Heinrich et al.[20] and Sawatzky and Jones.[26] In an electron microprobe instrument that has a facility for measuring sample current, it can be assumed that the x-ray photon rate reaching the detector is proportional to the sample current:

$$N = k\,i, \quad (6)$$

where (i) is the sample current. Using the linear approximation we obtain:

$$k\ i = N'/(1 - N'\ \tau) \tag{7}$$

or:

$$N'/i = k - k\ N'\ \tau \tag{8}$$

Thus, a plot of N'/i vs. N' should yield a straight line with an intercept on the N'/i axis of (k) and a slope of (k τ). τ can be determined for the plot by using

$$\tau = 1/N' - 1/k\ i \tag{9}$$

after the intercept has been determined.

Some experimenters[27] have encountered detector systems which yield data suggesting that the deadtime is a function of count rate; that is, that:

$$N = N'/(1 - N'\ \tau(N')) \tag{10}$$

Consideration of the above model for pulse shrinkage and coincidence losses suggests that an apparent increase in deadtime at high count rates is really a problem generated by a too high Pulse Height Analyzer baseline setting. A baseline set too closely at low count rates would cause an artificial decrease in counting rate at high photon fluxes due to the effect of pulse shrinkage.

An estimate of the quantitative effect of deadtime and pulse shrinkage can be obtained from a consideration of a counting rate of 10,000 counts per second (less than the rate usually obtained on pure iron or copper). If

the detector system has a deadtime of three microseconds, then to ignore the effect of deadtime on count rate would result in an error of 2.9% in the measured count rate. If 10,000 counts per second were the rate from the standard and the unknown produced 1000 counts per second (approximately a 10% alloy), the error in the resulting intensity ratio would be approximately 2.4%. Such an error would also appear in the calculated concentration.

If at 1000 counts per second, the linear amplifier output was centered at 10 volts, with a pulse distribution RMS deviation of 0.5 volts, then, assuming a Gaussian distribution, 95% of the pulses would occur between 9.0 and 11.0 volts. If the Pulse Height Analyzer was set with its upper and lower level discriminators at 8.0 and 12.0 volts respectively, and an increase in count rate to 10,000 cps resulted in a 10% decrease in pulse amplitude to a distribution centered at 9.0 volts, then approximately 4% of the counts at 10,000 cps would fall below the base-line. This loss of 4% of the standard counts would cause an error of approximately 4.5% in the intensity ratio and in the calculated concentration.

In the present experiments, the upper discriminator setting is chosen at low count rate, less than 100 per second. The lower level discriminator is set at high count rates, of the order of 10,000 counts per second. These criteria are chosen in reference to the discussion in

section III.C. The detection system deadtime is measured, as discussed in section III.D. and the correction is applied to all data.

B. Detector System

The precision of an analysis is directly related to the absolute number of x-ray quanta detected. If long counting time can be tolerated, low counting rates are acceptable. However, since in carbon analysis any significant sample surface carbon contamination will cause analysis errors, short counting times at low probe intensities are desirable. The analysis then requires diffracting crystals of high efficiency and detectors also of high quantum counting efficiency.

Rose and Korff[28] and Rose and Ramsey[29] investigated the amplification properties of proportional counters, and give specific recommendations for the use of an Argon-Methane gas mixture. Counting efficiencies of proportional counters and scintillation counters were investigated by Taylor and Parrish.[30] Their data indicate that no proportional counter can compete with a NaI(Tl) scintillator-photomultiplier tube detector for quantum counting efficiency and uniformity of spectral response, for wavelengths below 2 Å. For the wavelength interval 2 Å to 8 Å, the highest quantum counting efficiency is exhibited by an argon filled

side-window proportional counter with a Be window. The decrease in quantum counting efficiency of an (A-CH_4) - Be detector for wavelengths greater than 6 Å is due to the absorption by the window material. For wavelengths greater than 8 Å, thin organic film windows hold out the most promise for eliminating the absorption problem of Be. For example, Birks[31] has reported using a 0.25 μ nitrocellulose window for long wavelengths. More recently, Henke et al.[32] have calculated mass absorption coefficients for various organic film window materials.

For the present experiments, an argon-10% CH_4 filled proportional counter with a 0.005 in. Be window was used in the interval 1 Å to 8 Å; an aluminized 2500 Å nitrocellulose window flow proportional counter with argon-10% CH_4 gas was used for longer wavelengths.

C. Pulse Shrinkage Measurement

The data of Bender and Rapperport[17] suggest that for a given detector voltage the percent shift in output pulse amplitude decreases with wavelength to a zero shift for the silicon Kα emission line. It would seem likely then that the carbon Kα emission line should also exhibit no shift with increasing counting rates. To test this conclusion, the pulse height distribution of the carbon Kα emission line from natural diamond was measured as a func-

tion of counting rate. The pulse height spectra were obtained with a multi-channel analyzer. The channel number corresponding to the peak of the pulse height distribution is plotted as a function of counting rate in Figure 6. While little change in pulse height is observed for count rates greater than 6000 counts per second, a significant change, a reduction in output pulse amplitude with increasing count rate, is observed for lower counting rates. Since for samples containing carbon the expected carbon count rate is between 100 and 5000 counts per second, pulse shrinkage with increasing count rate cannot be ignored.

To include all possible effects of pulse shrinkage in the present analyses, the Pulse Height Analyzer upper level discriminator must be set equivalent to channel 50 in Figure 6. The lower level discriminator must be set equivalent to channel 38. These are approximately the conditions indicated at the end of section III.A.

D. Detector System Deadtime Measurement

The x-ray detection-counting system is shown schematically in Figure 7. Because each component in the system has its own effect on the net pulse pair resolution, the "deadtime" was determined for the entire detection system. This was done for each of the three spectrometers at

Figure 6. Pulse height decrease with counting rate for carbon Kα emission line.

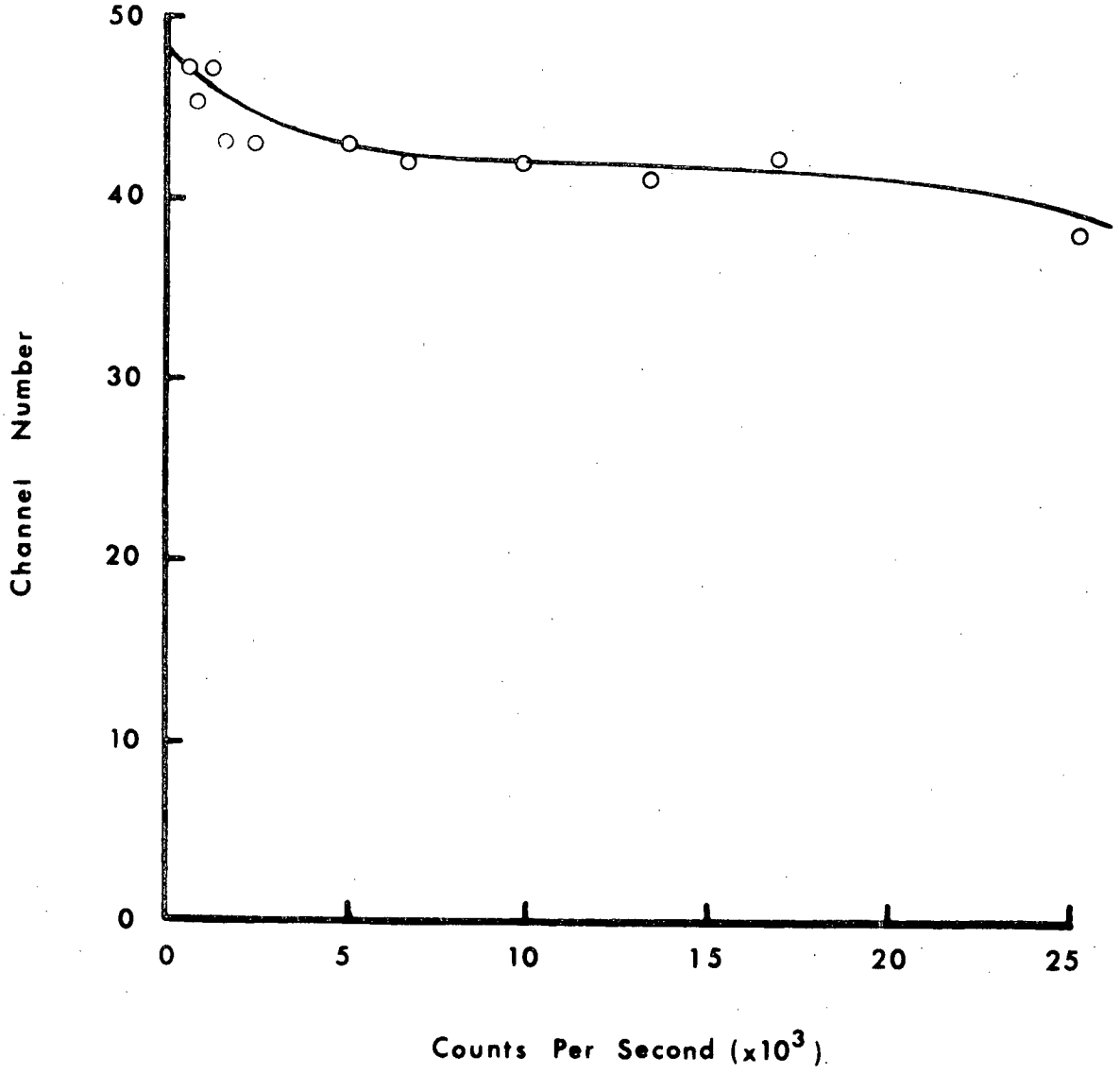
50
40
30
20
10
0
Channel Number
0
5
10
15
20
25
Counts Per Second (x10^3)

Figure 7. Schematic diagram of detector-counting system.

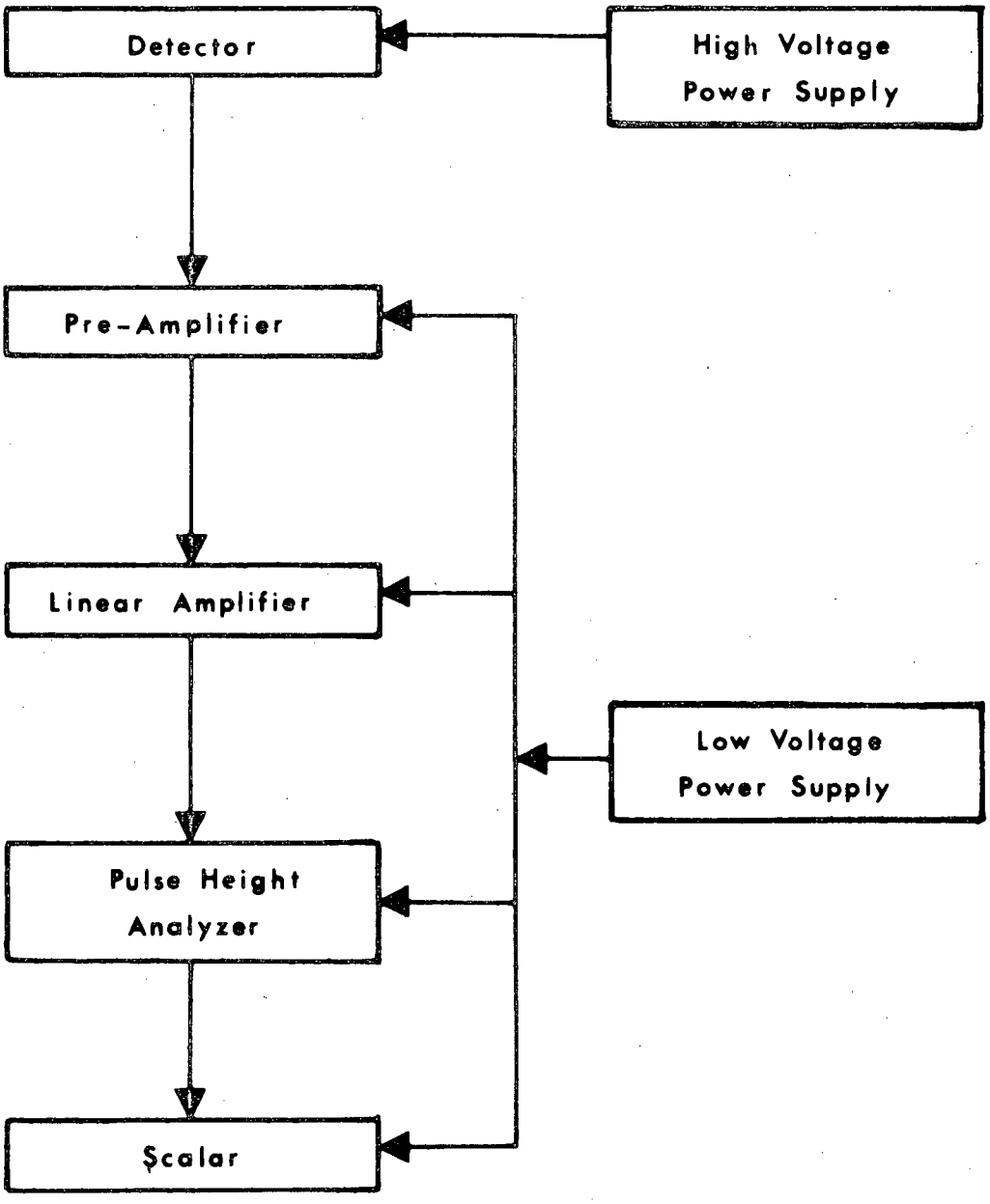
Detector
High Voltage Power Supply
Pre-Amplifier
Linear Amplifier
Low Voltage Power Supply
Pulse Height Analyzer
Scalar

several wavelengths. The data were plotted following the method of section III.A. The values of the deadtime τ were also determined mathematically using the method of least squares.[33] If there are n observations of sample current I_j and count rates N'_j, then the relations:

$$\sum_{j=1}^{n} (N'_j/I_j) = n\,k - n\,\tau \sum_{j=1}^{n} N'_j \qquad (11)$$

$$\sum_{j=1}^{n} (N'^2_j/I_j) = k \sum_{j=1}^{n} N'_j - k\,\tau \sum_{j=1}^{n} N'^2_j \qquad (12)$$

are solved for τ. A computer program, written for use in the evaluation of deadtime, is given in Appendix A. This program was written specifically to make use of the automatic readout capability added to the present instrument.

The results of several deadtime determinations are given in Table II. The values of deadtime as determined experimentally for the present instrumentation are slightly lower than that assumed in the estimate of errors made in section III.A. Thus, while the magnitude of the errors that would be encountered if we ignored the deadtime correction are slightly less than the estimates in that section, those errors are nevertheless significant. For an intensity ratio of 1000 cps/10,000 cps, the error introduced in this intensity ratio by ignoring the deadtime correction would be of the order of 2%. We thus conclude that in using the present instrumentation, a deadtime correction using

Table II. Experimental Deadtime Determinations

Detector	Wavelength	Number of Determinations	Mean τ, μ sec.
Sealed Prop. Counter #1	Si Kα	2	2.08
	Al Kα	2	2.28
			Mean 2.18 μ sec.
Sealed Prop. Counter #2	Sn Lα	2	2.53
	Fe Kα	3	2.49
	Zn Kα	3	1.94
			Mean 2.32 μ sec.
Flow Prop. Counter	C Kα	2	2.85
	Fe Kα	2	2.07
	Zn Kα	1	1.84
			Mean 2.25 μ sec.

Equation (5) with deadtime values from Table II must be made to all measured intensities.

E. Instrument Drift

In order that statistical errors in recorded data be held small, less than the errors in other input parameters, sufficient data must be accumulated. The low fluorescence yield of the light elements (less than 0.01) necessitates long counting times, ten seconds or more. During the counting interval, short term instabilities in the electron gun are encountered. Further, when many data points are taken, long term drift in the electron gun and magnetic lenses result in a changing probe intensity. Some microprobe instruments have been fitted by the manufacturers with a feedback network for stabilizing the probe current. The constancy of probe intensity is achieved by either adjusting the electron gun grid bias voltage or adjusting the condenser lens excitation current. As has been pointed out by Reed,[34] either method results in a defocusing of the electron probe, the extent of which is dependent on the amount of stabilization required. In addition, changes in condenser lens excitation can shift the position of the probe unless the electron optics column is completely aligned. Since probe intensity drift is usually due to

a shift in position of the filament with respect to the center of the gun grid aperture, the drift itself is a misalignment of the electron optics column. Thus, before implementation, all methods of instrumental compensation for probe instabilities must be critically evaluated since they might only aggravate the problem.

Correction for probe intensity drift is possible without instrumental adjustments. For example, if the probe current is measured and recorded, rather than stabilized, all x-ray counts can be normalized to constant probe current. The difficulty with this approach is that the x-ray intensity cannot be measured at the same time as the probe intensity. It is possible, however, to measure a "monitor" current, a fraction of the total beam current, which strikes an insulated aperture located above the magnetic objective lens pole piece. The x-ray intensity is then normalized to constant "monitor" current. This method relies on the proportionality between "monitor" current and probe current, which may not hold in the case of a badly misaligned column.

It is well to mention here that the current measured is NOT the sample current, the current collected by the sample and usually fed to ground via a current meter. Because of the change in electron scattering properties with atomic number, a constant probe current can be accom-

panied by a changing sample current. The changing sample current is correlatable in a general way with composition and thus is not a true measure of probe stability.

In the present instrument, much care has been taken to insure that the electron optics column is aligned before any analysis is performed. With an initially aligned column, misalignment caused by filament drift or warpage caused no detectable change in the proportionality between "monitor" current and probe current. Thus, in the present situation, a correction for probe intensity drift was accomplished by digitizing the "monitor" current as the x-ray data were taken. The x-ray data were then normalized to constant "monitor" current.

F. Contamination

The instrumental problems introduced by sample surface contamination have been discussed by Ong,[35] Ranzetta and Scott[36] and Neuhaus.[37] Consideration of the problem leads to the conclusion that contamination cannot be eliminated. However, the rate of buildup of a contamination layer on the sample surface can be reduced with certain precautionary measures.

Initial studies made in conjunction with the present work indicated that the rate of contamination buildup was independent of the type of sample surface introduced into

the electron microprobe. Likewise, these studies indicated that the generation of a visible contamination spot on the surface of a sample under probe bombardment occurred much more rapidly if the sample was left in the sample chamber overnight than if the sample was freshly introduced into the system. It was concluded that the contamination was due to the interaction at the sample surface, of the electron probe with organic vapors present in the probe enclosure, and the deposition of carbon products on the sample surface.

To reduce the amount of organic vapor in the probe enclosure the diffusion pump oil was changed from the manufacturer supplied Octoil to low back-streaming Convolex-10. The probe chamber was supplied only with an inefficient water cooled baffle for trapping back-streaming pump oil. The pumping system was thus modified to include a liquid nitrogen cold trap of the chevron type. This cold trap was separated from the diffusion pump by an air-cooled baffle also of the chevron type. The air-cooled baffle served as thermal insulation between the pump and the trap. It also served as an intermediate trap which reduced the amount of back-stream pump oil frozen on the nitrogen trap. This second function proved to be of considerable import since the nitrogen trap could be kept cooled for many days without too much concern being paid to the possi-

bility of depletion of pump oil from the diffusion pump reservoir. The addition of these baffles produced no significant effect on pumping speed.

To further reduce the possibility of contamination effects, the present instrument was modified to permit an automatic readout of accumulated data by way of a teletypewriter unit. Accumulated data were read out at the rate of 10 characters per second. Several channels of data, each containing six digits, were printed out and simultaneously punched on paper tape. Four channels of data, beam current monitor and three x-ray data channels, were read out in four seconds.

A test for contamination rate was made after the above modifications had been performed. Figure 8 shows the total carbon x-ray counts accumulated in ten second intervals as a function of time under three conditions of probe bombardment of a titanium sample. This obviously is a more sensitive test for contamination than looking for a visible contamination spot. It will be noted that on the average about seven minutes were required for the carbon count rate to double. At the intended probe intensity of 0.05 microamps, approximately six minutes passed before the carbon count rate due to contamination increased by six counts per second. Analysis of titanium carbide samples

Figure 8. Carbon contamination rate for three analysis conditions.

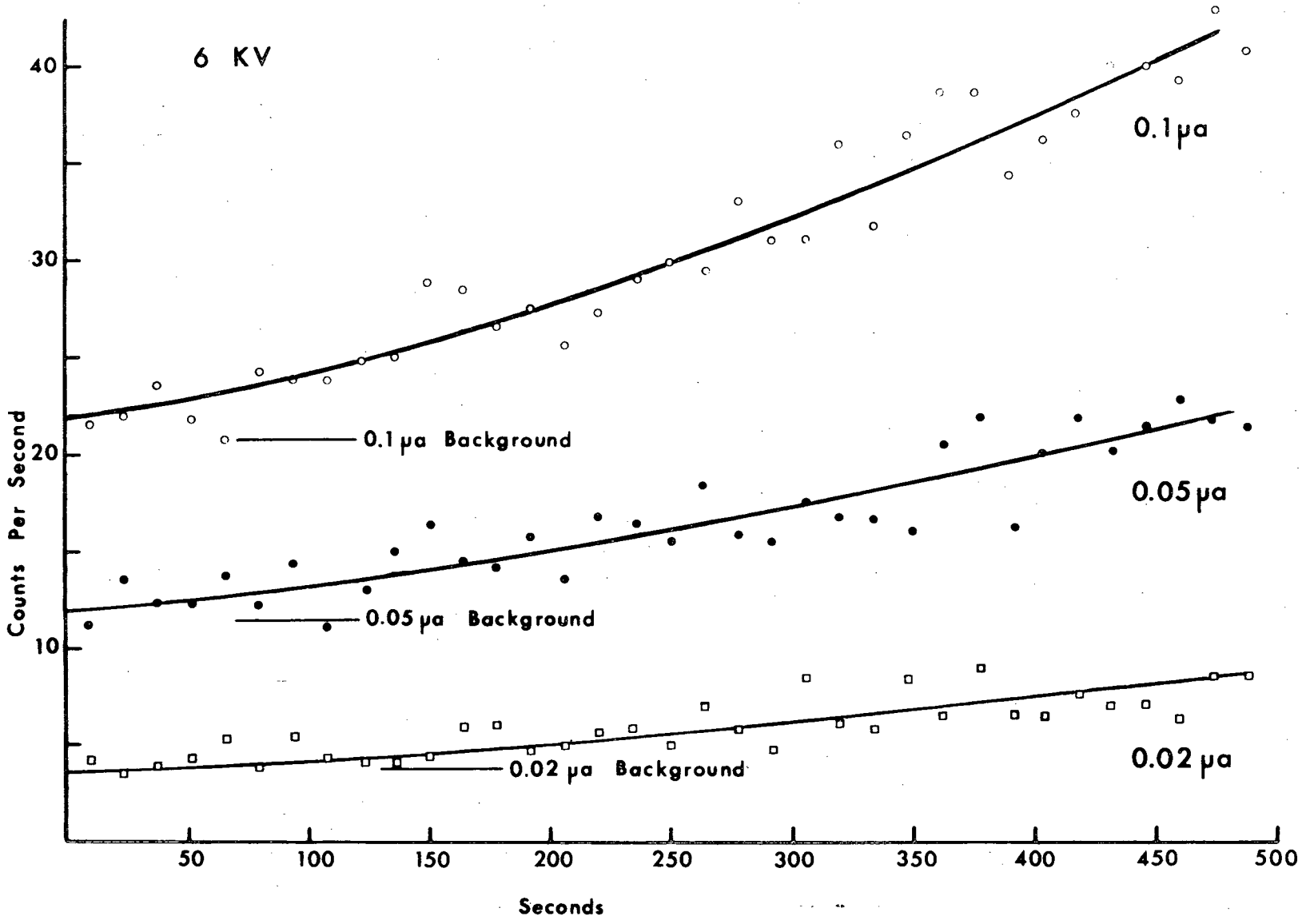
6 KV
40
30
20
10
Counts Per Second
0.1 μa
0.1 μa Background
0.05 μa
0.05 μa Background
0.02 μa
0.02 μa Background
50
100
150
200
250
300
350
400
450
500
Seconds

was expected to yield count rates in excess of 100 counts per second. It was thus concluded that counting times up to 50 seconds could be employed, if necessary, without significant changes in carbon intensity due to contamination. That is, the change in carbon counts due to contamination was less than the expected statistical error in the count data.

IV. SAMPLE EFFECTS

A. Absorption Correction

We turn, now, to the absorption within the sample of the characteristic x-rays generated by the electron probe. Several experimental determinations of the absorption correction for specific alloy systems and analysis conditions have been made. Castaing[1] and Kirianenko et al.[38] tilted the target, thus altering the electron probe angle of incidence and the x-ray emergence angle. Castaing and Descamps[39] and Castaing and Henoc[40] covered a thin tracer layer of element A by increasing layers of element B, thus changing only the total electron retardation and the total x-ray attenuation between the sample surface and the layer of the tracer element under study. Green[41] varied the x-ray emergence angle. Based on slightly different models, Philibert,[4] Theisen,[14, 42] and Helgesson[43] developed analytical methods for calculating the absorption correction in the general case.

We follow, in general, the approach of Castaing and Descamps and Philibert, with several modifications. We assume at this point that all intensity is generated by the electron probe; that is, there are no secondary flurescence effects. Letting the probe be incident normally to the surface of a sample containing element A in mass concentration C_A, the x-ray intensity generated in a thin

layer of mass thickness $d(\rho z)$, ρ = density, at a depth (ρz) is:

$$d I_{A,z} = m_o \phi(\rho z) d(\rho z) C_A, \quad (13)$$

where $\phi(\rho z)$ gives the distribution in depth of the generated intensity. m_o is the number of probe electrons per unit area incident on the specimen. Because of absorption in the specimen, the intensity emitted by the layer is:

$$d I_{A,z} = m_o C_A \phi(\rho z) \exp [-(\mu/\rho)_u^A \rho z \csc\theta] d(\rho z) \quad (14)$$

where $(\mu/\rho)_u^A$ is the mass absorption coefficient of the sample for A characteristic radiation, say Kα radiation, and θ is the x-ray take-off angle, as defined in Figure 9.

For the entire sample, the emitted intensity is:

$$I_u^A = \int_{\rho z=0}^{\infty} m_o C_A \phi(\rho z) \exp [- \chi_u^A \rho z] d(\rho z) \quad (15)$$

where $\chi_u^A = (\mu/\rho)_u^A \csc \theta$. Since the take-off angle, θ, is determined by the instrument, we need to know two quantities, $\phi(\rho z)$, the distribution in depth of the generated intensity, and (μ/ρ), the mass absorption coefficient for A Kα radiation.

Letting an incident electron have an energy $E_o > E > E_c$, where E_o is the probe accelerating potential and E_c is the critical excitation potential for A Kα radiation, the number of ionizations per unit path length could be expressed as:

Figure 9. Relationship between incident electron probe and x-ray emergence angle, θ.

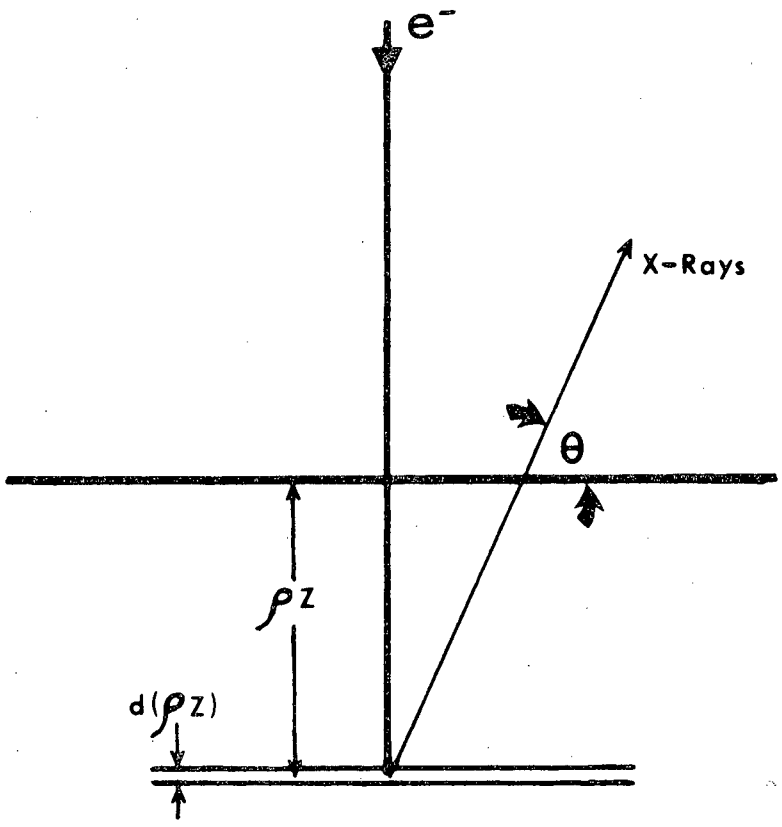
e⁻
X-Rays
θ
ρz
d(ρz)

$$d\,n_A = \psi(E, E_c, n)\,d\,x, \tag{16}$$

where (n_A) is the number of "ionizable" electrons per cm^3. If ψ depends only on the element A, and if (n) is not a function of atomic number (as, for example, the number of K electrons), then:

$$d\,n_A = \frac{\rho\,N}{A}\,\psi_A(E, E_c)\,d\,x, \tag{17}$$

where N is Avogadro's number and A is the atomic weight of A. ψ_A now has the characteristics of a cross section. We now consider the number of ionizations of A atoms per layer (d z) at the depth (z) in a sample containing element A in concentration C_A. If an electron traversing (d z) makes an angle β_i with the normal, then, with β_i defined in Figure 10, we have:

$$d\,n_{A,z} = C_A\,\frac{\rho\,N}{A}\,\psi_A\,\frac{d\,z}{\cos\,\beta_i} \tag{18}$$

For all electrons crossing d z:

$$d\,I_{A,z} = \sum_i d\,n_{A,z} = C_A\,\frac{\rho\,N}{A}\,\psi_A\,\sum_i \frac{d\,z}{\cos\,\beta_i}. \tag{19}$$

The summation must be taken over all electrons crossing (d z), not just those moving downward. If (m_o) is the number of electrons per unit area in the probe at the specimen surface, then at depth (z), this number will be reduced to (m_z). But these are only the downward traveling p be electrons. Since the possibility of backscattering does exist, the net number of electrons crossing (d z) is $(r_z\,m_z)$, with $1 \leq r_z \leq 2$. At the depth of complete diffusion,

Figure 10. Relationship between incident electron probe and electron traverse angle, β.

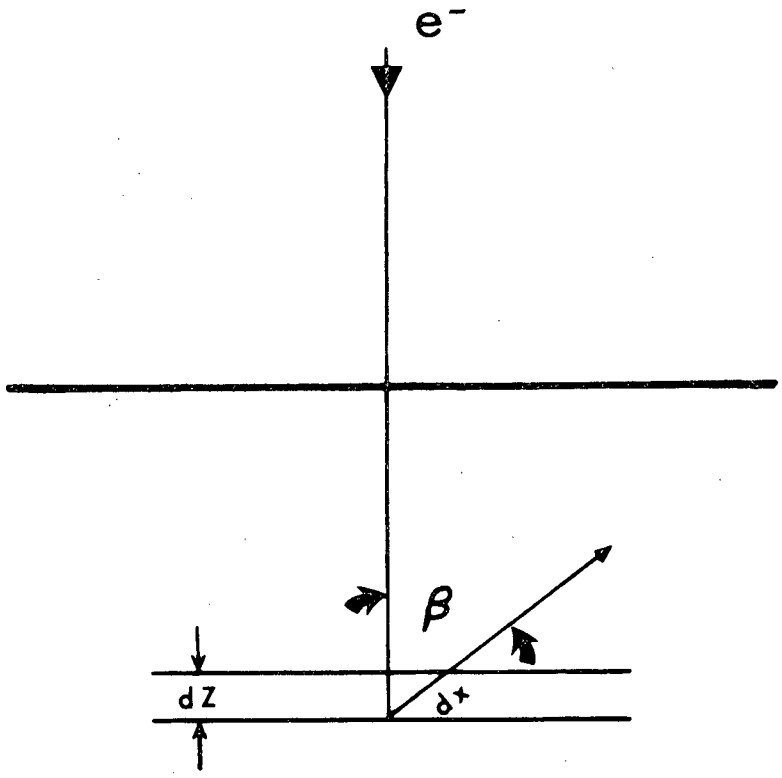
e⁻
β
dZ
δ+

$r_z = 2$. At the surface, $r_z = 1$. Thus we write:

$$d\, I_{A,z} = C_A \frac{\rho\, N}{A} \psi_A \sum_{i=1}^{r_z m_z} \frac{1}{\cos\, \beta_i}\, d\, z. \qquad (20)$$

Since, for a given set of conditions, the mean scattering angle, or the angle of traverse across (d z), will vary with (z), we set:

$$\sum_{i=1}^{r_z m_z} \frac{1}{\cos\, \beta_i} = m_z\, R(\rho\, z), \qquad (21)$$

and:

$$d\, I_{A,z} = C_A \frac{N}{A} \psi_A\, m_z\, R(\rho\, z)\, \rho\, d\, z. \qquad (22)$$

Before proceeding, it is well to recall that the only reason for the present manipulations is the desire to obtain some form for the distribution in depth of the generated x-ray intensity. Such a distribution is needed to obtain an estimation for the effect of specimen absorption of the generated intensity. It will be seen later that the distribution in depth can effectively be removed from the consideration of absorption.

Philibert assumed an exponential form for the dependence of R on (ρ z) as:

$$R(\rho\, z) = R(\infty) - (R(\infty) - R(0)) \exp\, (-\, k\, \rho\, z) \qquad (23)$$

He also assumed that the number of downward traveling electrons varies with depth following Lenard's[44] law:

$$(m_z/m_o) = \exp\, (-\, \sigma\, \rho\, z). \qquad (24)$$

The first serious problem arises now, since the Lenard (σ)

depends only on E_o, and not on E_c. Duncumb and Shields[45] noted this problem and Duncumb and Melford[46] have suggested that the critical excitation potential dependence should be of the form:

$$\sigma = \frac{\text{const.}}{E_o^{1.5} - E_c^{1.5}} \tag{25}$$

Substituting for $R(\rho z)$ and (m_z), we obtain:

$$d I_{A,z} = C_A \frac{N}{A} m_o \psi_A e^{-\sigma\rho z} [R(\infty) - (R(\infty) - R(0)) e^{-k\rho z}] \tag{26}$$

From Equation (13), we had:

$$d I_{A,z} = m_o C_A \phi(\rho z) d(\rho z) \tag{13}$$

Thus we obtain:

$$\phi(\rho z) = \frac{N}{A} \psi R(\infty) e^{-\sigma\rho z} [1 - (1 - \frac{R(0)}{R(\infty)}) e^{-k\rho z}]. \tag{27}$$

With absorption, we previously had:

$$d I_{A,z} = m_o C_A \phi_u(\rho z) \exp(-(\mu/\rho)_u^A \rho z \csc\theta d(\rho z)) \tag{14}$$

or:

$$I_u^A = m_o C_A \int_{\rho z=0}^{\infty} \phi_u(\rho z) \exp(-\chi_u^A \rho z) d(\rho z), \tag{15}$$

which is just the form of the LaPlace transform of $\phi(\rho z)$. Likewise, for a standard of pure A:

$$I_s^A = m_o' \int_{\rho z=0}^{\infty} \phi_s(\rho z) \exp(-\chi_s^A \rho z) d(\rho z), \tag{28}$$

where χ_s^A is the product of $\csc\theta$ and the mass absorption coefficient of element A for A radiation. Forming the ratio of intensities:

$$\frac{I_u^A}{I_s^A} = C_A \frac{m_o}{m_o'} \frac{\int \phi_u(\rho\ z)\ e^{-\chi_u \rho z}\ d(\rho\ z)}{\int \phi_s(\rho\ z)\ e^{-\chi_s \rho z}\ d(\rho\ z)} , \tag{29}$$

We see that it is absolutely imperative that the probe intensity be the same for the unknown and the standard.

Taking the transform:

$$F(\chi) = \left(\frac{1}{1+\frac{\chi}{\sigma}} + \frac{\sigma}{k}\frac{R(0)}{R(\infty)}\right)\left(\frac{1}{1+\frac{\sigma}{k}+\frac{\chi}{k}}\right) \tag{30}$$

and letting $h = \frac{\sigma}{k}$ we have:

$$F(\chi) = \left(\frac{1}{1+\frac{\chi}{\sigma}} + h\frac{R(0)}{R(\infty)}\right)\left(\frac{1}{1+h(1+\frac{\chi}{\sigma})}\right) \tag{31}$$

If $m_o = m_o'$, the intensity ratio now becomes:

$$\frac{I_u^A}{I_s^A} = K = C_A \frac{F_u(\chi)}{F_s(\chi)} . \tag{32}$$

Since we had to assume some form for the rate of energy loss by the probe electrons, the above relation contains not only the correction for sample absorption, but also the effect of atomic number. It is possible to separate the two effects if we consider that in the absence of absorption ($\chi = 0$):

$$F(0) = \frac{1 + h\ R(0)/R(\infty)}{1 + h} . \tag{33}$$

Then, defining:

$$f(\chi) = F(\chi)/F(0) \tag{34}$$

we can write:

$$\frac{I_u^A}{I_s^A} = C_A \frac{f_u(\chi_u)}{f_s(\chi_s)} \frac{F_u(0)}{F_s(0)} \tag{35}$$

or:

$$C_A = \frac{I_u^A}{I_s^A} \frac{f_s(\chi_s)}{f_u(\chi_u)} g \tag{36}$$

where

$$f(\chi) = \frac{1 + \frac{h\,R(0)}{R(\infty) + h\,R(0)} \frac{\chi}{\sigma}}{(1 + \frac{\chi}{\sigma})(1 + \frac{h}{1+h} \frac{\chi}{\sigma})} \tag{37}$$

and (g) is a function containing the effect of atomic number.

At this point, we are faced with the evaluation of the various factors in $f(\chi)$. It has been usual to assume that $R(0) = 0$ (Philibert[4]). However, from consideration of our model, such an assumption ignores any ionization occurring near the target surface, and would thus tend to overcorrect the intensity ratio. To a first approximation, $R(0) = 1 + \varepsilon$, where ε would be determined by the backscattered electron intensity. However, all backscattered electrons do not have the same energy. Thus the energy distribution would have to be considered. Such an approach has been suggested by Bishop.[47] In the present case, we assume that $R(0) = 1.1$. If we assume, in Equation (21) that an approximate value for the average of $\cos \beta_i$ is 1/2, then we obtain $R(\infty) = 4$. Philibert had shown that h can be expressed as a function of

(A/Z^2) where Z is the atomic number. Using values of $R(0)$ and $R(\infty)$ similar to the above, Duncumb and Melford evaluated $h = 4.5 \frac{A}{Z^2}$. This value will be assumed here. The final evaluation is that of the mass absorption coefficients. As Yakowitz and Heinrich[48] have shown, it is the accuracy of (μ/ρ) which dominates the accuracy of $f(\chi)$, and thus the accuracy of the absorption correction, Equations (36) and (37). We deal in some detail with mass absorption coefficients in the next section.

A. 1. Mass Absorption Coefficients

Since the analytical method of electron probe microanalysis can be applied to any solid sample, the correction for sample absorption of generated x-rays must be able to be applied to any sample. Necessary inputs to that correction are the values of the sample and standard mass absorption coefficients for the x-ray wavelengths used in the analysis. Two of the most recent "generalized" tables of x-ray mass absorption coefficients have been published by Heinrich[8] and by Frazer.[49] Several comments are pertinent to both sets of values. Both authors use the approach initially suggested by Siegbahn,[50] discussed by Allen,[51] Grosskurth,[52] Laubert,[53] and formalized by Leroux[54] to interpolate between measured values of (μ/ρ). Leroux claimed that experimental mass absorption coefficients could be fit to an analytic relation of the form:

$$(\mu/\rho) = C\ \lambda^{n}. \qquad (38)$$

The exponent was said to be characteristic of the wavelength interval between absorption edges and the coefficient dependent on atomic number. These two authors tested experimental values from various investigators for internal consistency based on a minimum random error from the assumed relation, Equation (38). The data were then weighted accordingly and fit by the method of least squares to obtain values for the coefficient and exponent. Both authors obtained a set of C's and n's for several elements

and wavelength intervals. In particular, these authors found that the exponent was not independent of atomic number, as had been suggested by Leroux. Heinrich graphically fitted the C's and n's he obtained by a smooth curve. A linear dependence of the exponent on atomic number and a polynomial dependence of the coefficient on atomic number were finally assumed by Frazer. These fittings assumed a smooth variation of the mass absorption coefficients with atomic number and thus permitted a tentative interpolation to atomic numbers for which no experimental mass absorption data had been obtained.

Other methods, based on semi-theoretical grounds, have been suggested for estimation of mass absorption coefficients. Victoreen[55,56] dealt primarily with very short wavelengths, generating a semi-empirical relation for mass absorption coefficients below the K-edge. Also obtaining a semi-empirical function, Henke et al.[57] calculated mass absorption coefficients of elements up to Gallium. They give values for (μ/ρ) for wavelengths between 8.34Å and 44.Å, stopping short of the L III edge. The calculations of Bearden[58] and Henke et al.,[32] leading directly to photo-effect cross sections, are based on assumed hydrogen-like wave functions for the initial and final states of the electron involved in the photo-ionization. Bearden gives calculated and experimental

values of (μ/ρ) for wavelengths less than or just greater than the K edge, for 9 elements. Henke et al. present results of similar calculations for elements to Calcium up to the L III edge, but also give experimental data to 113 Å for carbon and for elements found in the gaseous state.

Since it is impossible to predict the elements that might be involved in any particular microanalysis, including the light elements, some method must be used to obtain at least a reasonable estimate of the numerical value of mass absorption coefficients. Several compilations of mass absorption coefficients, generally containing only experimental values, but not necessarily, have been published by Birks,[13] Allen,[59] Liebhafsky et al.,[60] Compton and Allison,[61] Sagel,[62] and Stainer.[63] However, in any of these compilations, it is generally not possible to determine which values presented are really experimental and which are values obtained by the author's own method of interpolation. Further, these tables are generally limited to wavelengths less than ten Angstroms.

The interpolated, calculated tables of Heinrich do not contain mass absorption coefficients for wavelengths longer than 11.9 Å. Thus, no numerical values, even interpolated ones, are presented for the emission lines of elements lighter than sodium. An additional difficulty arises because certain of the values presented differ by several percent

from recently measured (μ/ρ) values. For example, the Heinrich given value for nickel absorbing the tin Lα line differs from that measured by Hughes and Woodhouse,[64] being low by more than 4%. Likewise, for zirconium as an absorber, the Heinrich values for wavelengths between 5.7 and 8.4 Å are higher than the Hughes and Woodhouse[64] values by more than 7%.

Although the calculated values of Frazer include mass absorption coefficients for wavelengths to the fluorine Kα line (18.32 Å), it is in the cases of long wavelengths (greater than the silicon Kα, 7.125 Å) that significant errors appear. For example, when compared to the experimental values of Henke et al.,[32] the Frazer values for (μ/ρ) for a carbon absorber for the emission lines of fluorine (18.32 Å), magnesium (9.89 Å) and aluminum (8.339 Å) are in error by 9.8%, 16.6% and 17.5% respectively. For nitrogen as the absorber, the errors are 2.0%, 12.7% and 14.3%. For oxygen as the absorber, the errors are 1.0%, 7.2% and 10.0%. For fluorine absorbing fluorine Kα, the difference amounts to 96.5%.

The lack of an apparently trustworthy set of self-consistent mass absorption coefficients for the refractory metals and for light elements prompted a search for experimental data with these materials as absorbers. Some data

for the refractory metals are available in the literature.[8,52,53,64-71] These data do not necessarily include values of (μ/ρ) for the emission lines of carbon, nitrogen and oxygen. Figure 11 is a log-log plot of experimental mass absorption coefficient data as a function of wavelength for zirconium. The solid line is a fit of that data by the method of least squares to a relation of the form of Equation (38). The data only covers wavelengths less than 9 Å. Data taken with titanium as the absorber, to wavelengths greater than 100 Å, is shown in Figure 12. Again, the solid line is a least squares fit of the data to Equation (38). Even allowing that the data of Ershov et al.[69] might be 5-15% low, a serious deviation from linearity is observed in this plot. Figure 13 shows the mass absorption data for a Group VB metal, Tantalum. Equation (38) seems to fit below the M I edge, although absence of data near that edge precludes any real test.

The coefficients and exponents obtained by our fit of the data available at the present time, for these three elements, were sufficiently different from those postulated or obtained by Heinrich or Frazer to warrant a re-evaluation of estimates of mass absorption coefficients for other elements, particularly in light of recently available data.[32,68-79]

This re-evaluation was undertaken. That work required consideration of experimental and theoretical work on both

Figure 11. Mass absorption coefficient of zirconium.

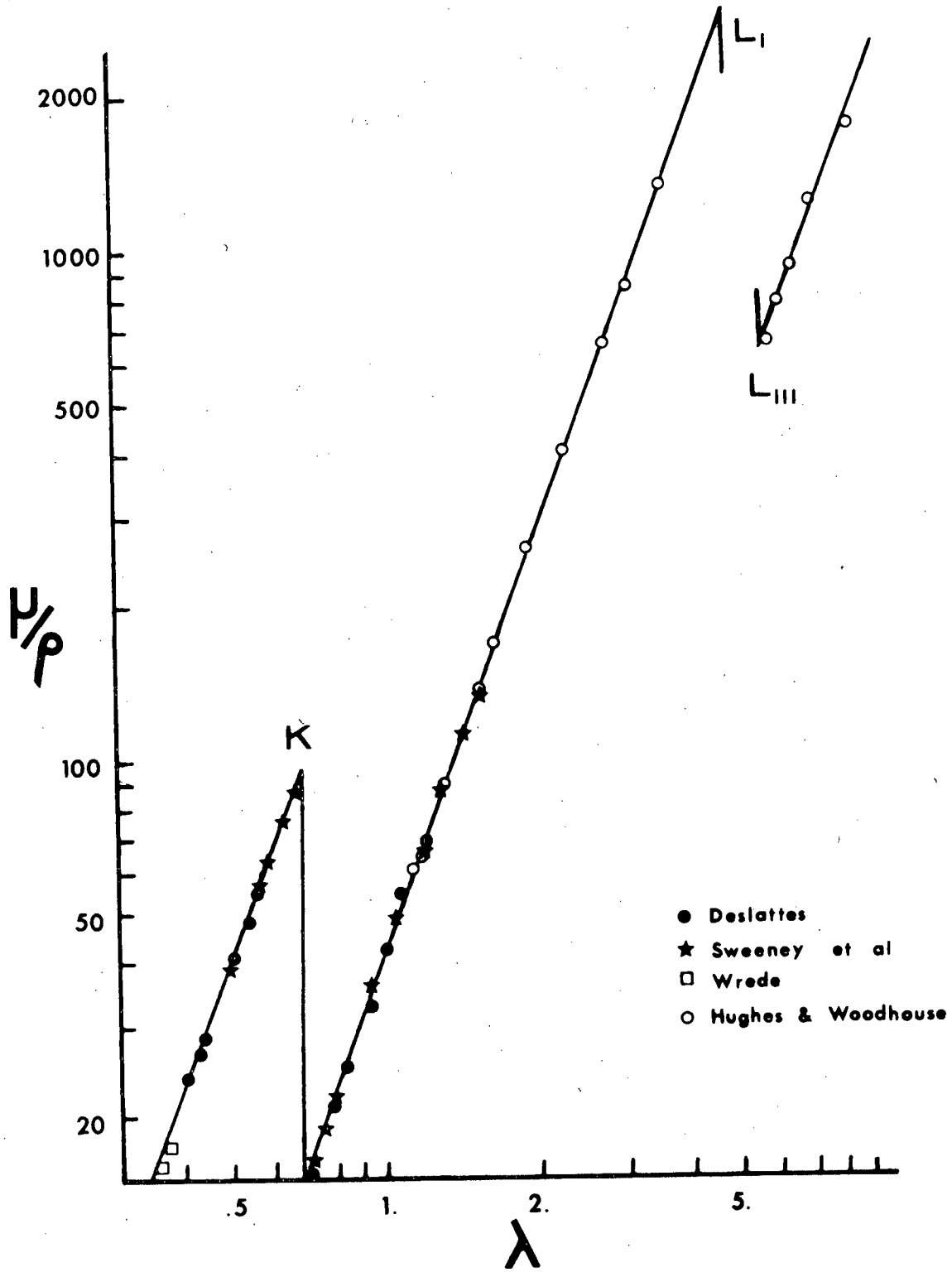
2000
1000
500
100
50
20
μ/ρ
K
L_I
L_III
.5
1.
2.
5.
λ
Deslattes
Sweeney et al
Wrede
Hughes & Woodhouse

Figure 12. Mass absorption coefficient of titanium.

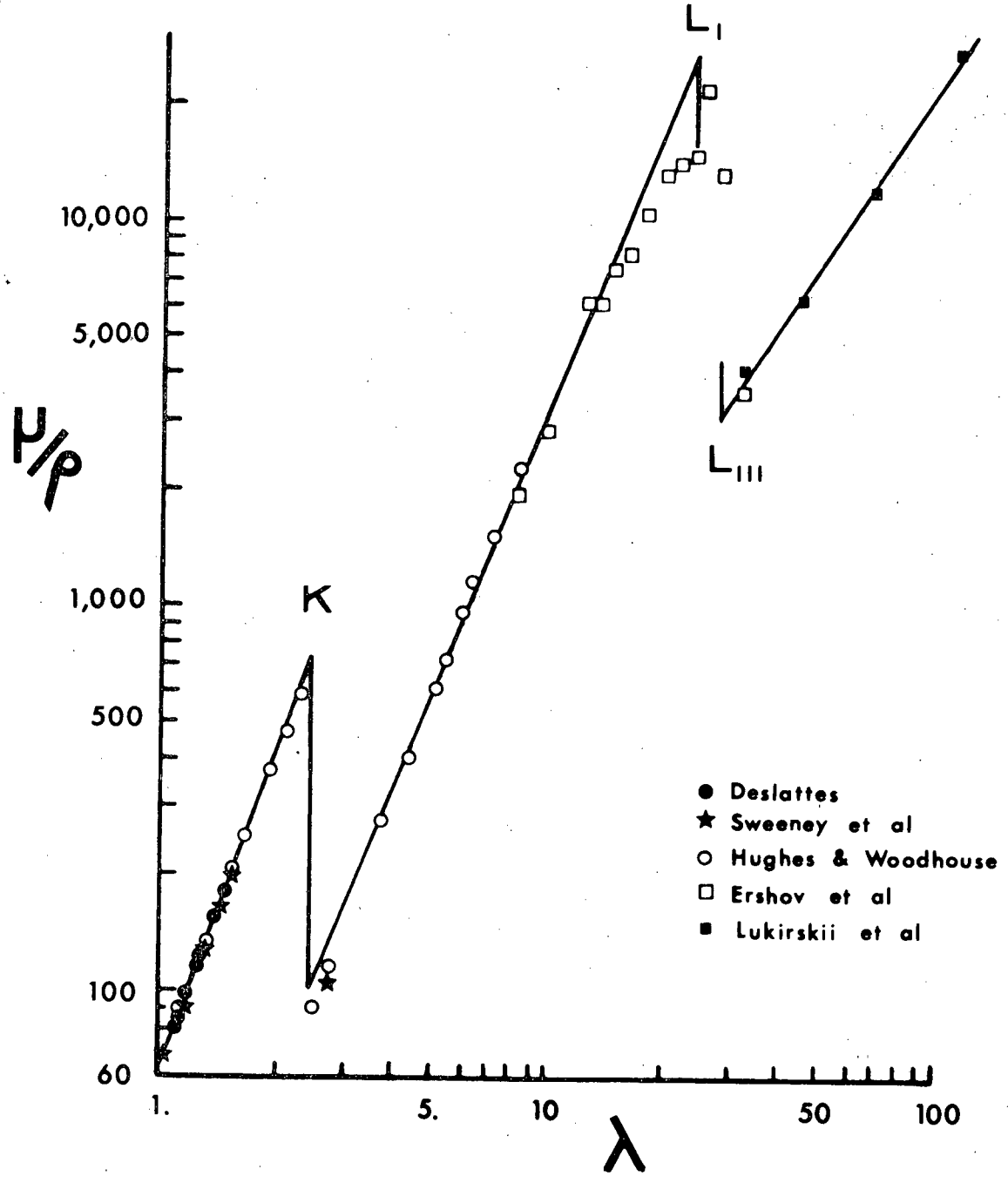
L_I
L_III
K
10,000
5,000
1,000
500
100
60
μ/ρ
1.
5.
10
50
100
λ
Deslattes
Sweeney et al
Hughes & Woodhouse
Ershov et al
Lukirskii et al

Figure 13. Mass absorption coefficient of tantalum.

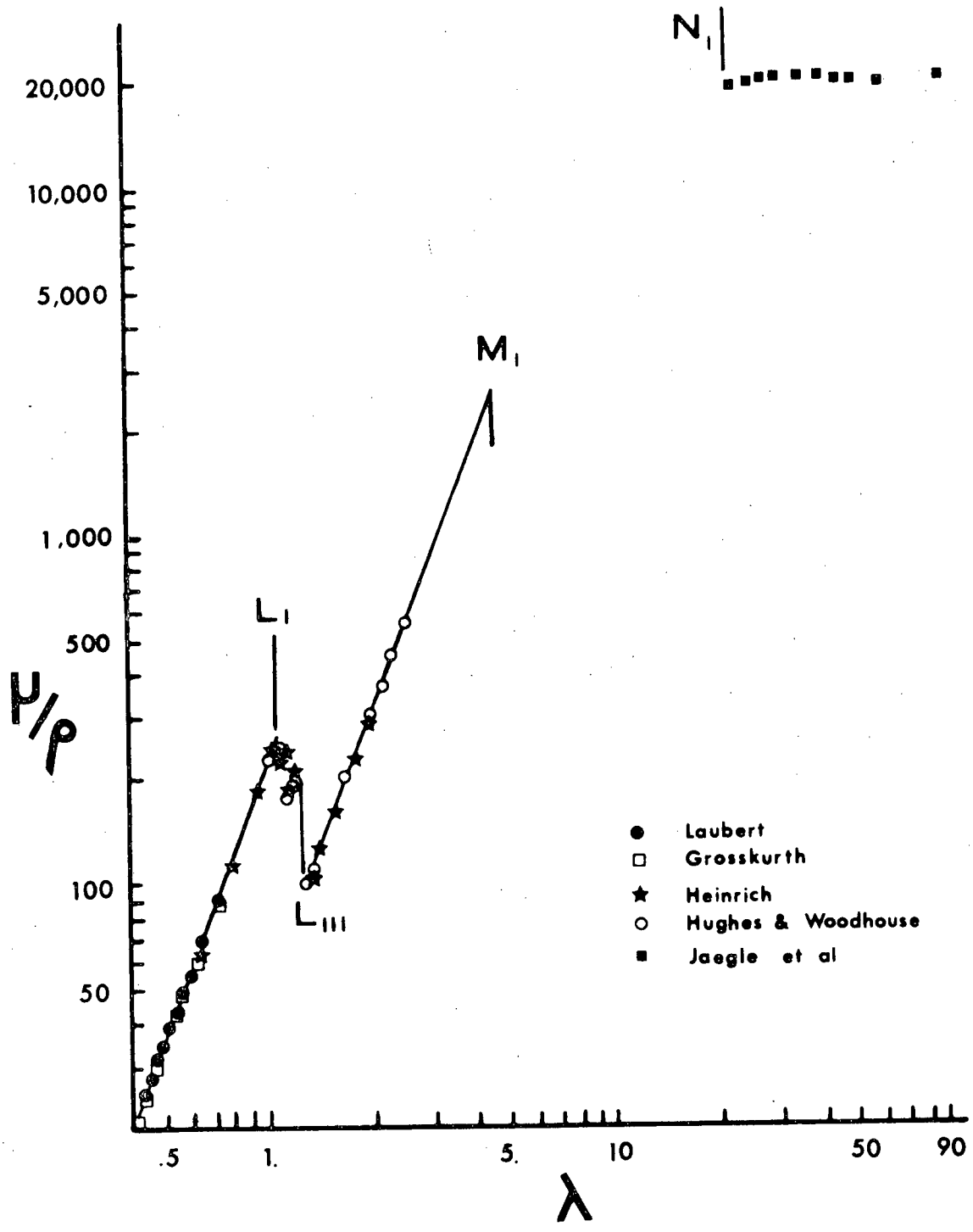
N1
20,000
10,000
5,000
M1
1,000
L1
500
μ/ρ
100
LIII
50
Laubert
Grosskurth
Heinrich
Hughes & Woodhouse
Jaegle et al
.5
1.
5.
10
50
90
λ

the characteristic energies of emission lines and absorption edges, and mass attenuation coefficients. The work is discussed in the following sections.

A. 2. Evaluation of Emission Line and Absorption Edge Wavelengths.

Since the present interest in mass absorption coefficients includes a desire to estimate values for the rate of attenuation of the carbon, nitrogen and oxygen emission lines, it was necessary to know the wavelengths of the emission lines and the position of the absorption edges of the various elements. Again, in this data, we are particularly concerned with long wavelengths.

Heinrich[8] included a listing of absorption edges with his calculated and interpolated coefficients and exponents. These values, however, are also limited to wavelengths less than 12. Å. Further, several errors become apparent. For example, the L I edge of zinc, as given by Heinrich, differs from the value listed by Bearden[80] by 0.5 Å. Several other edges were found to differ from Bearden's values by several tenths of an Angstrom. The relatively large size of these errors indicated that a critical evaluation of published absorption edge and emission line wavelengths was needed. In addition, as indicated by the fact that Bearden's compilation is incomplete, the L sub-shell edges and M sub-shell edges had not been determined in the case of many elements.

A listing of primary ($K\alpha_1$, $L\alpha_1$, $M\alpha_1$) emission wavelengths and critical excitation potentials for the principle atomic series is given in Table III.

Table III. Principle Emission Line Wavelengths and Critical Excitation Potentials for K, L and M Series

At. Wt.	Ele.	E_K(Kev)	E_L(Kev)	E_M(Kev)	$\lambda_{K\alpha_1}$ Å	$\lambda_{L\alpha_1}$ Å	$\lambda_{M\alpha_1}$ Å
1.008	H	.014					
4.003	HE	.025					
6.939	LI	.055			228.		
9.012	BE	.111			114.		
10.811	B	.188	.005		67.6		
12.011	C	.284	.006		44.7		
14.007	N	.400	.009		31.60		
15.999	O	.532	.007		23.62		
18.998	F	.685	.009		18.32		
20.183	NE	.867	.018		14.610		
22.990	NA	1.072	.031		11.910		
24.312	MG	1.303	.049		9.890		
26.982	AL	1.560	.073		8.339		
28.086	SI	1.840	.101		7.125		
30.974	P	2.144	.132		6.157		
32.064	S	2.470	.165		5.372		
35.453	CL	2.820	.200		4.728		
39.948	AR	3.203	.245		4.192		
39.102	K	3.608	.295		3.741		
40.080	CA	4.038	.346		3.358	36.33	
44.956	SC	4.489	.402	.007	3.031	31.35	
47.900	TI	4.965	.455	.004	2.749	27.42	
50.942	V	5.464	.513	.002	2.504	24.25	
51.996	CR	5.989	.575	.002	2.290	21.64	
54.938	MN	6.538	.640	.003	2.102	19.45	
55.847	FE	7.111	.707	.004	1.936	17.59	
58.933	CO	7.710	.779	.003	1.789	15.972	
58.710	NI	8.332	.854	.004	1.658	14.561	
63.540	CU	8.980	.933	.002	1.541	13.336	
65.370	ZN	9.661	1.022	.008	1.435	12.254	

Table III. Continued

At. Wt.	Ele.	E_K(Kev)	E_L(Kev)	E_M(Kev)	$\lambda_{K\alpha_1}$ Å	$\lambda_{L\alpha_1}$ Å	$\lambda_{M\alpha_1}$ Å
69.720	GA	10.368	1.117	.017	1.340	11.292	
72.590	GE	11.104	1.217	.029	1.254	10.436	
74.922	AS	11.865	1.323	.041	1.176	9.671	
78.960	SE	12.655	1.434	.054	1.105	8.990	
79.909	BR	13.470	1.553	.069	1.040	8.375	
83.800	KR	14.324	1.677	.089	.980	7.817	
85.470	RB	15.202	1.807	.110	.926	7.318	
87.620	SR	16.107	1.941	.133	.875	6.863	
88.905	Y	17.038	2.079	.157	.829	6.449	
91.220	ZR	17.999	2.223	.180	.786	6.071	
92.906	NB	18.987	2.371	.205	.746	5.724	
95.940	MO	20.004	2.523	.227	.709	5.407	
99.000	TC	21.047	2.678	.253	.675	5.115	
101.070	RU	22.119	2.838	.279	.643	4.846	
102.905	RH	23.220	3.002	.307	.613	4.597	
106.400	PD	24.348	3.173	.335	.585	4.368	
107.870	AG	25.517	3.351	.398	.559	4.154	
112.400	CD	26.716	3.538	.440	.535	3.956	
114.82	IN	27.942	3.730	.443	.512	3.772	
118.690	SN	29.195	3.929	.511	.491	3.600	
121.750	SB	30.486	4.132	.528	.470	3.439	
127.600	TE	31.811	4.342	.572	.451	3.289	
126.904	I	33.167	4.559	.631	.433	3.149	
131.300	XE	34.590	4.782	.672	.416	3.017	
132.905	CS	35.987	5.011	.726	.400	2.892	
137.340	BA	37.452	5.247	.780	.385	2.776	
138.910	LA	38.934	5.484	.832	.371	2.666	14.88
140.120	CB	40.453	5.723	.883	.357	2.562	14.04
140.907	PR	42.002	5.963	.926	.344	2.463	13.343
144.240	ND	43.574	6.209	.973	.332	2.370	12.68

Table III. Continued

At. Wt.	Ele.	E_K(Kev)	E_L(Kev)	E_M(Kev)	$\lambda_{K\alpha_1}$ Å	$\lambda_{L\alpha_1}$ Å	$\lambda_{M\alpha_1}$ Å
147.	PM	45.198	6.461	1.027	.320	2.282	12.
150.35	SM	46.849	6.717	1.073	.309	2.200	11.47
151.96	EU	48.519	6.981	1.126	.298	2.121	10.96
157.250	GD	50.233	7.243	1.185	.288	2.047	10.46
158.924	TB	52.002	7.515	1.241	.279	1.977	10.00
162.500	DY	53.793	7.790	1.295	.270	1.909	9.59
164.93	HO	55.619	8.068	1.351	.261	1.845	9.20
167.26	ER	57.487	8.358	1.401	.252	1.784	8.82
168.934	TM	59.380	8.650	1.461	.244	1.727	8.48
173.04	YB	61.300	8.944	1.528	.237	1.672	8.149
174.97	LU	63.310	9.249	1.589	.229	1.620	7.840
178.49	HF	65.310	9.558	1.662	.222	1.570	7.539
180.948	TA	67.403	9.877	1.743	.215	1.522	7.252
183.85	W	69.508	10.200	1.814	.209	1.476	6.983
186.20	RE	71.658	10.531	1.890	.203	1.433	6.729
190.2	OS	73.856	10.868	1.967	.197	1.391	6.490
192.2	IR	76.101	11.212	2.048	.191	1.351	6.262
195.09	PT	78.381	11.562	2.133	.186	1.313	6.047
196.967	AU	80.720	11.921	2.220	.180	1.276	5.840
200.590	HG	83.109	12.286	2.313	.175	1.241	5.648
204.37	TL	85.533	12.660	2.406	.170	1.207	5.460
207.19	PB	88.005	13.041	2.502	.165	1.175	5.286
208.980	BI	90.534	13.426	2.603	.161	1.144	5.118
210.	PO	93.105	13.814	2.683	.156	1.114	
210.	AT	95.730	14.214	2.787	.152	1.085	
222.	RN	98.404	14.619	2.892	.148	1.057	
223.	FR	99.999	15.031	3.000	.144	1.030	
226.	RA	99.999	15.444	3.105	.140	1.005	
227.	AC	99.999	15.871	3.219	.136	.980	
232.038	TH	99.999	16.300	3.325	.133	.956	4.138

Table III. Continued

At. Wt.	Ele.	E_K(Kev)	E_L(Kev)	E_M(Kev)	λK_{α_1} Å	λL_{α_1} Å	λM_{α_1} Å
231.	PA	99.999	16.733	3.436	.129	.933	4.022
238.030	U	99.999	17.165	3.545	.126	.911	3.910
237.	NP	99.999	17.610	3.666		.889	
244.	PU	99.999	18.054	3.778		.868	
243.	AM	99.999	18.504	3.887		.848	
247.	CM	99.999	18.930	3.971			
247.	BK	99.999	19.452	4.132			
251.	CF	99.999	19.930	4.253			
254.	ES	99.999	20.410	4.374			
253	FM	99.999	20.900	4.498			

Table IV lists values for the wavelengths corresponding to the various atomic absorption edges.

Data included in this assembly were derived from several primary sources[80-83] and secondary sources.[61,84,85] In the case of discrepancies between optical data, x-ray data and photoelectric data, the x-ray data were selected. In the absence of any experimental data, either mathematical interpolation[83] or graphical interpolation was used to obtain absorption edge wavelengths.

Having obtained a compilation of emission line and absorption edge wavelengths, it is now possible to discuss mass absorption coefficients in the various wavelength intervals delineated by absorption edges. We thus proceed to a discussion of experimental (μ/ρ) data.

Table IV. Characteristic Absorption Edge Wavelength

	ABSORPTION EDGES Å									
ELE.	K	LI	LII	LIII	MI	MII	MIII	MIV	MV	NI
H	999.	999.	999.							
HE	499.	999.	999.							
LI	226.5	999.	999.							
BE	111.	999.	999.							
B	65.6	999.	999.	999.						
C	43.68	999.	999.	999.						
N	30.99	999.	999.	999.						
O	23.32	524.	999.	999.						
F	18.09	398.	999.	999.						
NE	14.302	275.	677.	677.491	999.					
NA	11.569	247.3	398.8	405.	999.					
MG	9.512	197.3	249.3	250.700	999.					
AL	7.948	142.5	169.49	170.490	999.					
SI	6.738	105.0	123.	124.960	999.					
P	5.784	81.0	93.7	94.000	999.					
S	5.019	64.1	75.2	75.800	999.					
CL	4.397	52.1	61.8	61.990	708.462	999.				
AR	3.871	43.2	50.2	50.563	490.043	999.846	999.846			
K	3.437	36.4	41.8	42.278	365.572	696.522	696.522	999.		
CA	3.070	30.7	35.13	35.491	283.709	488.114	488.114	999.		
SC	2.762	26.8	30.6	30.826	230.447	383.842	383.842	999.		
TI	2.497	23.4	26.94	27.290	205.606	358.326	358.326	999.		
V	2.269	19.72	23.8	24.172	186.437	327.992	327.992	999.		
CR	2.070	17.84	21.24	21.581	167.315	291.720	291.720	999.		
MN	1.896	16.15	19.05	19.380	147.772	255.104	255.104	999.		

Table IV. Continued

	ABSORPTION EDGES Å									
Ele.	K	LI	LII	LIII	MI	MII	MIII	MIV	MV	NI
FE	1.743	14.65	17.202	17.525	133.456	229.594	230.000	999.		
CO	1.608	13.38	15.618	15.915	123.119	202.000	208.371	999.		
NI	1.488	12.3	14.242	14.525	110.895	182.057	188.400	999.		
CU	1.381	11.27	13.014	13.288	110.600	159.500	166.000	999.		
ZN	1.283	10.06	11.862	12.131	91.230	137.000	143.900	999.		
GA	1.196	9.517	10.828	11.100	78.419	116.087	120.487	712.534	712.534	999.
GE	1.117	8.773	9.924	10.187	68.878	96.936	102.633	431.989	431.989	999.
AS	1.045	8.107	9.125	9.367	60.924	84.686	88.243	300.924	300.924	999.
SE	.980	7.503	8.407	8.646	53.556	73.710	76.579	218.661	227.800	999.
BR	.920	6.959	7.753	7.984	48.336	65.494	68.309	176.863	179.682	399.000
KR	.866	6.47	7.168	7.392	43.07	55.672	57.989	129.500	139.461	421.000
RB	.816	6.008	6.644	6.862	38.491	50.114	51.984	110.895	112.403	388.000
SR	.770	5.592	6.173	6.387	34.680	44.310	46.072	91.838	93.149	317.000
Y	.728	5.217	5.756	5.962	31.499	39.687	41.286	77.682	78.768	275.600
ZR	.689	4.879	5.378	5.579	28.475	35.565	36.972	66.137	67.185	240.000
NB	.653	4.575	5.031	5.230	26.469	32.709	34.154	59.779	60.597	214.100
MO	.620	4.304	4.719	4.913	24.413	30.084	31.402	53.278	54.201	186.900
TC	.589	4.058	4.436	4.630	22.5	27.578	28.853	47.508	48.140	162.
RU	.561	3.835	4.180	4.369	20.945	25.461	26.511	42.660	43.039	145.500
RH	.534	3.629	3.943	4.130	19.454	23.342	24.492	38.561	39.286	136.800
PD	.509	3.437	3.723	3.907	18.109	21.603	22.699	34.941	35.494	122.600
AG	.486	3.256	3.516	3.700	16.878	20.119	21.061	30.82	31.14	110.500
CD	.464	3.085	3.326	3.505	15.874	18.603	19.614	28.13	29.50	101.000
IN	.444	2.926	3.147	3.324	14.764	17.314	18.285	26.718	27.166	91.100
SN	.425	2.777	2.982	3.156	13.867	16.050	17.200	24.28	24.90	85.800
SB	.407	2.639	2.830	3.000	13.020	15.072	16.014	22.699	23.114	76.600
TE	.309	2.510	2.688	2.856	12.275	14.186	15.080	21.124	21.528	72.000

Table IV. Continued

	ABSORPTION EDGES Å									
Ele.	K	LI	LII	LIII	MI	MII	MIII	MIV	MV	NI
I	.374	2.388	2.554	2.720	11.575	13.345	14.193	19.660	20.050	66.900
XE	.358	2.274	2.429	2.593	10.8	12.410	13.232	17.8	18.441	60.1
CS	.345	2.167	2.314	2.474	10.186	11.641	12.428	16.766	17.089	53.718
BA	.331	2.068	2.205	2.363	9.590	10.907	11.672	15.560	15.890	49.004
LA	.318	1.978	2.105	2.261	9.108	10.294	11.036	14.612	14.907	45.851
CE	.30	1.893	2.012	2.166	8.642	9.741	10.459	13.756	14.036	42.811
PR	.295	1.814	1.926	2.079	8.205	9.270	9.975	13.122	13.394	40.716
ND	.285	1.739	1.844	1.997	7.870	8.838	9.556	12.459	12.737	39.334
PM	.274	1.667	1.768	1.919	7.55	8.426	9.137	11.791	12.073	37.6
SM	.265	1.600	1.695	1.846	7.196	8.047	8.732	11.288	11.552	35.864
EU	.256	1.538	1.627	1.776	6.888	7.682	8.374	10.711	11.013	34.420
GD	.247	1.478	1.563	1.712	6.592	7.344	8.030	10.186	10.461	32.991
TB	.238	1.422	1.502	1.650	6.301	7.014	7.694	9.724	9.989	31.159
DY	.230	1.369	1.445	1.592	6.057	6.732	7.399	9.304	9.574	29.782
HO	.223	1.319	1.391	1.537	5.825	6.448	7.120	8.910	9.174	28.456
FR	.216	1.271	1.339	1.484	5.619	6.181	6.843	8.601	8.847	27.606
TM	.209	1.225	1.289	1.433	5.374	5.933	6.579	8.186	8.487	26.284
YB	.202	1.182	1.243	1.386	5.170	5.706	6.359	7.865	8.115	25.448
LU	.196	1.140	1.199	1.341	4.977	5.477	6.127	7.562	7.805	24.492
HF	.190	1.100	1.155	1.297	4.767	5.241	5.882	7.223	7.461	23.040
TA	.184	1.061	1.114	1.255	4.585	5.020	5.650	6.870	7.110	21.924
W	.178	1.025	1.075	1.216	4.407	4.815	5.435	6.590	6.830	20.837
RE	.173	.989	1.037	1.177	4.236	4.620	5.234	6.330	6.560	19.837
OS	.168	.956	1.001	1.141	4.071	4.433	5.043	6.073	6.300	18.949
IR	.163	.924	.967	1.106	3.915	4.260	4.861	5.830	6.050	17.966
PT	.158	.893	.934	1.072	3.762	4.093	4.686	5.590	5.810	17.172
AU	.154	.864	.903	1.040	3.616	3.936	4.518	5.374	5.584	16.339
HG	.149	.835	.872	1.009	3.478	3.783	4.355	5.157	5.360	15.492
TL	.145	.808	.843	.979	3.346	3.634	4.198	4.952	5.153	14.664
PB	.141	.782	.815	.951	3.217	3.492	4.047	4.757	4.955	13.874

Table IV. Continued

	ABSORPTION EDGES Å									
Ele.	K	LI	LII	LIII	MI	MII	MIII	MIV	MV	NI
BI	.137	.757	.789	.923	3.094	3.359	3.904	4.572	4.764	13.215
PO	.133	.732	.763	.898	2.988	3.217	3.755	4.431	4.621	12.457
AT	.129	.709	.739	.872	2.872	3.093	3.619	4.262	4.449	11.898
RN	.126	.687	.715	.848	2.766	2.981	3.504	4.103	4.286	11.301
FR	.123	.665	.692	.825	2.665	2.865	3.385	3.952	4.133	10.753
RA	.119	.645	.671	.803	2.571	2.762	3.270	3.817	3.993	10.260
AC	.116	.625	.650	.781	2.479	2.663	3.172	3.679	3.852	9.770
TH	.115	.606	.630	.761	2.392	2.567	3.068	3.557	3.729	9.325
PA	.110	.587	.610	.741	2.310	2.479	2.970	3.433	3.602	8.938
U	.107	.570	.592	.722	2.235	2.392	2.884	3.333	3.497	8.605
NP	.104	.553	.574	.704	2.166	2.310	2.796	3.220	3.382	8.262
PU	.102	.537	.557	.687	2.090	2.237	2.721	3.121	3.282	7.955
AM	.099	.521	.540	.670	2.026	2.171	2.656	3.030	3.190	7.667
CM	.097	.507	.521	.655	1.972	2.103	2.584	2.933	3.122	7.546
BK	.091			.637	1.891	2.017	2.491	2.840	3.000	7.064
CF	.091	.475	.491	.622	1.836	1.950	2.427	2.757	2.915	6.892
ES	.089	.461	.476	.607	1.777	1.886	2.361	2.678	2.834	6.637
FM	.087	.448	.462	.593	1.721	1.825	2.297	2.601	2.756	6.401

A. 3. Mathematical Fitting of Experimental Mass Absorption Data.

Experimental mass absorption coefficient results obtained for more than 70 elements in various wavelength intervals by several authors[8,32,52,53,58,64-79,86-99] were obtained from the literature. These data were plotted versus wavelength on a log-log scale. The experimental points for several elements are given in Figures 11 to 13 and Figures 14 to 18.

We now assume that for any element, between two absorption edges, the mass absorption coefficient can be represented as a function of wavelength by:

$$(\mu/\rho)_Z = C_Z \lambda^{n_Z} \qquad (39)$$

The experimental data were fitted by the method of least squares to Equation (39). The exponent for each element in each wavelength interval was determined first. The data of each investigator were not treated separately. Rather, all data were taken together. The coefficients were evaluated using the determined value of the exponent. The curves resulting from this mathematical fitting of experimental data are represented by the solid lines in Figures 10 to 18. These curves are typical in their closeness of fit.

Before proceeding, we must make several observations. The first point to be mentioned is that we have no a priori reason to expect that the experimental data will fit exactly

Figure 14. Mass absorption coefficient of carbon.

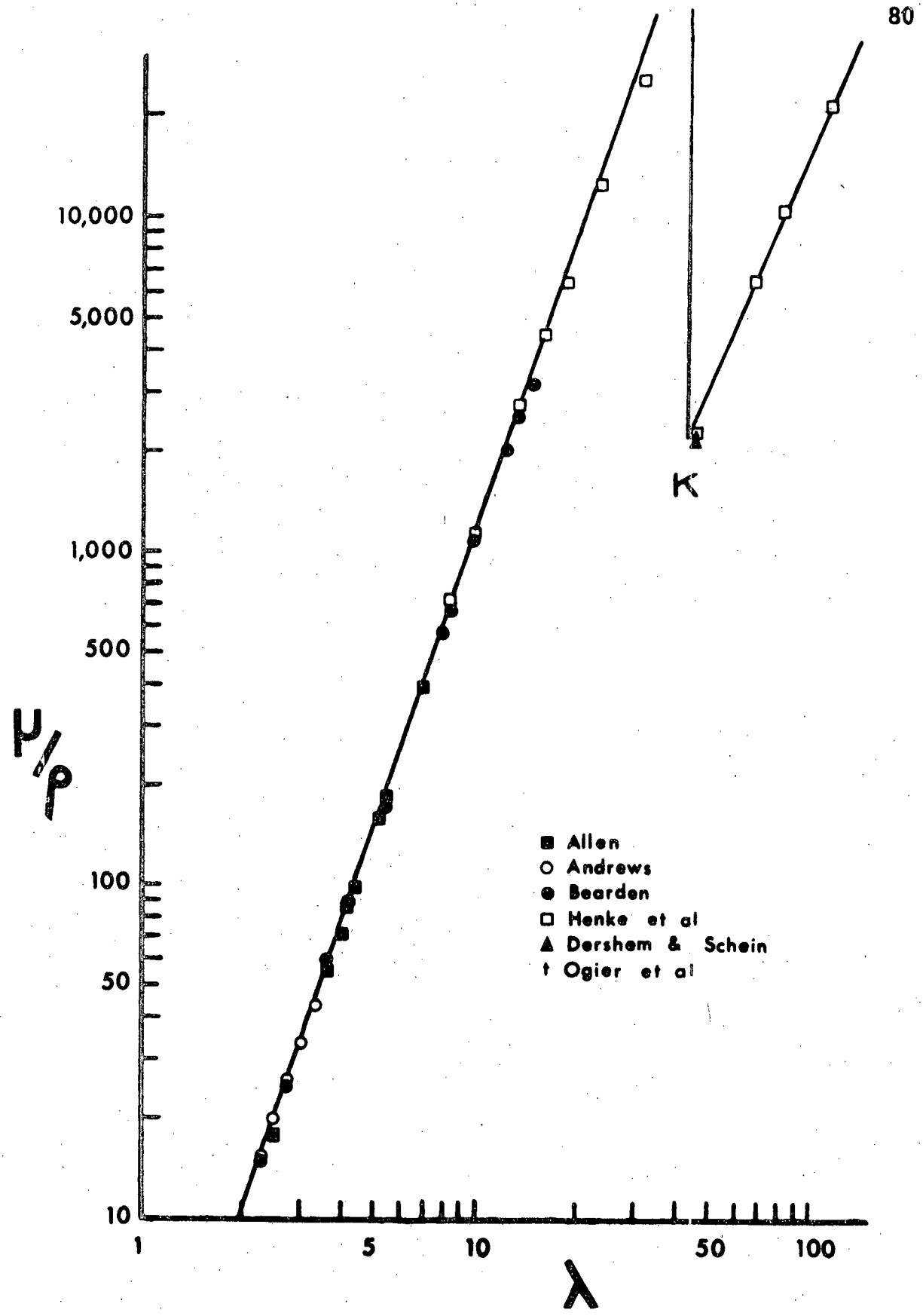
10,000
5,000
1,000
500
100
50
10
μ/ρ
1
5
10
50
100
λ
K
Allen
Andrews
Bearden
Henke et al
Dershem & Schein
Ogier et al

Figure 15. Mass absorption coefficient of nitrogen.

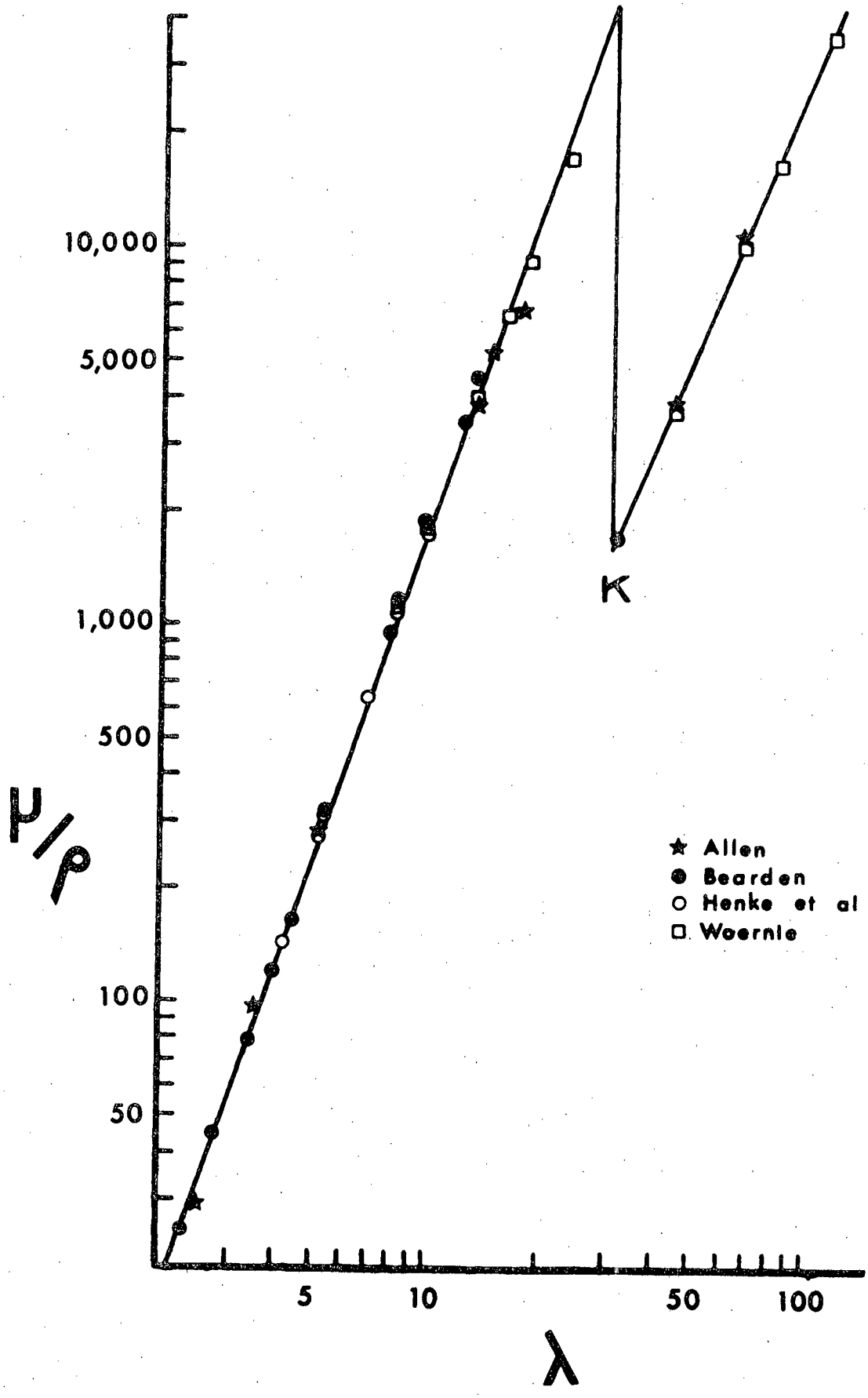
10,000
5,000
1,000
500
100
50
μ/ρ
K
5
10
50
100
λ
Allen
Bearden
Henke et al
Woernle

Figure 16. Mass absorption coefficient of oxygen.

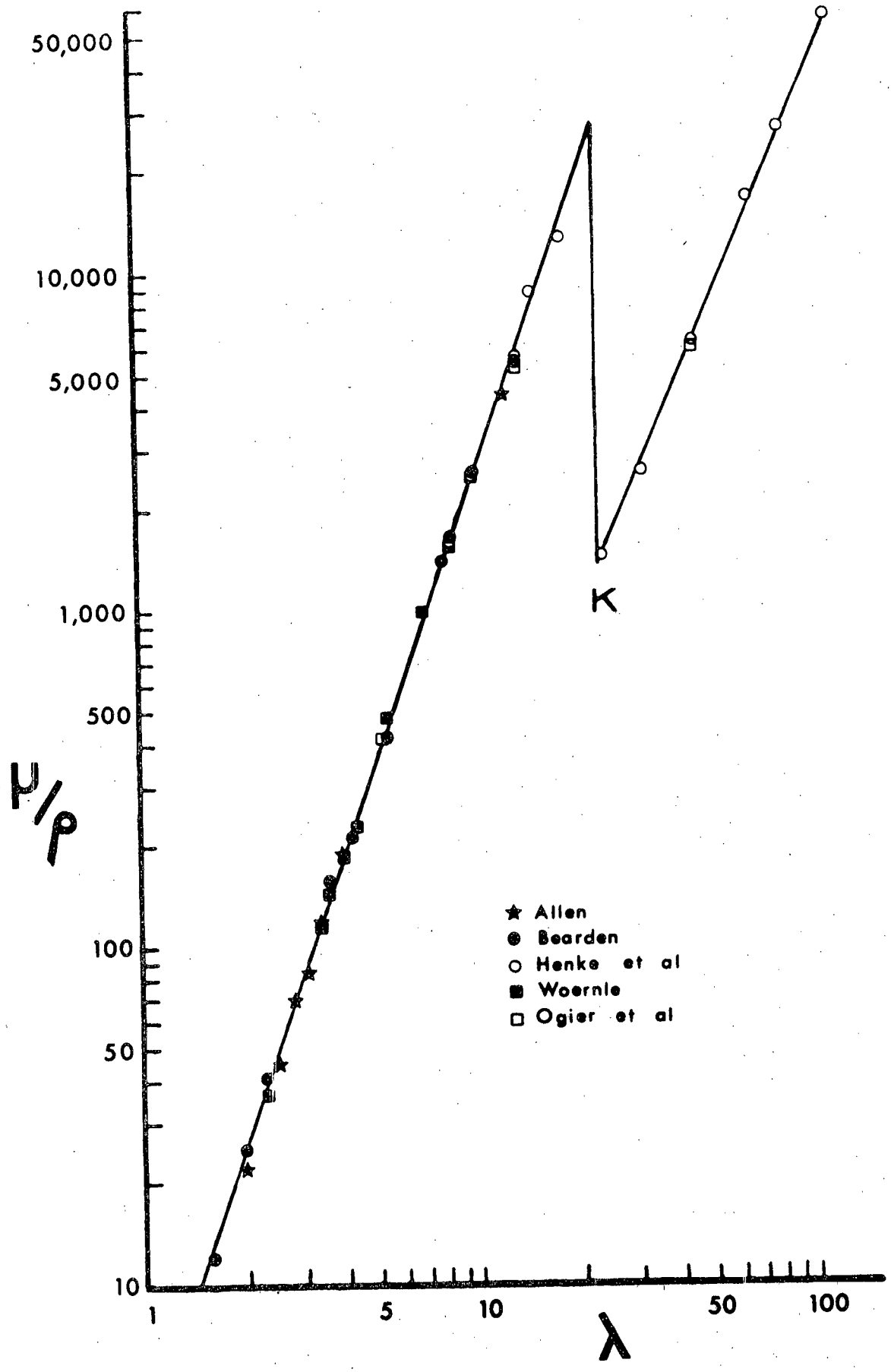
50,000
10,000
5,000
1,000
500
100
50
10
μ/ρ
K
1
5
10
50
100
λ
Allen
Bearden
Henke et al
Woernle
Ogier et al

Figure 17. Mass absorption coefficient of vanadium.

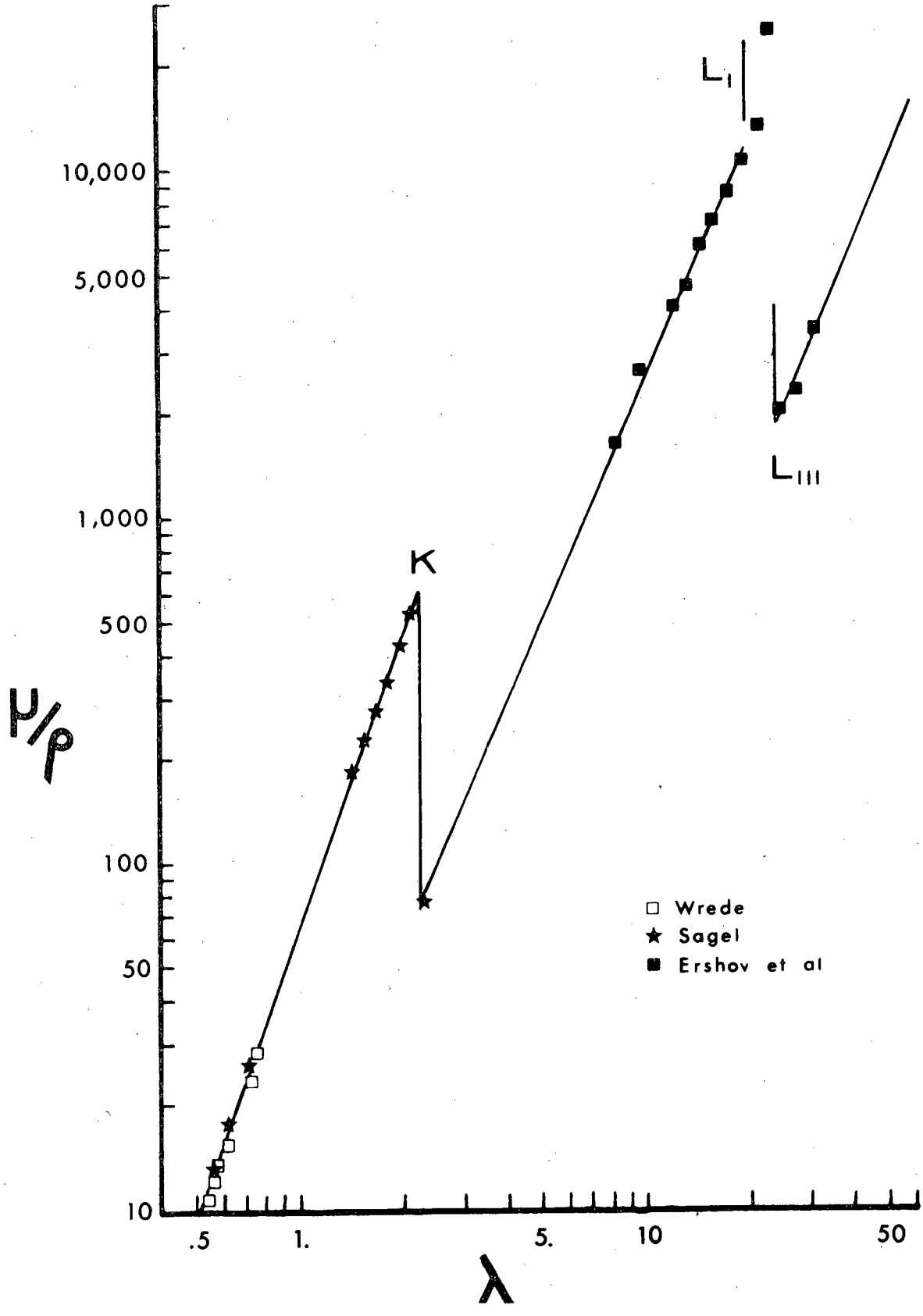
10,000
5,000
1,000
500
100
50
10
μ/ρ
K
L_I
L_III
.5
1.
5.
10
50
λ
Wrede
Sagel
Ershov et al

Figure 18. Mass absorption coefficient of niobium.

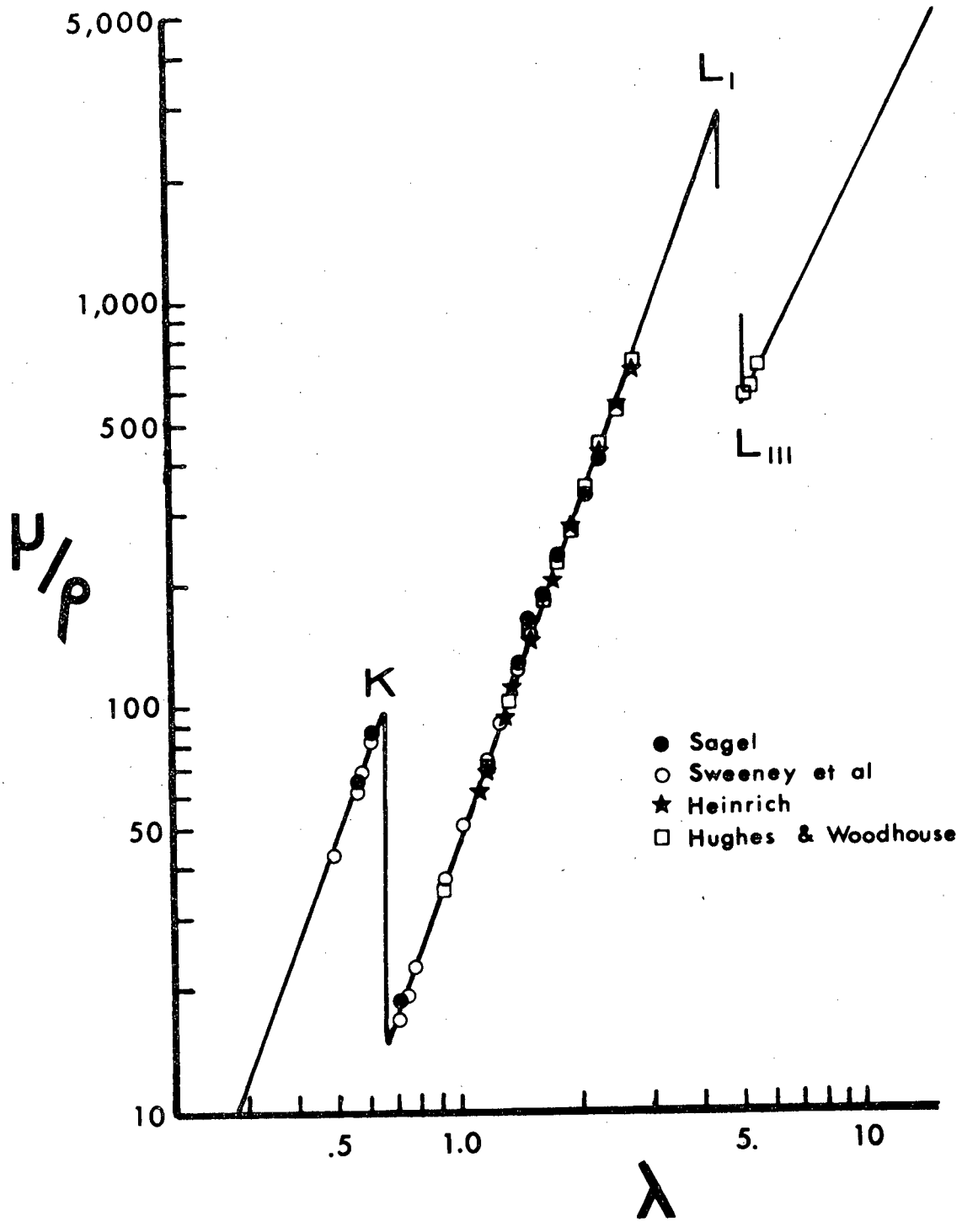
5,000
1,000
500
100
50
10
μ/ρ
K
L_I
L_III
.5
1.0
5.
10
λ
Sagel
Sweeney et al
Heinrich
Hughes & Woodhouse

to Equation (39). Rather, Equation (39) is simply a semi-empirical relation that reasonably approximates the change in photoattenuation with wavelength between absorption edges. However, we can make certain observations about the relation between the data and the fitted curves, and about the relation between various curves.

Let us consider the data for zirconium and titanium, Figures 11 and 12. The most obvious deviation from linearity between log (μ/ρ) and log λ is found near the L I-edge of titanium. Lesser deviations from linearity are seen at the K-edges of both elements. In each case, the data near the absorption edge suffer a depression from the mathematical fit. The data below the K-edges exhibit a steeper slope than the data between the K-edges and the L I-edges. The latter data show a steeper slope than that of the data above the L III-edges. Between the same absorption edges, the data for titanium exhibit a lower slope than that for zirconium. However, the data for titanium below the K-edge show approximately the same slope as the data for zirconium between the K and L I-edges. A similar relation is observed between the data for titanium between the K and L I-edges and the data for zirconium above the L III-edge.

The fitted values of the coefficient, C, and the exponent, n, are plotted, for wavelengths below the K-edge, between the K- and L I-edges and between the L III- and M I-edges, in Figures 19 to 24.

Figure 19. Calculated values of coefficient, C, for function $(\mu/\rho) = C\ \lambda^n$ for $\lambda <$ K edge.

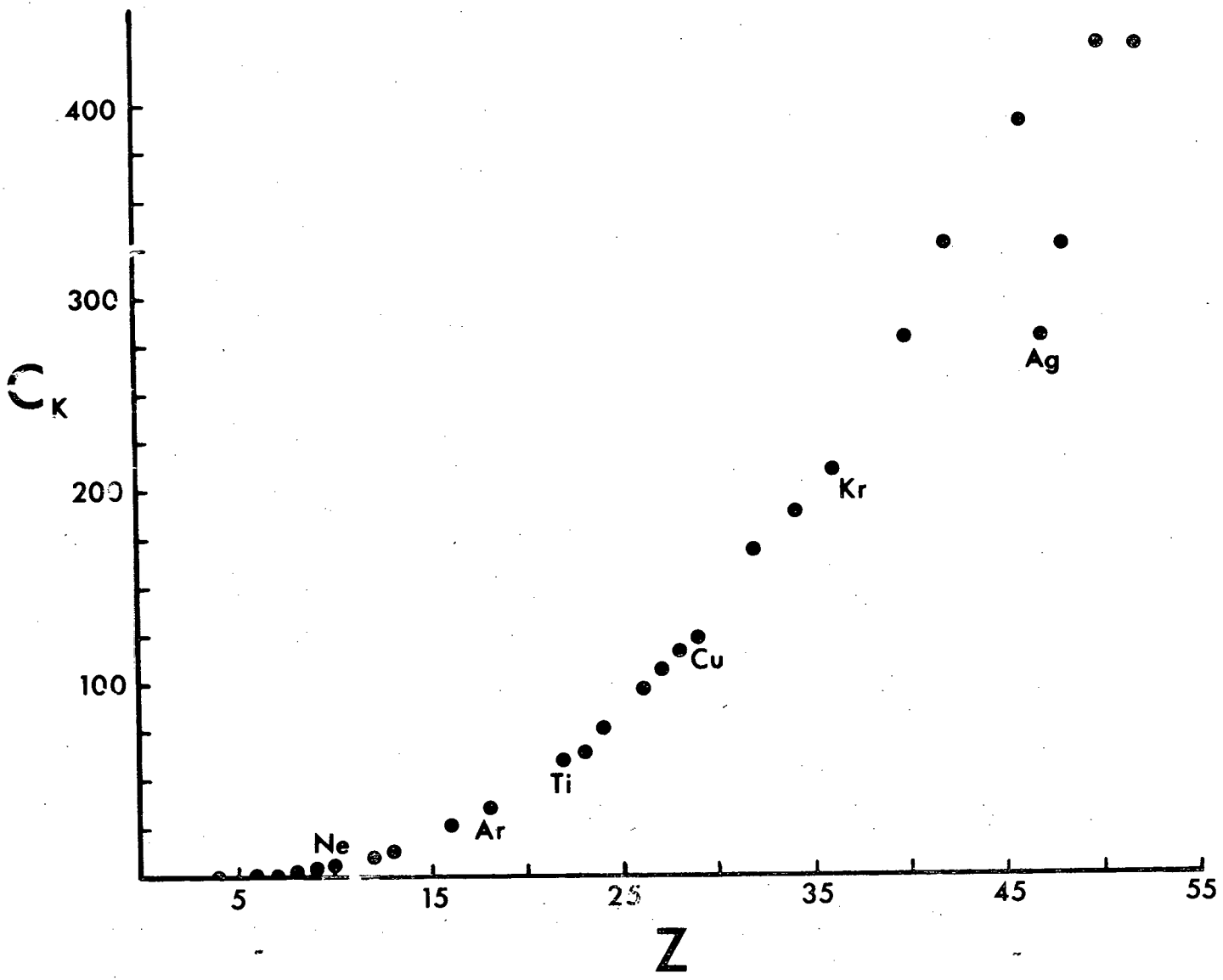
400
300
200
100
C_K
Ne
Ar
Ti
Cu
Kr
Ag
5
15
25
35
45
55
Z

Figure 20. Calculated values of exponent, n, for function $(\mu/\rho) = C\ \lambda^n$ for $\lambda <$ K edge.

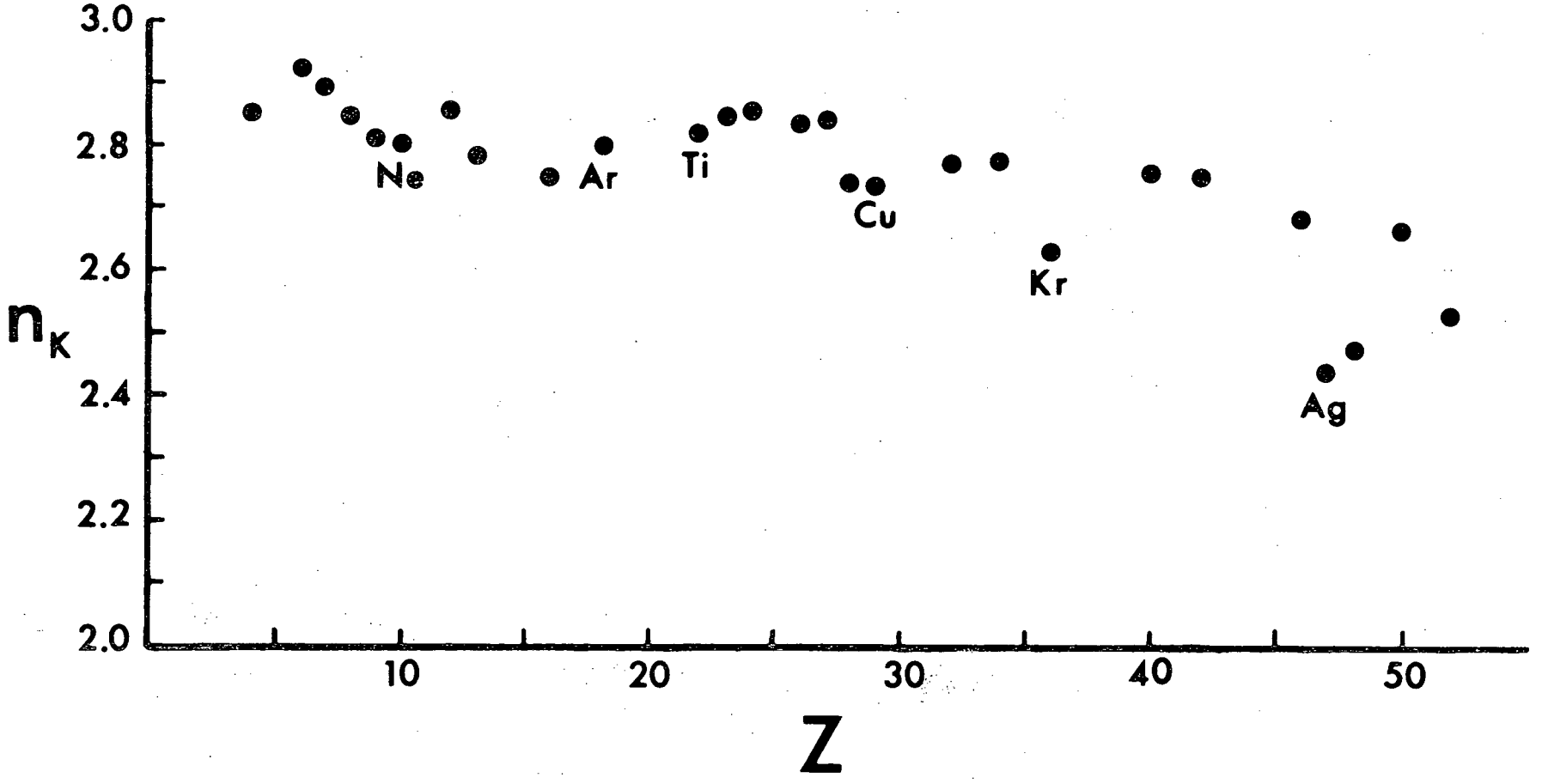
3.0
2.8
2.6
2.4
2.2
2.0
n_K
Ne
Ar
Ti
Cu
Kr
Ag
10
20
30
40
50
Z

Figure 21. Calculated values of coefficient, C, for function $(\mu/\rho) = C\ \lambda^n$ for λ between K and L I edges.

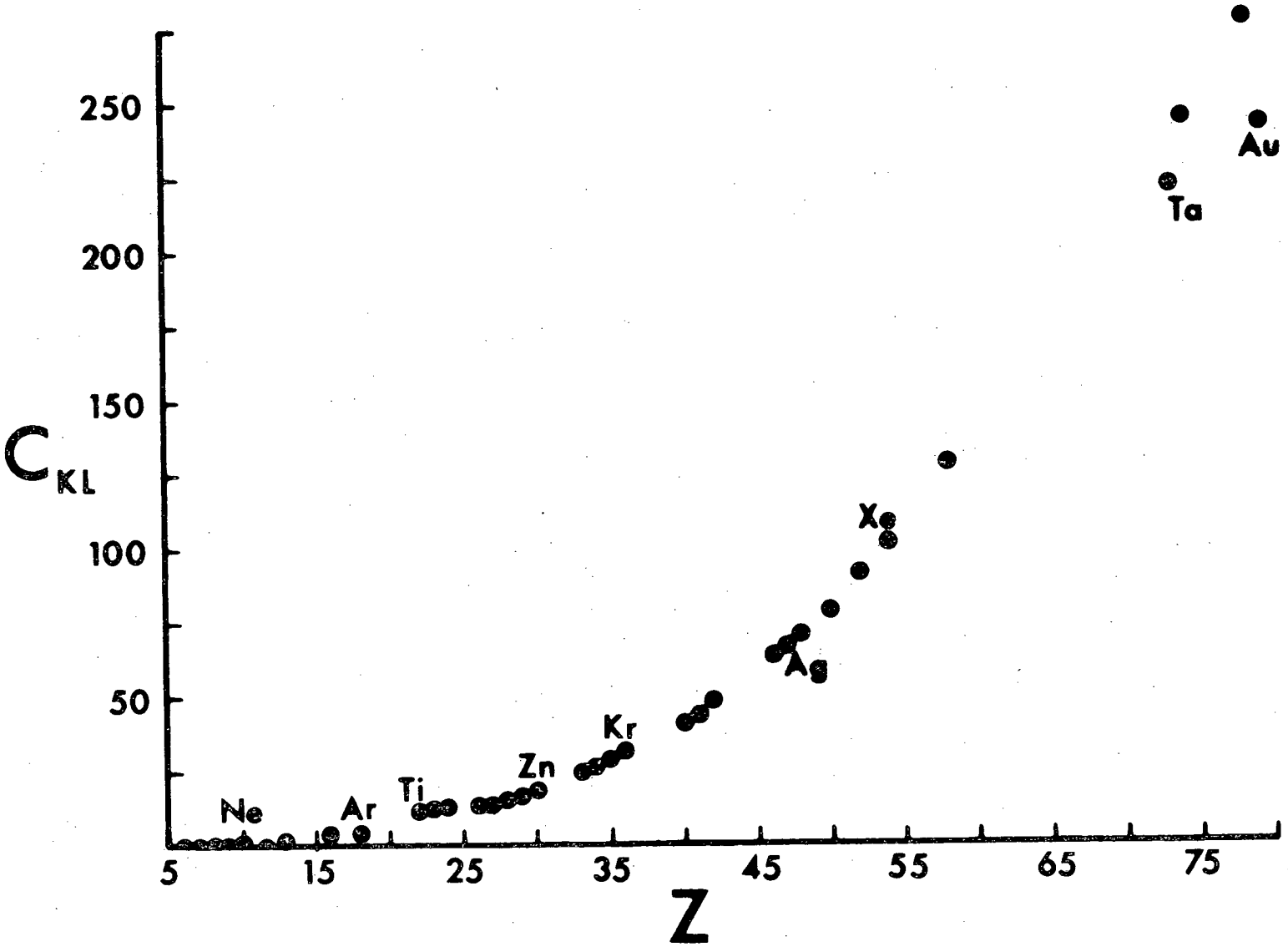
250
200
150
100
50
C_{KL}
Ne
Ar
Ti
Zn
Kr
Xe
Ag
Ta
Au
5
15
25
35
45
55
65
75
Z

Figure 22. Calculated values of exponent, n, for function $(\mu/\rho) = C\ \lambda^n$ for λ between K and L I edges.

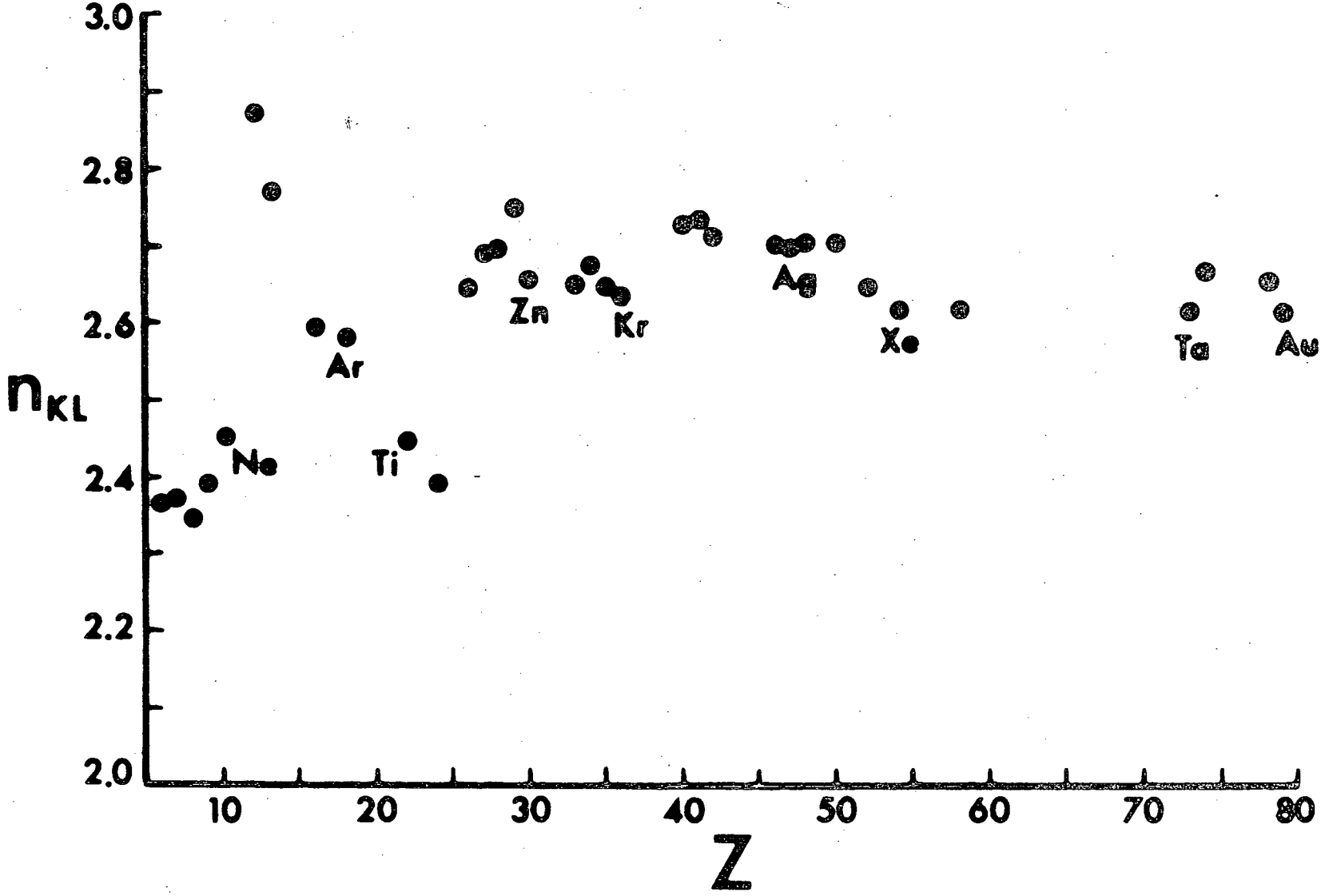
3.0
2.8
2.6
2.4
2.2
2.0
n_{KL}
Ne
Ar
Ti
Zn
Kr
Ag
Xe
Ta
Au
10
20
30
40
50
60
70
80
Z

Figure 23. Calculated values of coefficient C, for function $(\mu/\rho) = C\ \lambda^n$ for λ between L III and M I edges.

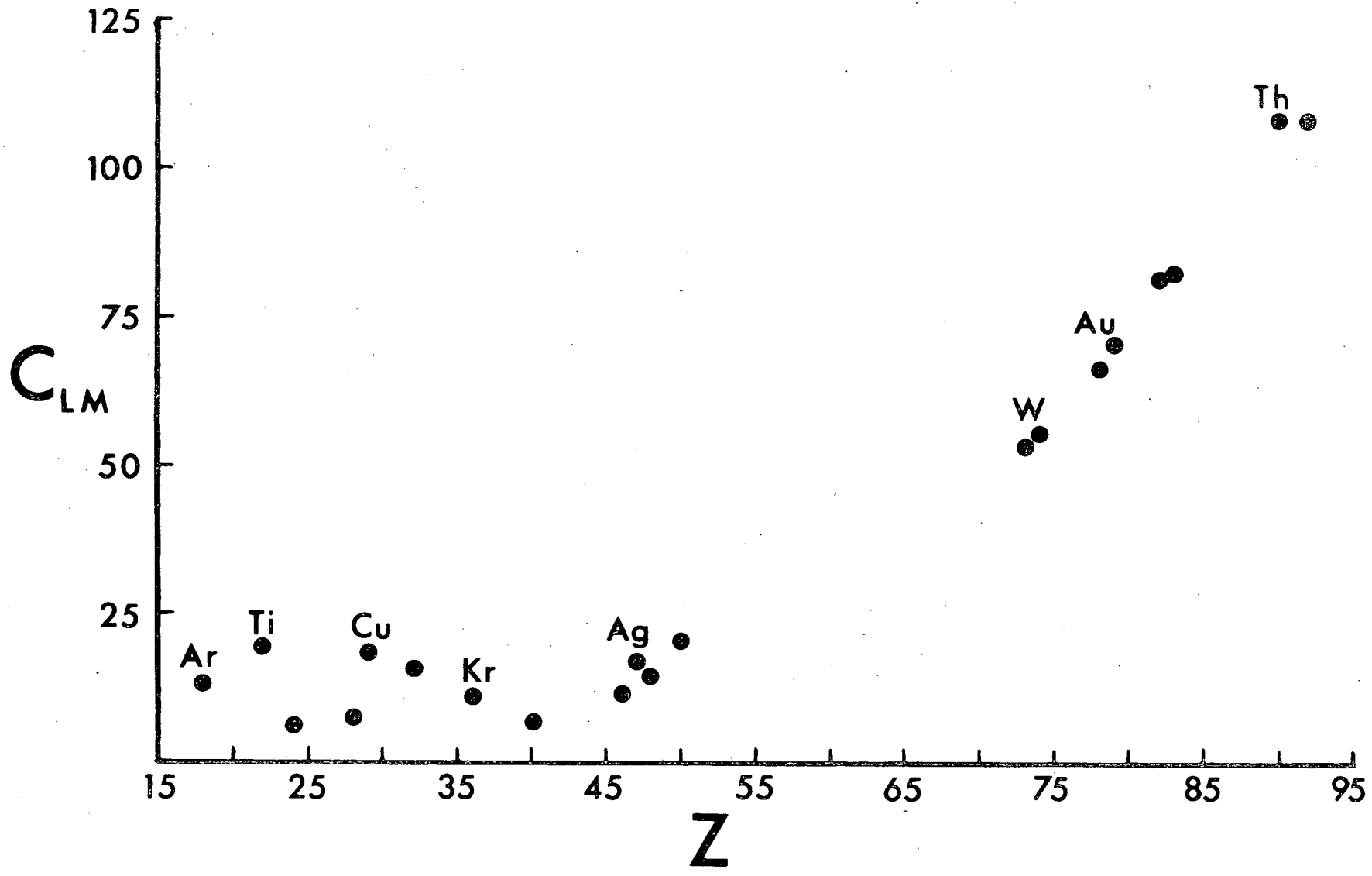
125
100
75
50
25
C_{LM}
Th
Au
W
Ar
Ti
Cu
Kr
Ag
15
25
35
45
55
65
75
85
95
Z

Figure 24. Calculated values of exponent, n, for function $(\mu/\rho) = C\ \lambda^n$ for λ between L III and M I edges.

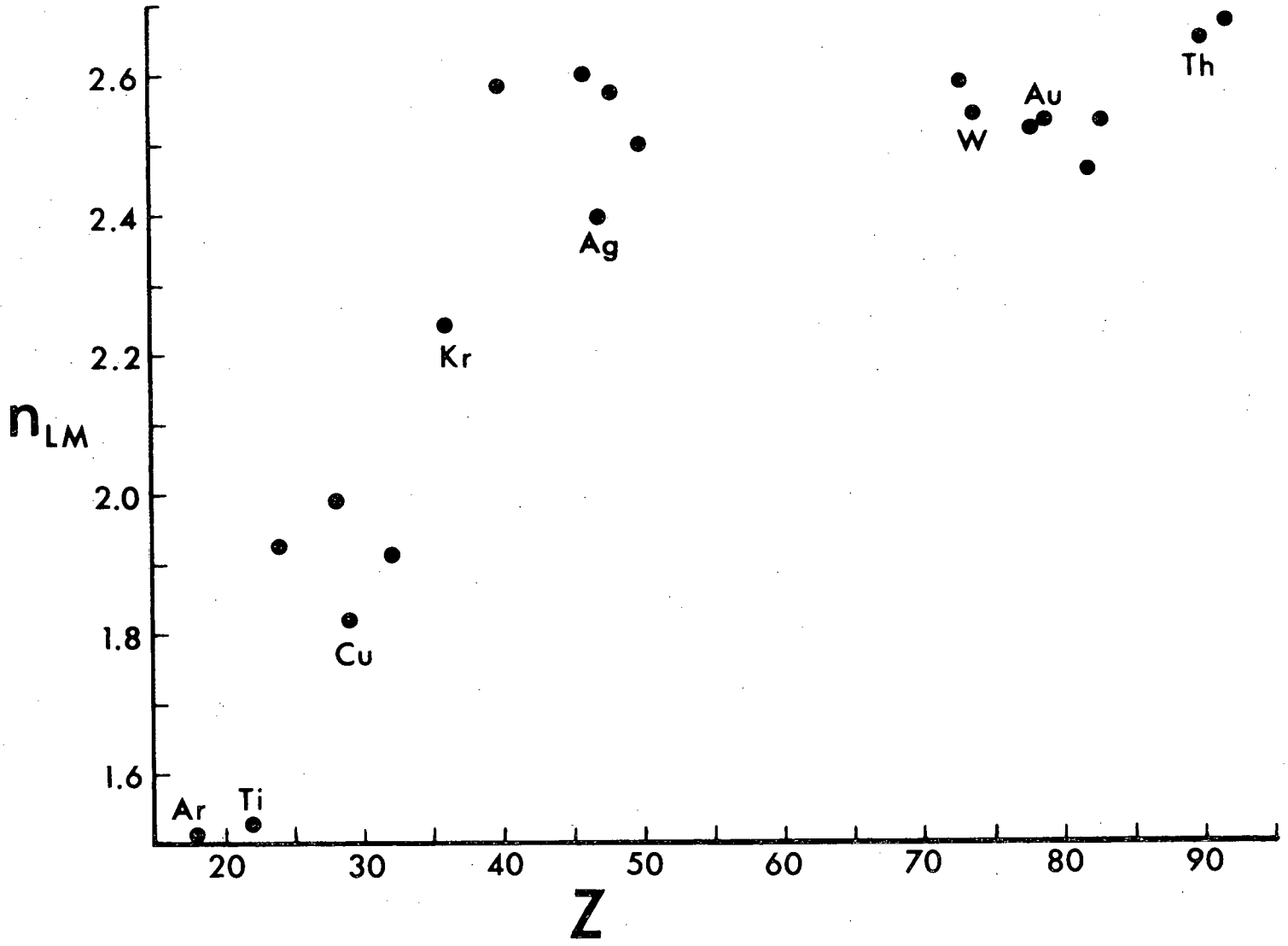
2.6
2.4
2.2
2.0
1.8
1.6
n_{LM}
Ar
Ti
Cu
Kr
Ag
W
Au
Th
20
30
40
50
60
70
80
90
Z

The surprising feature of these plots is the relative smoothness of the dependence of the coefficients, C, on atomic number. No such smooth variation is seen in the distribution of the exponents, n. It will be noticed, however, that if attention is directed to the variation of the exponent with atomic number, relatively sharp minima in n occur at the noble gases and at the noble metals. We conclude that the filling of atomic electronic shells and sub-shells has a distinct effect on the change of photoionization with energy. In particular, we suggest, at this point, that the filled outer electronic shells and sub-shells act as a type of barrier which must be overcome by an inner electron being ejected from an atom by a photoionization event.

In view of the above discussion, we will show in succeeding sections that there is some theoretical justification for concluding that a non-smooth variation in the exponent of Equation (39) with atomic number is physically meaningful. Further, it will be shown that based on atomic potential calculations, a physically sound foundation can be established for an interpolation of mass absorption coefficients. The conclusion to be reached is that while the fitting function assumed is not the best over the entire wavelength range from 1 to 80 Å, it is nevertheless possible to explain the variations in the atomic number dependence of the exponent and coefficient. The result will be that the large differ-

ences between experimental mass absorption coefficients and interpolated or mathematically estimated values can generally be eliminated.

A. 4. Discussion of Photoeffect Cross Section Calculations

At usual x-ray wavelengths, 0.5 - 5 Å, almost all atomic species exhibit the familiar hydrogen-like behavior of mass absorption coefficient or photoionization cross section. (While it is reasonable to consider Compton scattering and pair production as photo-attenuation processes at higher energies than considered here, we assume here that photo-attenuation and photoionization are equivalent processes.) This usual behavior is characterized by sharp increases in photo-attenuation at absorption edges, followed by a smooth decrease with increasing energy. Recent experiments[71,73-79] have suggested that at wavelengths longer than 5 Å, involving photoionization of intermediate and outer electron shells, this behavior is by no means universal. In particular, these experiments indicate that maxima in the photoionization occur as much as 30 ev higher than the supposed absorption edge.

Theoretical calculations of atomic photoeffect cross sections have been based on a variety of models. The mentioned work of Bearden[58] and Henke et al.[32] result in photoeffect cross sections based on modified Coulomb or hydrogen-like wave functions. These results are close to experimental values of (μ/ρ) for light elements where the K shell is primarily involved in the photoionization. Likewise, reasonable

values are calculated for elements in which the L shell plays the most prominent part with only a small effect from K shell screening of the nucleus. Bearden presents theoretical and experimental values for nine elements, dealing with the wavelength interval 0.3 - 14.5 Å. Henke et al. present theoretical values from 2.0 - 200 Å and experimental values from 8.34 - 113 Å. Both authors refrain from giving theoretical values near absorption edges. Schmickley and Pratt[100] report numerical results from computations designed to study the effects of some inner electron screening. They deal with photon energies between 10 kev and 3 Mev, generally much higher than of interest here.

Cooper[101,102] and Manson and Cooper[103] report calculations of photoionization cross sections, dealing primarily with energies in the vicinity of absorption edges up to approximately 100 ev above an edge. These authors obtain their results using a one-electron model with a modified central potential.[104] The results presented are significantly different from the gross spectral shape of photoionization cross sections predicted by the hydrogenlike model. Particularly, these calculations do indicate accurately the general spectral distribution of photoattenuation near thresholds, that is, near absorption edges corresponding to electron levels located some distance from the nucleus.

Rau and Fano[105] have recently considered the variation with atomic number of the potential assumed by Cooper[102] and Manson and Cooper.[103] Rau and Fano consider the mean potential energy of a test electron as a function of its distance from the nucleus within an atom of atomic number Z. The potential energy as calculated by those authors exhibits large variations, of the order of 20%. These variations are attributed to changes in inner and outer electron screening, which may be related to the average number of electrons inside and outside a sphere of radius r. The variations of potential energy should have an increased effect on atomic properties when the influence of electronic centrifugal potential energy is also considered. The combined effect of the electrostatic and centrifugal potentials results in the occurrence of a potential barrier separating two potential wells, for various combinations of Z and ℓ, the orbital angular momentum quantum number. The maximum barrier heights occur for copper, silver or palladium and gold with lesser heights at the noble gases.

The existence of the potential barrier and extremum values of that barrier should exhibit themselves as extremum values of the exponent in Equation (39). Maxima in the barrier would cause a greatest depression in the rate of change of an atomic photoionization cross section with wavelength between two thresholds, when compared to nearby atomic

species. Likewise, the barrier would exhibit itself through the shifting of the maximum of the mass absorption coefficient from the threshold to some wavelength shorter than the threshold (absorption edge).

Indeed, as can be seen in Figures 20, 22, and 24, a minima of the exponent does occur in various wavelength intervals at the noble metals, with other minima at the noble gases. We attribute these depressions in the rate of change of the mass absorption coefficient with wavelength to the outer screening generated by the filling of outer electron sub-shells.

We do not say that variations in the exponent with atomic number are significant in every detail. Such a statement would imply a greater confidence in published mass absorption coefficient data than is had by this writer. Rather, our contention is that an attempt to fit some smooth analytical form to the atomic number dependence of the coefficients and exponents in Equation (39) ignores certain periodicities in these data.

A. 5. Numerical Estimates of Mass Absorption Coefficients

Since our goal is to obtain a reasonable estimation of mass absorption coefficients for use in microprobe analysis, we direct ourselves to that task. Based on the preceeding discussion, and on the general applicability of Equation (39) as expressing the wavelength dependence of the mass absorption coefficient on wavelength in the interval 1 to 80 Å, an interpolation between fitted exponents and coefficients was performed. The large number of fitted points, as shown in Figures 19 to 24, permitted graphical interpolation without too much difficulty. The results of that interpolation are given in tabular form in Table V. This tabulation permits the use of Equation (39) in the simple calculation leading to an estimation of mass absorption coefficients.

Serious consideration of the experimental difficulties encountered in the measurements of mass absorption coefficients has led the present author to question the introduction of the term accuracy at any point in the discussion of experimental values of (μ/ρ). The discussion should perhaps be limited to consideration of precision and absence of systematic errors.

If, however, we assume that experimental values are "true" values with a precision of such and such percent, then the limits on the accuracy of the present fitted and calculated values of (μ/ρ) can be estimated.

Table V. Values of C and n for $(\mu/\rho) = C\,\lambda^{n}$ for Various Wavelength Intervals

Z	n_K	n_{KL}	n_{LM}	n_{MN}	n_N	C_K	C_{KL}	C_{LM}	C_{MN}	C_N
1	2.335					000.144				
2	2.786					.084				
3	2.65					.250				
4	2.852					.404				
5	2.661					.889				
6	2.921	2.365				1.350	.295			
7	2.889	2.370				2.311	.471			
8	2.850	2.346				3.529	.818			
9	2.813	2.390				4.943	.904			
10	2.803	2.452				7.322	1.098			
11	2.784	2.59				9.322	.80			
12	2.851	2.870				11.601	.700			
13	2.780	2.770	1.309			14.87	1.110	7.338		
14	2.780	2.68	1.34			18.122	1.88	8.5		
15	2.773	2.61	1.38			22.020	2.6	10.0		
16	2.748	2.592	1.42			27.626	3.330	11.2		
17	2.847	2.652	1.46			27.864	3.548	12.5		
18	2.796	2.581	1.520			35.312	4.567	13.715		
19	2.802	2.54	1.522			42.038	5.8	15.		
20	2.810	2.52	1.524			48.678	7.3	16.8		
21	2.795	2.495	1.526			54.052	8.8	18.1		
22	2.821	2.478	1.529			60.083	10.927	19.593		
23	2.847	2.308	2.453			64.977	12.056	.742		
24	2.847	2.389	1.926			77.899	12.661	6.095		
25	2.864	2.660	1.94			83.305	10.979	6.4		
26	2.836	2.644	1.965			97.144	12.734	6.8		
27	2.841	2.688	1.98			108.210	14.322	7.2		
28	2.734	2.693	1.991			117.098	15.520	7.839		
29	2.734	2.749	1.820			123.080	15.783	18.830		
30	2.771	2.656	1.85			146.550	19.124	18.2		

Table V. Continued

Z	n_K	n_{KL}	n_{LM}	n_{MN}	n_N	C_K	C_{KL}	C_{LM}	C_{MN}	C_N
31	2.560	2.636	1.88			142.035	20.238	17.0		
32	2.769	2.471	1.915			169.094	24.425	16.246		
33	2.589	2.650	1.97			156.083	24.434	14.6		
34	2.782	2.672	2.05			188.918	26.852	13.5		
35	2.771	2.647	2.14			207.363	29.204	12.0		
36	2.626	2.633	2.242			209.178	32.008	10.150		
37	2.593	2.606	2.34			217.375	35.425	9.2		
38	2.668	2.791	2.44			238.313	34.296	8.6		
39	2.578	2.594	2.53			261.398	42.122	7.8		
40	2.752	2.728	2.583	.40		277.847	41.921	7.356	6.	
41	2.661	2.734	1.923	.48		291.277	44.976	22.304	8.	
42	2.751	2.712	1.99	.70		325.568	49.133	20.0	14.	
43	2.70	2.675	2.19	1.2		332.	53.	18.4	18.	
44	2.613	2.657	2.46	1.46		338.246	57.048	15.0	28.	
45	2.426	2.682	2.55	1.56		266.121	60.395	13.0	66.	
46	2.674	2.701	2.604	1.59		380.209	62.906	11.593	155.	
47	2.427	2.700	2.393	.385		278.270	66.473	18.157	1478.19	
48	2.469	2.703	2.574	1.60		325.561	70.806	14.947	108.	
49	2.396	2.701	2.55	1.60		291.804	75.185	16.8	44.	
50	2.656	2.702	2.500	1.593		429.243	79.510	20.595	34.465	
51	2.475	2.618	2.37	1.48		360.505	87.573	30.1	51.8	
52	2.526	2.644	2.16	1.26		428.535	90.994	57.0	86.	
53	2.453	2.648	1.94	.92		391.501	94.983	74.0	156.	
54	2.44	2.616	1.880	.757		393.	102.108	83.443	403.675	
55	2.435	2.609	1.92	.83		396.	107.580	76.	340.	
56	2.415	2.657	1.96	.90		400.642	108.976	64.	259.	
57	2.375	2.606	2.04	1.24		406.	117.488	52.	210.	
58	2.326	2.615	2.13	1.44		415.658	128.292	42.	155.	
59		2.617	2.28	1.72			133.322	36.	120.	
60		2.611	2.43	1.95			138.475	31.8	81.	

Table V. Continued

Z	n_K	n_{KL}	n_{LM}	n_{MN}	n_N	c_K	c_{KL}	c_{LM}	c_{MN}	c_N
61		2.61	2.58	2.12			143.5	30.8	57.	
62		2.623	2.722	2.26			150.262	30.254	34.	
63		2.674	2.746	2.36			164.053	31.414	19.5	
64		2.711	2.755	2.4			171.439	32.195	9.0	
65		2.740	2.685	2.39			182.478	35.891	5.0	
66		2.755	2.664	2.38			191.747	37.859	4.0	
67		2.760	2.632	2.37			203.031	40.695	6.0	
68		2.768	2.601	2.36			210.729	42.976	8.8	
69		2.769	2.600	2.35			222.047	45.248	9.9	
70		2.763	2.568	2.34			227.861	47.589	11.8	
71		2.764	2.558	2.32			239.732	50.412	14.5	
72		2.744	2.533	2.31	.018		247.226	53.018	16.2	19900.
73	2.517	2.613	2.589	2.30	.018	785.744	221.796	53.096	18.4	19011.799
74	2.043	2.668	2.541	2.28	.018	344.007	244.065	55.507	21.0	18100.
75		2.725	2.51	2.25	.017		271.	60.5	23.0	17300.
76		2.762	2.492	2.22	.017		290.700	63.573	25.5	16500.
77		2.703	2.468	2.17	.016		291.982	67.423	27.6	15700.
78		2.653	2.520	2.06	.016		277.059	66.215	27.8	14935.4
79		2.511	2.528	2.068	.043		241.237	70.331	27.626	10444.5
80		2.595	2.474	2.12	.058		290.	75.655	24.6	9100.
81		2.699	2.333	2.19	.073		342.330	85.413	21.0	7800.
82		2.601	2.456	2.280	.088		311.716	81.287	20.128	6500.
83	2.228	2.587	2.527	2.313	.106	631.182	325.828	82.053	20.591	5216.8
84		2.60	2.36	2.24			348.	82.	23.0	
85		2.62	2.18	2.09			371.	96.	27.5	

Table V. Continued

Z	n_K	n_{KL}	n_{LM}	n_{MN}	n_N	C_K	C_{KL}	C_{LM}	C_{MN}	C_N
86		2.653	2.147	1.92			394.339	112.607	36.0	
87		2.685	2.15	1.82			420.	117.	47.0	
88		2.727	2.154	1.76			440.969	121.092	57.0	
89		2.715	2.28	1.73			441.	114.	62.0	
90		2.689	2.647	1.74			441.914	108.024	58.0	
91			2.66	1.81				108.	51.0	
92		3.147	2.676	1.888			649.224	108.019	46.169	
93			2.74	1.95				122.	47.0	
94			2.819	2.03				144.388	48.	
95			2.82	2.08				155.	51.	
96			2.83	2.13				164.	56.	
97			2.84	2.17				166.	63.	
98			2.85	2.22				169.5	67.	
99			2.86	2.25				173.	74.	
100			2.87	2.27				175.	80	

Consideration of the precision of the experiments that provided the data for the present computations indicates that conservative estimates of the accuracy of the calculated values of the mass absorption coefficients limit that accuracy, at the extremes of error, to 5% below ten Angstroms and 15% above that wavelength.

As can be seen from Figures 11 to 18, the difference between experimental values of the mass absorption coefficient at any given wavelength below ten Angstroms and the fitted curve generally is less than 2%. The large error limits are, however, approached in some cases near absorption edges, particularly where one would expect the effect of outer electron screening to be the greatest. The error limits for wavelengths greater than ten Angstroms simply reflects the precision of experiments in this wavelength range. Generally, the calculated values as given by the solid curves in Figures 11 to 18 differ from the experimental values by less than 5%.

In consideration of the fact that some investigators would prefer numerical values of the mass absorption coefficients, Table VI lists a set of mass absorption coefficients for the emission lines of carbon, nitrogen, and oxygen.

Table VI. Mass Absorption Coefficients for Carbon, Nitrogen and Oxygen Kα Emission Lines

Absorber	44.6 Å	31.68 Å	23.57 Å
C	2280	25400	12200
N	3820	1730	17200
O	6000	2550	12620
F	8700	3700	1700
Ne	13600	5600	2600
Al	33000	15900	(7800)
S	47500	25400	13000
Ar	45000	29000	15900
Ti	6300	3900	(10000)
V	8400	3500	(25000)
Cr	11500	6000	2300
Ni	-	6900	4500
Ge	23100	(13000)	(8000)
Kr	31400	21500	12300
Ag	6340	5680	18800
Xe	7130	6200	4250
Ta	20440	20400	19600
Pt	15920	15800	-
Au	13000	12730	9700
Bi	7800	7550	(7100)

B. Background

The x-ray intensity measured in an electron probe instrument includes, of necessity, some background radiation. In the most general case, this background consists of continuum radiation, cosmic rays, spurious pulses in the counting electronics and secondary line radiation from other elements in the sample than that of interest. If the measurement time on the element standard is the same as that on the unknown, all background contributions can be grouped together, and measured together. This intensity is then subtracted from the peak intensities measured.

For instruments with scanning x-ray spectrometers, the usual method for measuring background is to detune the spectrometer to a wavelength both above and below the peak wavelength. The subtracted background is then taken as the average of these two readings. Obviously, this method necessitates an increase in the number of spectrometer settings by a factor of three. To be completely precise, then, the background should be measured on the standard and at each observation point on the unknown.

Two alternatives have also been used for the determination of background. Based on the concept that the amount of detuning of the spectrometer must be chosen arbitrarily, the continuum generated at the peak wavelength, but in elements adjacent in the periodic table to the element of in-

terest, could be measured. The continuum background would then be the average of these two readings. This intensity would then be subtracted from all intensity measurements, whether on the standard or on the unknown.[106] This method has two inherent difficulties. The biggest problem would occur when the concentration of the element of interest is less than approximately 30% in the unknown. Subtraction of the background as determined above is equivalent to subtraction of the standard background, generally 100% of that element, from intensities corresponding to much lower concentrations. The result is a serious overestimation of the unknown background. The determined unknown concentrations would then be artificially low, the error reaching in some cases 60%. The second difficulty with this method is that while the measurement taken on the element of atomic number (Z + 1) may be free from interference by secondary emission lines, the measurement on the sample (Z - 1) will almost always encounter interference from subsidiary lines in the emission spectrum of element (Z - 1). This will again result in an overestimation of the standard background with an even more serious overestimation of the unknown background. This fact was determined in the determination of the tin concentration (1.5% nominal) in five samples of Zircaloy-2. Following the above method, the probe determined concentration was 0.6% tin.

The third method for the determination of background is that used in the present analyses. Its greatest advantage occurs when many observations must be taken. Using the scanning ability of the x-ray spectrometers, an intensity vs. wavelength recording was made for each analytical line, both on the standards and on the unknowns. The full width at half maximum of the analytical line was measured, along with the position of the line peak. If no significant shift, greater than 3%, was found in the position of the analytical line, and no obvious changes in the line symmetry were observed, the background on the standard was measured at 5/2 FWHM off the peak both above and below the line peak. The magnitude of the background subtracted from each peak intensity measurement, whether on the standard or on the unknown, was taken as proportional to the concentration of the element in the sample measured. This approach necessitates some iteration and such a procedure was employed.

C. Fluorescence Correction

The incidence of the electron probe on a target sample is followed by loss of energy of the probe electrons as electron-atom collisions occur. The lost energy is exhibited by the characteristic emission spectra of the elements present in the target and by the continuum spectrum. The characteristic emission spectra are usually called primary fluorescent radiation. Secondary fluorescent radiation is

generated when the characteristic emission line wavelength, say of element B, falls below the absorption edge corresponding to another characteristic line, of element A. That is, in addition to electron excited A emission, some A emission is caused by photoionization of A atoms by B radiation. The x-ray continuum will also fluoresce the characteristic A line, since part of the continuum radiation falls below the absorption edge corresponding to A radiation. Both possibilities are indicated in Figure 25. The shaded portion of the emission spectrum is capable of causing secondary fluorescence of A radiation. The measured line intensity of the A line would be enhanced by these effects and must be corrected to obtain the true probe generated intensity.

Figure 26a illustrates how iron may be reported erroneously in the analysis of a small iron free inclusion present in an iron base matrix. The continuum emitted from the inclusion can excite the iron in the matrix, yielding an apparent iron content of the inclusion. Effects such as these can be large when the inclusion approaches, within a factor of three, the probe diameter. It is possible to minimize such errors by using an excitation potential as low as possible for the inclusion and by reducing the probe size. These operations will reduce the electron penetration volume and increase the minimum wavelength of the continuum.

Figure 25. Typical emission spectrum from compound target. Shaded region represents part of spectrum capable of fluorescing Kα (A) line.

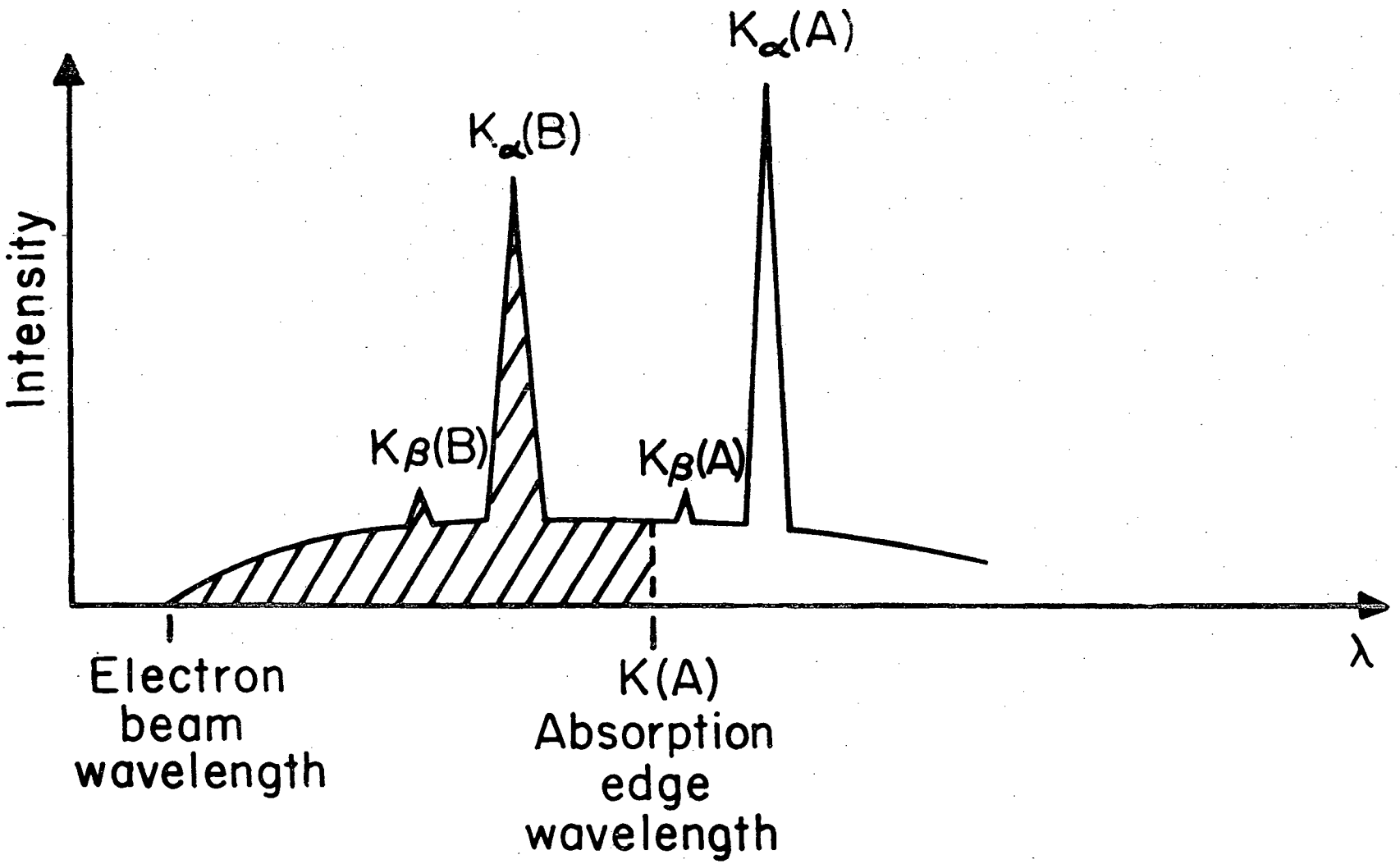
$K_\alpha(A)$
$K_\alpha(B)$
Intensity
$K\beta(B)$
$K\beta(A)$
λ
Electron beam wavelength
K(A) Absorption edge wavelength

Figure 26b illustrates an analysis made near the boundary of two phases containing different amounts of iron. Fluorescence of the iron rich region by characteristic lines and/or the continuum from the iron poor region will result in an overestimation of the iron content of the iron poor phase. Obviously this is a most difficult error to correct, and can be done only if the geometrical nature of the phase boundary is known.

Castaing[1] derived an expression for K line fluorescence by K lines. Other expressions have been obtained by Wittry,[2,5] Reed and Long,[107] Birks,[108] and Reed.[109] Duncumb and Shields[110] and Colby[111] have considered the various formulations proposed, and have attempted to show the range of validity and accuracy of these postulated relationships. From comparative studies by Colby, the method of Reed appears to be the most generally applicable. In particular, Reed's formulation overcomes the objections to the other formulations, by including a dependence on accelerating potential and allowing for K-K, K-L and L-K types of fluorescence. Without reviewing the details of the formulation, we make use of the results of the previously mentioned studies.

If $I_{A,u}$ is the directly excited intensity of the analytical line and I_f is the intensity contributed to the analytical line due to fluorescence by a shorter wavelength charac-

Figure 26. Examples of fluorescence effects: a) fluorescence of the matrix by the continuum generated in an inclusion containing no elements with characteristic lines capable of exciting iron; b) fluorescence due to the continuum and characteristic lines from a phase containing elements with characteristic lines capable of exciting iron.

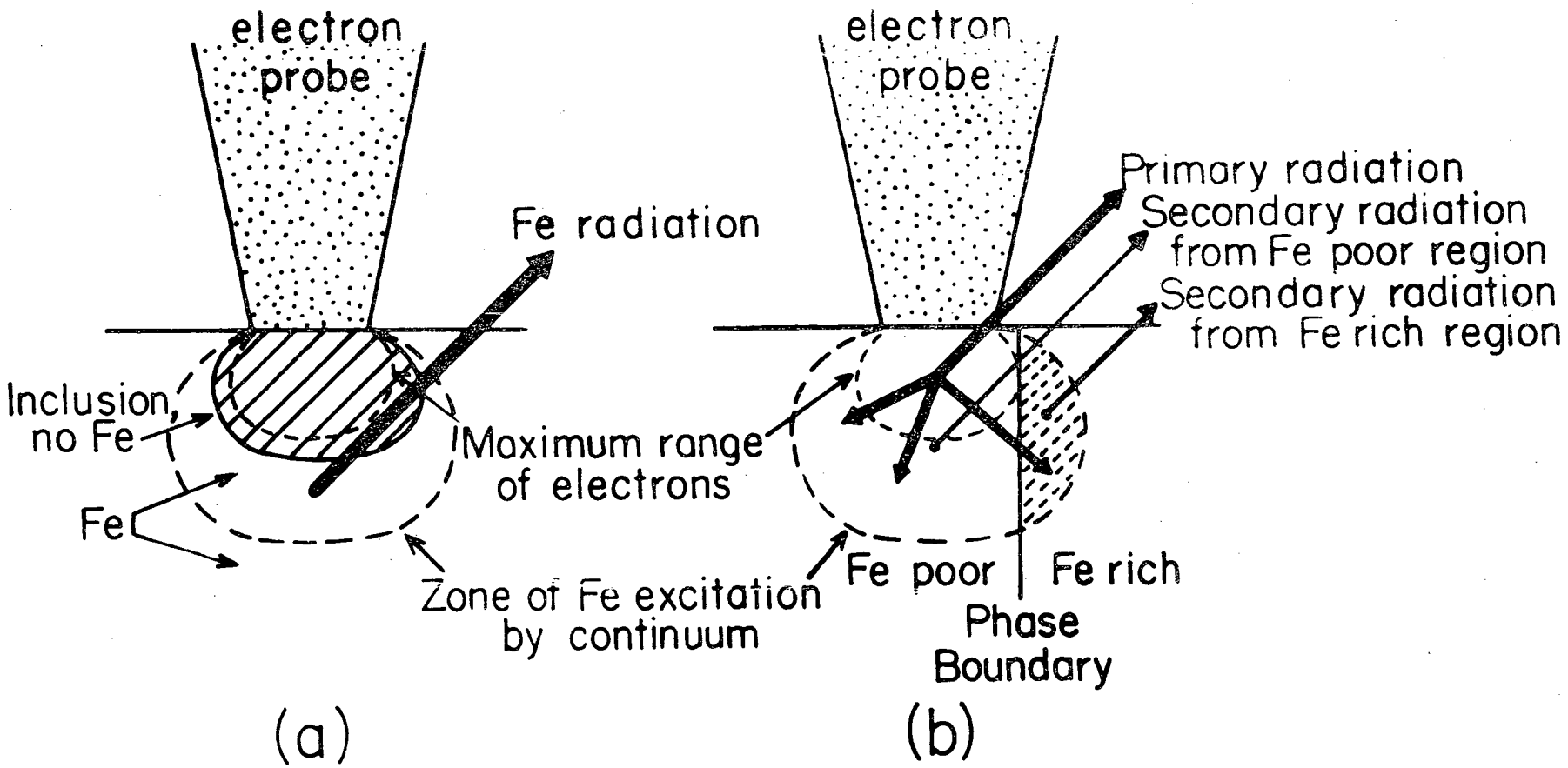
electron probe
Fe radiation
Inclusion, no Fe
Fe
Maximum range of electrons
Zone of Fe excitation by continuum
(a)
electron probe
Primary radiation
Secondary radiation from Fe poor region
Secondary radiation from Fe rich region
Fe poor
Fe rich
Phase Boundary
(b)

teristic line from element B, then:

$$\frac{I_f}{I_{A,u}} = K_{fA} = 0.5\, P_{ij}\, C_B\, \frac{r_A - 1}{r_A}\, \omega_B\, \frac{A}{B} \left(\frac{U_B - 1}{U_A - 1} \right)^{1.67}$$

$$\frac{(\mu/\rho)_A^B}{(\mu/\rho)^B} \left[\frac{\ell n(1 + y)}{y} + \frac{\ell n(1 + v)}{v} \right] \qquad (40)$$

where:

C_B = weight fraction of element B,

r_A = ratio of mass absorption coefficients on either side of the absorption edge for element A (absorption jump ratio),

ω_B = fluorescence yield for element B,

A = Atomic weight of element A,

B = atomic weight of element B,

$U_B = \frac{E_o}{E_c}$ for element B,

$(\mu/\rho)_A^B$ = mass absorption coefficient of element A for B radiation,

$(\mu/\rho)^B = \sum_i \left(\frac{\mu}{\rho}\right)_i^B$ C_i = mass absorption coefficient for B radiation by the specimen,

$y = \frac{(\mu/\rho)^A}{(\mu/\rho)^B}$ cosec θ,

$v = \frac{\sigma}{(\mu/\rho)^B}$ where σ is defined in Equation (25).

P_{ij} = a constant which takes different values for different fluorescence types: $P_{KK} = 1$; $P_{LL} = 1$; $P_{KL} = 2.4$ and $P_{LK} = 0.42$.

If I_{mA} is the measured intensity of A radiation it follows that:

$$I_{mA} = I_{A,u} + I_f. \tag{41}$$

Since

$$\frac{I_f}{I_{A,u}} = K_{fA} \tag{42}$$

$$I_{mA} = I_{A,u} + I_{A,u}K_{fA} = I_{A,u}(1 + K_{fA}). \tag{43}$$

Therefore:

$$I_{A,u} = \frac{I_{mA}}{(1 + K_{fA})} \tag{44}$$

and

$$\frac{I_{A,u}}{I_{A,s}} = C_A = K \frac{1}{1 + K_{fA}}. \tag{45}$$

Numerical values of the absorption jump ratios are obtained from the calculated mass absorption coefficients described in section IV. A. 3. The fluorescence yields of various elements have been reviewed by Fink et al.[112] In lieu of working with a possibly ambiguous set of tables of fluorescence yields, it is possible to fit the experimental data given by Fink et al. to the semi-empirical relation due to Burhop:[113]

$$\left(\frac{\omega}{1-\omega}\right)^{1/4} = A + BZ + CZ^3 \qquad (46)$$

The constants in Equation (46) have been evaluated by several authors,[113-115] most recently by Colby,[106] using the complete compilations of Fink et al. and by Bailey and Swedlund,[116] using their new data and the data of Fink et al. The constants used for K, L, and M fluorescence yield, in the present case are given in Table VII.

Table VII. Constants for Calculating Fluorescence Yields (ω)

	K	L	M
A	-0.03795	-0.11107	-0.00036
B	0.03426	0.01368	0.00386
C	-0.11634×10^{-5}	0.21772×10^{-6}	0.20101×10^{-6}

Castaing and Descamps[39] and Kirianenko et al.[38] showed that the contribution, by continuum fluorescence, to the total x-ray line intensity was generally small. This fluorescence radiation is generated deeper in the specimen than the primary radiation, resulting in greater absorption of the former. Theoretical considerations are difficult since fluorescence by the continuum is produced by a whole spectrum of wavelengths.

Castaing and Descamps,[39] Green and Cosslett,[117] and Henoc[118] give correction procedures for pure elements and binary compounds. The expression derived by Henoc is very

complex, but is also considered to be the most accurate (Henoc et al.[119]). Henoc followed the same approach as Castaing[1] for the fluorescence by characteristic lines, but he integrated over all the continuum from the short wavelength limit to the absorption edge of the particular analytical line.

Corrections for secondary fluorescence by the continuum are seldom made. Henoc's relation is very lengthy and is not used in the present work.

V. X-RAY GENERATION EFFECTS

In section IV. A., we began the analysis of the effect of sample absorption on the probe generated x-ray intensity with a discussion of the distribution in depth of the generated intensity. This distribution was shown to depend heavily on the atomic properties of the sample components. It was finally shown that this dependence on atomic number could effectively be removed from the absorption considerations (Equation 36). We now return to a specific consideration of the effect of atomic number on the generation of x-rays by the incident electron probe.

Electrons incident on a sample are in general subjected to interactions that can be broadly divided into two classes. The first class of scattering involves a negligible loss of energy but a significant change of direction, an elastic scattering event. The second type of scattering, inelastic scattering, involves a significant energy loss by the incident electron. Elastic scattering determines, primarily, the spatial distribution of the incident electrons within the sample. Inelastic scattering determines the rate of energy loss by the incident electrons. Ionization of an inner shell electron, K or L shell, is one form of an inelastic scattering event. Such an event is, in a certain fraction of the occasions, followed by the emission of a K or L characteristic x-ray photon. Inelastic interactions with the outer electrons

probably form the biggest contribution to the stopping of incident electrons. The model thus formed is one in which the incident electrons are more or less continuously slowed down by ionization losses, undergoing slight changes in direction by multiple scattering while still being able to experience large changes of direction by Rutherford scattering events, some electrons coming to rest inside the sample, others completely leaving the sample. Such processes have been discussed recently by several authors.[120-126]

In view of the realization that electron stopping is really not a continuous process, several attempts have been made to simulate electron trajectories within a target by a series of step-like paths. Worthington and Tomlin[127] had assumed for their calculation a simple straight line path. Archard[121,128] proposed a model based on an assumption of two types of paths, one straight into the sample, the other involving 90° scatterings. Green[129] proposed the use of Monte Carlo techniques to simulate the increasing complexity of the electron paths as they lose energy by inelastic collisions. Similar calculations of a more sophisticated nature have been undertaken by Bishop.[130,131]

In spite of the fact that these authors have considered step-like paths, they nevertheless assumed a continuous energy loss function. Thus, they did achieve a distribution for the incident electrons after they had lost all their energy, and they do give a distribution in depth of ionization. However,

while these calculations might be of interest for themselves, it would not be practical to attempt such a calculation every time a microprobe analysis was performed. Thus, we shall sidestep the step-like path approach and confine ourselves to the continuous energy loss approximation.

We had previously shown that the number of ionizations of A atoms per unit path length of the incident electron could be expressed as:

$$d\, n_K = \frac{\rho N\, C_A}{A}\, \psi\, (E, E_C)\, d\, x \qquad (17)$$

where C_A is the mass concentration of element A in the target, ρ is the material density in grams/cc, N is Avogadro's number, and A is the atomic weight of the sample. ψ has the characteristics of a cross section. This can now be put in a form explicitly dependent on the energy of the incident electron, as:

$$d\, n_K = \frac{\rho N\, C_A}{A}\, \frac{Q_A}{dE/dx}\, d\, E, \qquad (47)$$

with Q_A being the ionization cross section and the incremental (dE) is the mean energy change in traveling the path length (dx). Assuming that all incident electrons remained in the sample, the total number of ionizations produced by an incident electron as it decelerates from its initial energy E_o to the critical excitation potential of the A atomic K-shell, E_c, would be:

$$n_K = \frac{N\, C_A}{A} \int_{E_o}^{E_c} \frac{Q_A}{\frac{1}{\rho}\frac{d\,E}{d\,x}}\, d\,E. \qquad (48)$$

We have here assumed that the energy loss process is a continuous one, rather than a step-like phenomenon.

Following the suggestion of Poole and Thomas,[6] we define a stopping power, S, which describes the ability of a given material to decelerate incident electrons, as:

$$S = -\frac{1}{\rho}\frac{d\,E}{d\,x} \quad \left(\frac{Kev}{cm}\right). \qquad (49)$$

Defined this way, S should be approximately constant for each atomic species regardless of its chemical state. Thus:

$$n_K = \frac{N\, C_A}{A} \int_{E_c}^{E_o} \frac{Q_A}{S_A}\, d\,E. \qquad (50)$$

We now remove the assumption that all the incident electrons remain in the sample, by introducing a factor $R < 1$. Following several authors,[6,117,132] we define R as the fraction of the ionization remaining when the losses due to backscattered electrons are removed. Backscattered electrons are those which undergo large angle scattering such that they leave the sample surface with an energy greater than E_c. R will depend on the accelerating voltage and on the atomic number of the target.

Thus, the total number of ionizations per incident electron becomes:

$$n_K = \frac{N\, C_A}{A}\, R_A \int_{E_c}^{E_o} \frac{Q_A}{S_A}\, d\, E. \qquad (51)$$

A similar expression would hold for the standard A. If u is an alloy unknown, and s is the pure element standard, then the intensity ratio, K, can be written as:

$$\frac{I_u}{I_s} = K = \frac{m_o}{m_o'}\, C_A\, \frac{R_u}{R_s}\, \frac{\int_{E_c}^{E_o} \frac{Q_A}{S_u}\, d\, E}{\int_{E_c}^{E_o} \frac{Q_A}{S_s}\, d\, E}. \qquad (52)$$

The writing of the above relation assumes that the intensity ratio is experimental data corrected for instrumental effects and for any absorption and fluorescence effects in the sample. We assume that suitable expressions can be found for R, S, and Q, not only for the pure elements but also for alloys. We discuss each of these three quantities separately.

A. Ionization Cross Section

Bethe[133] derived a non-relativistic expression for the total ionization cross section of an atom as a function of the energy of an incident electron. Two adjustable constants in this relation were evaluated by Mott and Massey.[134] Worthington and Tomlin,[127] however, indicate that this formulation holds for large values of $U = E/E_c$ only, and modify that relation to apply to all low energy electrons, based on the silver data of Webster, Hansen and Duveneck.[135]

Recently Moiseiwitsch and Smith[136] have performed a complete reanalysis of cross sections. However, they deal primarily with cross sections of particular atomic levels. Glupe and Mehlhorn[137] have measured the total cross sections of four light elements and indicate that their data can be fit best to a semi-empirical relation due to Drawin.[138] The difference between the relation of Worthington and Tomlin and Drawin is a factor $(1 - 1/U)$. Since this factor would have significance only for heavy elements at low overvoltages, the relation of Worthington and Tomlin is used here:

$$Q\, E_c^2 = \text{constant}\, \frac{1}{U}\, \ell n\, U \qquad (53)$$

with E_c expressed in kev.

B. Electron Stopping Power

The rate of energy loss for non-relativistic electrons has been described by Bethe[133] and written by Mott and Massey[134] as:

$$S = \text{constant}\, \left(\frac{Z}{A}\right) \frac{1}{E}\, \ell n\, \frac{E\sqrt{e/2}}{J} \qquad (54)$$

Since the Bethe relation was obtained for hydrogen as the target, the extension to heavier target atoms required the introduction and evaluation of the mean ionization potential, J. (A recent formulation of the stopping power by Bishop[47] is in error since his expression excludes a dependence on atomic number.) Bloch[139] calculated J/Z concluding that the

ratio should be constant with a value of 13.5 ev. Jensen[140] derived a J/Z dependence of:

$$J/Z = K\,(1 + k\,Z^{-2/3})$$

with the two constants to be evaluated experimentally. Wilson[141] experimentally obtained a J/Z value of 11.5 ev for aluminum. Recent experiments by Duncumb and DaCasa[142] have shown that J/Z is only approximately constant, with significant deviations from either of the above constant values for atomic numbers less than 40. These authors have fitted their data to a relation of some complexity:

$$\frac{J}{\bar{Z}} = 14.0\,(1.0 - e^{-0.1\bar{Z}}) + \frac{75.5}{\bar{Z}\bar{Z}/7.5} - \frac{\bar{Z}}{100 + \bar{Z}} \qquad (55)$$

Since this relation was obtained from experimental data taken on a fairly wide range of sample compositions with varying atomic number, and with electron accelerating potentials similar to those used in microprobe analysis, we choose to use this form for the mean ionization potential.

C. Effective Current Factor

Some experimental work has been done toward the determination of the energy distribution of backscattered electrons.[143-147] Generally, the agreement between investigators is only fair. Defining $W = E/E_o$ ($W \leq 1$), Bishop[146] has shown that the energy distribution of backscattered electrons given as $d\eta/dW$, rather than in terms of the actual energy as $d\eta/dE$, retains essentially the same shape as

E_o is varied. Bishop has also shown that the electron backscatter coefficient, η, which is the fraction of incident electrons backscattered, is essentially a smoothly varying function of atomic number. The electron backscatter coefficient is also almost entirely independent of E_o. Similar results have been obtained by Weinryb and Philibert.[147]

It is recognized that if all electrons backscattered were backscattered with energy E_o, the factor R would be given by

$$R = 1 - \eta \quad . \tag{56}$$

However, there is a distribution in the energy of the backscattered electrons. Several methods have been proposed for calculating the effective current factor R.[132,148,149] Webster et al.[132] have shown that R may be calculated from the energy distribution of the backscattered electrons, $d\eta/dW$, if the form of the ionization cross section and the electron stopping power are known. Duncumb and Shields[150] have performed the numerical integration of:

$$R = 1 - \frac{\int_{W_c}^{1} \frac{dn}{dW} \int_{E_c}^{WE_o} \frac{Q}{S} \, dE \, dW}{\int_{E_c}^{E_o} \frac{Q}{S} \, dE} \tag{57}$$

using the experimental data of Kulenkampff and Spyra.[143] In this form, the effective current factor is given as the ratio of the ionization that would be caused by the electrons that were backscattered, had they remained in the target, to the ionization generated had all electrons remained in the target.

More recently Bishop[47] used an alternative form to calculate the effective current factor:

$$R = 1 - \frac{\int_{W_c}^{1} \eta\,(W)\,\frac{Q}{S}\,d\,W}{\int_{E_c}^{E_o} \frac{Q}{S}\,d\,E} \quad . \tag{58}$$

His results are given in graphical form as a function of atomic number and overvoltage ratio, U.

VI. COMPUTATIONAL METHODS

Thus far we have discussed the various concepts involved in the reduction of x-ray intensity ratios to composition. In the present section, we begin to describe the application of the relations obtained to the determination of concentration. We start by considering various approximations involved in the computational methods to be used.

The general relation connecting the measured intensity ratio, K, with composition can be written:

$$K = C \times (\text{absorption correction}) \times (\text{fluorescence correction}) \times (\text{atomic Number correction}) \qquad (59)$$

The various correction factors are written on the right side of Equation (59) since they themselves are functions of composition. The assumption made here is that all precautions necessary for the elimination of the effects of pulse shrinkage and of contamination have been taken. It is further assumed that the raw intensities have been corrected for deadtime losses. (In the accumulation of data, drift may be encountered, and it is assumed that this also is allowed for. The computer program to be discussed has provision for correction of both long and short time instabilities. Given a numerical deadtime input, the program also corrects the raw data for this effect.)

The absorption correction is applied following the method discussed in section IV. A.:

$$\frac{I_u^A}{I_s^A} = K_A = C_A \left[\frac{f_u(\chi_u)}{f_s(\chi_s)}\right] x \text{ (Fluorescence Correction)} \quad x \text{ (Atomic Number Correction)} \quad (36$$

The value of $f(\chi)$ is determined from Equation (37), with $R(0) = 1.1$ and $R(\infty) = 4$. In the parameter $\chi = (\mu/\rho) \csc \theta$, the proper value of the mass absorption coefficient must be used. For the case of the standard, assuming a pure element, the (μ/ρ) value is obvious. For the unknown, however, the other elements must also be accounted for. Thus, we use:

$$(\frac{\mu}{\rho})_u^A = \sum_i (\frac{\mu}{\rho})_i^A C_i \quad (60)$$

where: C_i is the weight fraction of the i^{th} element in the unknown, and (μ/ρ) is the absorption coefficient of the i^{th} element for A radiation. The numerical value of (μ/ρ) is obtained from section IV. A. 5.

There remain in $f(\chi)$ two factors to be determined. Since σ depends only on E_o and E_c, this value is the same for both standard and unknown:

$$\sigma = \frac{(2.54)(10^5)}{E_o^{1.5} - E_c^{1.5}} \quad (61)$$

The factor (h) contains the residue of the influence of atomic number on the absorbtion correction. Thus, we must use for the pure element standard:

$$h = 4.5 \frac{A_A}{Z_A^2} \quad (62)$$

and for the unknown:

$$h = 4.5 \sum_i C_i \left(\frac{A_i}{Z_i^2}\right) \qquad (63)$$

Had we limited ourselves to the simplified form of f(x):

$$f(\chi) = \frac{1 + h}{\left(1 + \frac{\chi}{\sigma}\right)\left[1 + h\left(1 + \frac{\chi}{\sigma}\right)\right]} \qquad (37')$$

then different values of h and σ would be necessary. These are given by Duncumb and Shields[150] as:

$$h = 1.2 \frac{\bar{A}}{\bar{Z}^2} \qquad (63')$$

$$\sigma = \frac{4.5 \times 10^5}{E_o^{1.67} - E_c^{1.67}} \qquad (61')$$

In these relations, $\bar{A}$ and $\bar{Z}$ are the mean atomic weight and mean atomic number of the target. E_o is the probe accelerating voltage and E_c is the critical excitation potential of the emission line used for analysis.

At this point we must consider the limitations of the model used. In their work, Duncumb and Melford[46] obtained the values of (h) and (σ) for the full f(χ)by comparison to the work of Castaing[1] and Green.[41] They then calculated carbon intensity ratios to be expected from SiC. When compared to their experimental data, the change of predicted intensity ratio with increasing (μ/ρ) (or correspondingly, increasing accelerating voltage and thus depth of penetration) was less than that found experimentally.

We would expect, then, at low kilovoltages for a light element, an over correction for absorption, and at high kilovoltages, an undercorrection for absorption. Since h and (σ)

were evaluated at 10 KV, we expect the proper magnitude correction in the range 8 to 12 KV. The errors found for elements heavier than aluminum were in the same direction, but significantly less in magnitude. Thus, for the metal components of a metal-light element system, we would expect approximately the proper correction for absorption at various KV, with possibly a slight undercorrection at high KV.

The fluorescence correction applied is of the form of Equations (40) and (45). Thus:

$$K_A = C_A \left[\frac{f_u(x_u)}{f_s(x_s)}\right] \quad (1 + K_{fA}) \times (\text{Atomic Number Correction}) \tag{64}$$

The fluorescence yields of the light elements are low, less than 0.01. The expected fluorescence correction for, say, carbon and titanium would be small, less than 1.005. However, for other systems, for example, iron and nickel, the fluorescence effect could account for up to 10% of the total emitted intensity.

The general form of the atomic number (generation) correction is given by Equation (52). The relation between the intensity ratio and concentration now becomes:

$$K_A = C_A \left[\frac{f_u(x_u)}{f_s(x_s)}\right] (1 + K_{fA}) \left[\frac{R_u}{R_s} \frac{\int_{E_c}^{E_o} \frac{Q_A}{S_u} dE}{\int_{E_c}^{E_o} \frac{Q_A}{S_s} dE}\right] \tag{52'}$$

with the R's evaluated by Equation (57). Numerical integra-

tions of Equation (52) have been performed. (Appendix B gives a computer program used in that evaluation of Equation (52).) For the pure element standard, Q and S can be evaluated from Equations (53), (54), and (55). For the unknown, Q is the same as for the standard. However, from the definition of the stopping power:

$$S = -\frac{1}{\rho}\frac{dE}{dx} \tag{49}$$

it is obvious that S is not the same for the standard and the unknown. Since, from Equation (49) we see the elemental dependence of S, the additive nature of electron retardation energy losses would lead to:

$$S_u = \sum_i C_i S_i \quad . \tag{65}$$

Bishop[47] has shown that using an integration performed by Worthington and Tomlin[127] and an approximation of Poole and Thomas[6] the ratio of integrals in Equation (52') can be simplified after substitution of Q and S to:

$$\frac{\left(\frac{Z}{A}\right)_A \ell n\,(1.166\,\bar{E}/J_A)}{\sum_i C_i \left(\frac{Z}{A}\right)_i \ell n\,(1.166\,\bar{E}/J_i)} \tag{66}$$

where:

$$\bar{E} = \frac{E_o + E_c}{2} \quad .$$

Bishop has also shown that to a very good approximation:

$$R_u = \sum_i C_i R_i \quad . \tag{67}$$

Thus, the relation between the intensity ratio and concen-

tration can now be written:

$$K_A = C_A \left[\frac{f_u(\chi_u)}{f_s(\chi_s)}\right](1 + K_{fA}) \left[\frac{\sum_i C_i R_i \left(\frac{Z}{A}\right)_A \ell n (1.166 \bar{E}/J_A)}{R_s \sum_i C_i \left(\frac{Z}{A}\right)_i \ell n (1.166 \bar{E}/J_i)}\right] \quad (68)$$

The error in this relation, compared to the full integration of Equation (52') is less than 1% for $E_o > 2 E_c$.

The problem arising at lower overvoltages is dual. As pointed out in the discussion of the ionization cross section, a more accurate mathematical form for the ionization cross section would yield a faster decrease in the ionization cross section with overvoltage, at low overvoltages, $1 < U < 3$. For the light elements, the backscatter factor is small, and the effective current factor, R, is approximately unity. The error in the backscatter factor, η, at low overvoltages increases with increasing atomic number. The second difficulty arises from the assumption that the mean ionization potential, J, is independent of E. In fact, the data of Duncumb and DaCasa[142] seems to indicate that J decreases with decreasing E. The net result of these errors would show up most in the analysis of a light element in combination with a heavy element at low kilovoltages.

The consideration of errors can be summarized as follows. In the atomic number interval 15 to 70, the approximations

appear to be applicable as long as the overvoltage for the analytical x-ray lines is 2 or greater. The biggest problem in this area would arise in the analysis of low concentrations. In the analysis of very heavy elements, e.g., uranium, the errors inherent in the effective current factor correction would limit the accuracy of the analysis. From consideration of the work of Duncumb and DaCasa[142] these errors could approach 5%.

For the analysis of light elements, the biggest problem arises when that element is in a matrix characterized by a high mass absorption coefficient for the light element's emission line, and when the atomic numbers differ by a factor of 3 or more. In such a case, it is not reasonable to expect high accuracy at low kilovoltages because of the errors in the atomic number correction and in the absorption correction. At high kilovoltages, the magnitude of the absorption would essentially limit any light element analysis. Nevertheless, reasonable results could be expected at intermediate kilovoltages, 8 to 12 KV, where mass absorption coefficients less than 10,000 cm^2/g are encountered.

A computer program which permits the reduction of raw microprobe data to concentration, and which uses the relations just described is given in Appendix C. The only input requirements are problem identification, kilovoltage used,

deadtimes, elements and lines used in the analysis and microprobe output. All constants are either stored internally in the computer or calculated at the time of a computer run. The data stored internally are given in Appendix D. A detailed description of input requirements is given in Appendix E. Appendix F gives a typical output.

VII. APPLICATIONS

We shall now discuss the application of the various corrections to eight metallurgical samples. Each type of analysis results points up particular characteristics of the correction procedure. The data was corrected by use of the computer program given in Appendix C. Corrections were applied for detector system deadtime, instrument drift, background, absorption, characteristic line fluorescence and atomic number effect.

Of the various constants used in the calculation, the following were stored internally: Atomic Number, Atomic Weight, Absorption Edge Wavelengths, Critical Excitation Potentials, Primary Emission Line Wavelengths, and constants for calculation of Absorption Coefficients. Data for the correction that was calculated included: Overvoltage Ratio, Effective Current Factor, Mass Absorption Coefficients, Absorption Jump Ratios, and Fluorescence Yields.

A. Copper-Zinc

A sample of National Bureau of Standards brass C-1102 was analyzed under three different analysis conditions. A total of 30 analyses were performed. The analyses were performed at 25 KV with two LiF crystals and two detectors, a sealed proportional counter and a flow proportional counter. For one-third of the analyses, pure element standards were used. For the rest of the analyses, standards supplied by the

probe manufacturer were used. The analyses using the probe manufacturer supplied standards always resulted in high concentrations. The cause was finally determined to result from the purity of these standards, approximately 98% of the element. The pure element standards contained at least 99.6% of the element. The results of the analyses using the pure element standards are given in Table VIII. The results are quite good when compared to the NBS certified composition:

Zinc: 27.10 wt %

Copper: 72.85 wt %

The significance of this analysis lies in the fact that the magnitude of the corrections should be small for this system containing adjacent elements. There is only a slightly greater correction for the absorption of the copper radiation than for the zinc radiation. The only fluorescence correction would be necessitated by the zinc K β_1 fluorescence of the copper line. The mass absorption coefficients calculated, for example, for the copper, agree well with the values measured by Hughes, Woodhouse and Bucklow.[68]

Line	(μ/ρ) calc.	(μ/ρ) exp.[68]
Zinc Kα	43.	42.7
Copper Kα	52.	52.2

Likewise, the Absorption Jump Ratio measured by Hopkins[93] for copper as 8.1 compares favorably with the calculated value of 7.77.

PROBLEM NUMBER A1242

SEPT. 14, 1967

SUBMITTED BY L. J. GRAY

DESCRIPTION - C-1102, NBS BRASS

MEAN CHEMICAL COMPOSITION AND TWO SIGMA LIMITS BASED ON 10 ANALYSES

ELEMENT	WEIGHT PERCENT	ATOMIC PERCENT
ZN	27.428 - 0.134	26.790 - 0.185
CU	72.670 - 0.575	73.220 - 0.194

MEAN INTENSITY RATIOS AND TWO SIGMA LIMITS

ELEMENT	K
ZN	0.2731 - 0.0015
CU	0.7279 - 0.0069

ACCELERATING VOLTAGE	25.0 KEV
X-RAY EMERGENCE ANGLE	52.5 DEGREES

STANDARD PEAK-TO-BACKGROUND RATIOS (P/B) AND MINIMUM DETECTABILITY LIMITS (MDL)

ELEMENT	P/B	MDL
ZN	101/1	0.1037 WT %
CU	133/1	0.0821 WT %

Table VIII. Results of Analyses of Copper-Zinc Sample of Certified Composition 27.10 wt % zinc, 72.85 wt %.

B. Nickel-Iron

This system should exhibit two effects, a fluorescence of the iron by the nickel and an effect of atomic number. Fifty analyses were performed on this sample. Intensity ratios were formed with respect to the pure elements (greater than 99.7%) after correction for deadtime, drift and background. In all cases the iron concentration was within 0.5% of the vendor* supplied chemical analysis of 43.55%. Likewise, all results for the nickel were high by about 1.0% when compared to the stated composition of 56.55%. A typical set of results is given in Table IX.

The effect of the fluorescence correction is seen in the comparison of the measured intensity ratio for iron: 0.4864, with the resultant composition: 43.38 wt %.

Since the action of the atomic number effect is to reduce the apparent concentration of the heavier element and to increase the apparent concentration of the lighter element, the fluorescence effect and the atomic number effect act in a direction opposite to the absorption effect for iron. However, for nickel, the atomic number effect and the absorption effect act in the same direction. Thus, errors in these corrections re-enforce each other, and a 1% error in concentration results.

*International Nickel Co., Inc.

PROBLEM NUMBER A1246

23 MARCH 1967

SUBMITTED BY L. J. GRAY

DESCRIPTION - PUG FE-NI CAM SICS SRC

MEAN CHEMICAL COMPOSITION AND TWO SIGMA LIMITS BASED ON 10 ANALYSES

ELEMENT	WEIGHT PERCENT	ATOMIC PERCENT
NI	57.582 - 0.217	55.810 - 0.166
FE	42.279 - 0.117	44.200 - 0.144

MEAN INTENSITY RATIOS AND TWO SIGMA LIMITS

ELEMENT	K
NI	0.5320 - 0.0023
FE	0.4864 - 0.0012

ACCELERATING VOLTAGE	25.0 KEV
X-RAY EMERGENCE ANGLE	52.5 DEGREES

STANDARD PEAK-TO-BACKGROUND RATIOS (P/B) AND MINIMUM DETECTABILITY LIMITS (MDL)

ELEMENT	P/B	MDL
NI	169/1	0.1226 WT %
FE	208/1	0.0963 WT %

Table IX. Results of Analyses of Nickel-Iron Sample of Reference Composition 43.55 wt % Iron, 56.55 wt % Nickel.

C. Tin-Zirconium

Zircaloy-2 contains nominally 1.5% tin in a zirconium matrix. The attempt in this case was to test the theoretical correction procedure in the determination of this low concentration. The analyses of five samples* yielded the tin results given in Table X. These results are particularly important because they show that the method for calculating background based on composition, as described in section IV. B., yields reasonable results. As pointed out in that section, use of the standard background in all cases resulted in a probe concentration of 0.6% tin in Zircaloy-2. The intensity ratios formed with respect to pure zirconium and pure tin were corrected for absorption, fluorescence and atomic number effects. Table X shows the more meaningful results obtained with the present background correction.

D. Titanium-Niobium

The alloy system of titanium and niobium forms an interesting challenge. It is necessary to use the niobium Lα line for the analysis. Thus, there is a fluorescence of the niobium by the titanium, and this effect acts opposite to the effect of atomic number and absorption for niobium. This situation is in contrast to that in the

*The Zircaloy-2 samples were provided by Dr. K. Tangri, Department of Mechanical Engineering, University of Manitoba.

Table X. Analyses of Nominal 1.5 wt % Tin in Zircaloy-2

Sample	Number of Analyses	Mean Tin Concentration	RMS Deviation
Y-1	40	1.473 %	0.017
Y-5	60	1.494 %	0.071
Y-6	29	1.423 %	0.024
Y-8	25	1.440 %	0.049
Y-9	39	1.396 %	0.208

nickel-iron system. The standards used in this analysis were again the pure elements. After correcting the data for deadtime, drift and background, the other corrections were applied with the results for analysis at 20 KV given in Table XI. Other analyses were performed at 25 KV and 30 KV. Those results exhibit an enhancement of the trends given in Table XI.

The results of chemical analysis by several laboratories* were averaged to yield reference compositions of:

Titanium: 34.97%

Niobium: 65.00%

In Table XI we again see a too high concentration for the heavy element, similar to the effect in the nickel-iron analysis. Since in the iron-nickel system, the fluorescence correction for iron yielded good results, we expect that the same would hold here. If that is so, then the error observed in the heavy element in both cases must be due to the atomic number correction over-correcting the intensity ratio. An additional complication enters in this system because of the ease of oxidation of any sample surface. Although the standards were polished to 1/4 micron diamond within 10 minutes of being put into the probe chamber, the definite possibility of a surface oxide layer still existed.

*Wet chemical analyses performed by the laboratories of various members of the Midwest Probe Users Group were averaged to obtain the results given here.

PROBLEM NUMBER A1256

19 SEPT 1967

SUBMITTED BY L. J. GRAY

DESCRIPTION - MAPLG TI-NB

MEAN CHEMICAL COMPOSITION AND TWO SIGMA LIMITS BASED ON 10 ANALYSES

ELEMENT	WEIGHT PERCENT	ATOMIC PERCENT
TI	33.435 - 0.258	48.474 - 0.238
NB	68.528 - 0.185	51.536 - 0.243

MEAN INTENSITY RATIOS AND TWO SIGMA LIMITS

ELEMENT	K
TI	0.3122 - 0.0026
NB	0.0625 - 0.0019

ACCELERATING VOLTAGE	20.0 KEV
X-RAY EMERGENCE ANGLE	52.5 DEGREES

STANDARD PEAK-TO-BACKGROUND RATIOS (P/B) AND MINIMUM DETECTABILITY LIMITS (MDL)

ELEMENT	P/B	MDL
TI	73/1	0.1252 WT %
NB	25/1	0.7268 WT %

Table XI. Results of Analyses of Titanium-Niobium Sample of Reference Composition 34.97 wt % Titanium, 65 wt % Niobium.

In spite of this possible face-saving problem, we still have an indication of difficulty in the atomic number correction.

Certain non-metallics occur as troublesome inclusions in steels. Two such materials were subjected to probe analysis. In each case, the light element of the binary compound was determined by difference since either no standard was available or the light element intensity was too low to obtain sufficient counts.

E. Silicon-Oxygen

An inclusion thought to be quartz from fluorescence data was tested in the probe. Pure silicon was the single standard. No oxygen data were taken because the oxygen intensity was of the order of the background intensity. In this work, care was taken to insure that peak intensities were measured on both the standard and the unknown. The reason for this lies in the fact that the silicon Kα line shifted in position between the pure element and the oxide. The analyses results are given in Table XII.

In this difficult system, where the magnitude of the corrections approaches 10% absolute, or 20% relative, the results are a little surprising. The silicon concentration is within 0.5% of the theoretical value for SiO_2.

PROBLEM NUMBER A1282

16 AUGUST 1967

SUBMITTED BY L. J. GRAY

DESCRIPTION - SI + C (SIC2)ON SIC2 PEAK

MEAN CHEMICAL COMPOSITION AND TWO SIGMA LIMITS BASED ON 11 ANALYSES

ELEMENT	WEIGHT PERCENT	ATOMIC PERCENT
SI	48.212 - 0.582	34.658 - 0.527
C *	51.788 - 0.582	65.342 - 0.529

* DETERMINED BY DIFFERENCE

MEAN INTENSITY RATIOS AND TWO SIGMA LIMITS

ELEMENT	K
SI	0.3964 - 0.0056

ACCELERATING VOLTAGE	25.0 KEV
X-RAY EMERGENCE ANGLE	52.5 DEGREES

STANDARD PEAK-TO-BACKGROUND RATIOS (P/B) AND MINIMUM DETECTABILITY LIMITS (MDL)

ELEMENT	P/B	MDL
SI	924/1	0.1125 WT %

Table XII. Results of Analyses of SiO_2 Sample.

F. Iron-Sulfur

A specimen thought to be FeS_2 was analyzed in the microprobe. FeS_2 has a theoretical composition of 46.54 wt % Fe; 53.46 wt % S. The phase, however, is apparently not stoichiometric.[151] With sulfur to be determined by difference, the iron intensity ratio was formed with respect to pure iron. The resultant corrections yielded:

Iron	43.30 $\pm$ 0.532 wt %
Sulfur	56.70 $\pm$ 0.532 wt %

These results are reasonable in view of the uncertainty of the phase diagram.

G. Titanium-Carbon

Previous attempts to perform quantitative microanalysis of metal carbides generally dealt with stoichiometric compositions.[36,46] We have analyzed four samples of defect titanium carbide. The samples were single crystals grown by the Verneuil technique.* The microanalysis was performed using standards of pure (99.97%) titanium and natural diamond. The data were first corrected for detector system deadtime, instrument drift and background. Intensity ratios were formed and corrected in two ways. The first method used the full absorption relations, Equations (37), (61), (62)

*The TiC samples were kindly provided by Professor W. Williams, University of Illinois, Materials Research Laboratory.

and (63). The second method used the simplified form for the absorption correction, as described in section VI, with Equations (37'), (63'), and (61').

In section VI, we considered the models on which these corrections are based. This review led to an expectation, in this type of metallurgical system involving carbon, of high concentrations for both titanium and carbon at low kilovoltages, less than 9 KV, and low concentrations for carbon at accelerating potentials greater than 12 KV.

One of the four samples contained a large number of graphite inclusions, and yielded a total composition in the two phase region between TiC and graphite. The other samples appeared quite homogeneous to the electron probe.

The results obtained from more than fifty analyses on each samples are given in Table XIII. The titanium intensity ratios exhibited a maximum at an excitation potential between 10 KV and 15 KV. The carbon intensity ratio continually decreases with increasing kilovoltage. With the full $f(\chi)$, the carbon concentration is higher by about 1.7% absolute than with the simplified $f(\chi)$. For titanium, the difference is approximately 0.2%.

For 6 and 8 KV the calculated carbon concentration is too high in all cases. For 10 KV, the results are within 1.0% of the result obtained by other methods, when the full absorption correction is used. A similar result is obtained for the titanium. At 15 KV, the effect of undercorrection

Table XIII. Results of Analyses of Three TiC Samples

Accelerating Potential KF	Element and Line Used	Intensity Ratio	Mass Concentration Full $f(\chi)$ wt %	Simple $f(\chi)$ wt %
Sample 1251-53b, reported composition: 17.3 wt% carbon				
6	Ti Kα	.683	79.5	79.5
	C Kα	.241	24.4	22.9
8	Ti Kα	.708	83.1	83.2
	C Kα	.232	22.0	20.2
10	Ti Kα	.816	85.3	85.4
	C Kα	.135	16.9	15.3
15	Ti Kα	.790	82.5	82.7
	C Kα	.104	16.0	14.3
Sample 1251-59, reported composition: 17.9 wt% carbon, estimated				
6	Ti Kα	.692	79.2	79.3
	C Kα	.243	23.3	21.8
8	Ti Kα	.755	83.9	83.9
	C Kα	.207	22.7	20.8
10	Ti Kα	.814	85.2	85.3
	C Kα	.134	16.9	15.3
15	Ti Kα	.779	81.6	81.7
	C Kα	.105	16.2	14.5
Sample 1251-53a, reported composition: 17.3 wt% carbon				
6	Ti Kα	.850	(88.5)	(88.6)
	C Kα	.228	22.5	20.9
8	Ti Kα	.791	84.5	84.5
	C Kα	.206	22.7	20.8
10	Ti Kα	.813	85.2	85.3
	C Kα	.133	16.7	15.1
15	Ti Kα	.784	82.1	82.2
	C Kα	.101	15.6	13.9

for absorption appears.

The overcorrection for absorption at low KV is explained by the fact that the Philibert model does not adequately account for surface ionization. The undercorrection for titanium at low KV is attributed to the fact that the model used for the atomic number correction does not consider the change in ionization cross section with decreasing kilovoltage and ignores the variation of the mean ionization potential with kilovoltage and with composition.

Nevertheless, in spite of the limits of the theoretical correction procedures used, it is possible to obtain estimates of the carbon concentration in refractory metal carbides by choosing analysis conditions so as to limit the theoretical errors. Such conditions exist for the titanium-carbon system when using beam accelerating potentials of approximately 10 KV.

H. Gold-Copper

The analysis of a binary containing an intermediate weight element and a heavy element would complete the variety of elements analyzed. The copper-gold system contains the phase Cu_3Au, and this system was analyzed in the microprobe. The results are given in Table XIV. The magnitude of the corrections approaches 7% absolute for both elements. However, in spite of this size of correction, the results are within 0.3% of the theoretical composition.

PROBLEM NUMBER A1259

AUGUST, 1966

SUBMITTED BY L. J. GRAY

DESCRIPTION - CU3AU

MEAN CHEMICAL COMPOSITION AND TWO SIGMA LIMITS BASED ON 10 ANALYSES

ELEMENT	WEIGHT PERCENT	ATOMIC PERCENT
AU	50.854 - 0.588	25.386 - 0.264
CU	48.184 - 0.302	74.624 - 0.274

MEAN INTENSITY RATIOS AND TWO SIGMA LIMITS

ELEMENT	K
AU	0.4473 - 0.0061
CU	0.5545 - 0.0037

ACCELERATING VOLTAGE 30.0 KEV

X-RAY EMERGENCE ANGLE 52.5 DEGREES

STANDARD PEAK-TO-BACKGROUND RATIOS (P/B) AND MINIMUM DETECTABILITY LIMITS (MDL)

ELEMENT	P/B	MDL
AU	60/1	0.7657 WT %
CU	204/1	0.2282 WT %

Table XIV. Results of Analyses of Cu_3Au Sample.

VIII. SUMMARY

A method, based on physical principles, for the estimation of mass absorption coefficients has been described. Mass absorption coefficients of several elements for the characteristic emission lines of carbon, nitrogen, and oxygen have been given.

A correction procedure for the conversion of microprobe x-ray intensity data to composition has been presented. This method was tested in the analysis of eight binary systems of metallurgical interest, containing elements from carbon to gold in various combinations. This method of data reduction has been shown to be generally applicable to this variety of elements. The analyses results are summarized in Table XV. The biggest difficulties were encountered in the analysis of carbon. Consideration of the principles of the corrections led to the definition of a set of analysis conditions which minimized the theoretical errors.

The method of estimation of mass absorption coefficients to within 5% in most cases will now permit modifications to be made to the theoretical correction relations. Particular work should be centered on the distribution in depth of the sample ionization, and on the change in ionization cross section and mean ionization potential with electron energy. Such modifications will increase the range of analysis conditions under which reasonable estimates of light element concentrations can be made by microprobe techniques.

Table XV. Summary of Analyses Results

System	Chemical Analysis	Microprobe Intensity Ratios	Microprobe Composition
Cu	72.85 wt%	.7279	72.87 wt%
Zn	27.10 wt%	.2731	27.43 wt %
Ni	56.55 wt%	.5320	57.58 wt%
Fe	43.55 wt%	.4864	43.38 wt %
Ti	34.97 wt%	.3122	33.44 wt%
Nb	65.00 wt%	.6625	68.94 wt%
Si	33.33 at% (theo.)	.3964	48.21 wt% 34.66 at%
O	66.67 at% (theo.)	diff.	51.79 wt% 65.34 at%
Fe	46.54 wt% (theo.)	.3808	43.30 wt%
S	53.46 wt% (theo.)	diff.	56.70 wt%
Ti	82.7 wt%	.816	85.3 wt%
C	17.3 wt%	.135	16.9 wt%
Cu	75.00 at% (theo.)	.5545	48.18 wt% 74.62 at%
Au	25.00 at% (theo.)	.4473	50.81 wt% 25.39 at%

LIST OF REFERENCES

1. Castaing, R., Ph. D. thesis, University of Paris, 1951; Office Nationale d'Etudes et Recharches Aeronautique, Publication No. 55, Paris, 1951. Translated by P. Duwez and D. B. Wittry, Interim Technical Report No. 3, under Contract DA-04-495-Ord-463, 1955; ASTIA Document No. Ad-135428.

2. Wittry, D. B., Ph. D. Thesis, California Institute of Technology, 1957; Interim Technical Report No. 5, under Contract DA-04-495-Ord-463, 1957; ASTIA Document No. AD-135429.

3. Zemany, P. D., in "Symposium on X-ray and Electron Probe Analysis," Atlantic City, New Jersey, June, 1963, American Society for Testing and Materials, Philadelphia, Pennsylvania, 1964, p. 1.

4. Philibert, J., in "X-ray Optics and X-ray Microanalysis" (H. H. Pattee, V. E. Cosslett, and A. Engstrom, Eds.), Academic Press, New York, 1963 , p. 379.

5. Wittry, D. B., University of Southern California Engineering Center Report 84-204, July, 1962.

6. Poole, D. M., and Thomas, P. M., J. Inst. Metals 90, 1962, p. 228.

7. Campbell, W. J., Brown, J. D., and Thatcher, J. W., Anal. Chem. 38, 1966, p. 416R.

8. Heinrich, K. F. J., in "The Electron Microprobe" (T. D. McKinley, K. F. J. Heinrich, and D. B. Wittry, Eds.), John Wiley and Sons, New York, 1966, p. 841.

9. Keil, K., Fortschr. Min. 44, 1967, p. 4.

10. Cescas, M., Tyner, E., and Gray, L. J., in "Advances in Agronomy," 20, Aqademic Press, New York. To be published.

11. Campbell, W. J. and Brown, J. D., Anal. Chem. 40, 1968, p. 346R.

12. Elion, H. A., "Instrument and Chemical Analysis Aspects of Electron Microanalysis and Macroanalysis," Pergamon Press, New York, 1966.

13. Birks, L. S., "Electron Probe Microanalysis," Interscience Publishers, New York, 1963.

14. Theisen, R., "Quantative Electron Microprobe Analysis," Springer-Verlag Publishers, New York, 1965.

15. Malissa, H., "Elektronenstrahl-Mikroanalyse, Handbuch der Mikrochemischen Methoden," 4, Springer-Verlag Pub., New York, 1966.

16. Castaing, R., in "Advances in Electronics and Electron Physics," XIII (L. Marton, Ed.), Academic Press, New York, 1960, p. 317.

17. Bender, S. L., and Rapperport, E. J., in "The Electron Microprobe" (T. D. McKinley, K. F. J. Heinrich and D. B. Wittry, Eds.), John Wiley and Sons, New York, 1966, p. 405.

18. Burkhalter, P. G., Brown, J. D., and Myklebust, R. L., Rev. Sci. Inst. 37, 1966, p. 1267.

19. Spielberg, N., Rev. Sci. Inst. 37, 1966, p. 1268.

20. Heinrich, K. F. J., Vieth, D., and Yakowitz, H., in "Advances in X-ray Analysis" (G. R. Mallett, M. Fay and W. M. Mueller, Eds.), 9, Plenum Press, New York, 1965, p. 208.

21. Schiff, L. I., Phys. Rev. 50, 1936, p. 88.

22. Ruark, A. E. and Brammer, F. E., Phys. Rev. 52, 1937, p. 322.

23. Beers, Y., Rev. Sci. Inst. 13, 1942, p. 72.

24. Lonsdale, K., Acta. Cryst. 1, 1948, p. 12.

25. Short, M. A., Rev. Sci. Inst. 31, 1960, p. 618.

26. Sawatzky, A. and Jones, S., J. Appl. Phys. 38, 1967, p. 4758.

27. Borelie, F. and Short, M. A., Proc. Third Nat. Conf. Electron Probe Microanalysis, Chicago, 1968, paper 38.

28. Rose, M. E. and Korff, S. A., Phys. Rev. 59, 1941, p. 850.

29. Rose, M. E. and Ramsey, W. E., Phys. Rev. 61, 1942, p. 504.

30. Taylor, J. and Parrish, W., Rev. Sci. Inst. 26, 1955, p. 367.

31. Birks, L. S., Rev. Sci. Inst. 22, 1951, p. 891.

32. Henke, B. L., Elgin, R. L., Lent, R. E., and Ledingham, R. B., Air Force Office of Aerospace Research, Report AFOSR 67-1254, Pomona College, Claremont, California, 1967.

33. Beckett, R. and Hurt, T., "Numerical Calculations and Algorithms," McGraw Hill Book Co., New York, 1967, p. 268.

34. Reed, S. J. B., J. Sci. Inst. Ser. 2, 1, 1968, p. 136.

35. Ong, P. S., in "X-ray Optics and Microanalysis" (R. Castaing, P. Deschamps and J. Philibert, Eds.), Hermann, Paris, 1966, p. 181.

36. Ranzetta, G. V. T. and Scott, V. D., in "X-ray Optics and Microanalysis" (R. Castaing, P. Deschamps and J. Philibert, Eds.), Hermann, Paris, 1966, p. 254.

37. Neuhaus, H., in Proc. of the Third Nat. Conf. on Electron Probe Microanalysis, Chicago, 1968, paper 19.

38. Kirianenko, A., Maurice, F., Calais, D., and Adda, Y., in "X-ray Optics and Microanalysis" (H. H. Pattee, V. E. Cosslett and A. Engstrom, Eds.), Academic Press, New York, 1963, p. 559.

39. Castaing, R. and Descamps, J., J. Phys. Radium 16, 1955, p. 304.

40. Castaing, R. and Henoc, J., in "X-ray Optics and Microanalysis" (R. Castaing, P. Deschamps and J. Philibert, Eds.), Hermann, Paris, 1966, p. 120.

41. Green, M., in "X-ray Optics and Microanalysis" (H. H. Pattee, V. E. Cosslett and A. Engstrom, Eds.), Academic Press, New York, 1963, p. 361.

42. Theisen, R., in "X-ray Optics and Microanalysis" (R. Castaing, P. Deschamps and J. Philibert, Eds.), Hermann, Paris, 1966, p. 224.

43. Helgesson, C. I., in "X-ray Optics and Microanalysis" (R. Castaing, P. Deschamps and J. Philibert, Eds.), Hermann, Paris, 1966, p. 284.

44. Lenard, P. and Becker, A., in "Handbuch der Experimentalphysik," XIV, Akad. Verlagages., Leipzig, 1927, p. 178.

45. Duncumb, P. and Shields, P. K., in "The Electron Microprobe" (T. D. McKinley, K. F. J. Heinrich and D. B. Wittry, Eds.), John Wiley and Sons, New York, 1966, p. 284.

46. Duncumb, P. and Melford, D. A., in "X-ray Optics and Microanalysis" (R. Castaing, P. Deschamps and J. Philibert, Eds.), Hermann, Paris, 1966, p. 240.

47. Bishop, H. E., Brit. J. Appl. Phys. Ser. 2, 1, 1968, p. 673.

48. Yakowitz, H. and Heinrich, K. F. J., Mikrochimica Acta., 1, 1968, p. 182.

49. Frazer, J. Z., S. I. O. Report Reference No. 67-29, University of California, LaJolla, California, 1967.

50. Siegbahn, M., Zeits. Physik. 15, 1914, p. 753.

51. Allen, S. J. M., Phys. Rev. 28, 1926, p. 907.

52. Grosskurth, K., Ann. Physik. 20, 1934, p. 197.

53. Laubert, S., Ann. Physik. 40, 1941, 553.

54. Leroux, J., in "Advances in X-ray Analysis" (W. M. Mueller, Ed.), 5, Plenum Press, New York, 1962, p. 153.

55. Victoreen, J. A., J. Appl. Phys. 14, 1943, p. 95.

56. Victoreen, J. A., J. Appl. Phys. 20, 1949, p. 1141.

57. Henke, B. L., White, R., and Lundberg, B., J. Appl. Phys. 28, 1957, p. 98.

58. Bearden, A. J., J. Appl. Phys. 37, 1966, p. 1681.

59. Allen, S. J. M., Mass Absorption Coefficients for X and Gamma Rays, "Handbook of Chemistry and Physics," The Chemical Rubber Publishing Co., Cleveland, Ohio.

60. Liebhafsky, H. A., Pfeiffer, H. G., Winslow, E. H., and Zemany, P. D., "X-ray Absorption and Emission in Analytical Chemistry," John Wiley and Sons, Inc. New York, 1960.

61. Compton, A. R. and Alisson, S. K., "X-rays in Theory and Experiment," D. Van Nostrand Co., New York, 1957.

62. Sagel, K., "Tables for X-ray Emission and Absorption Analysis," Springer-Verlag, Heidelberg, 1959.

63. Stainer, H. M., U. S. Department of the Interior, Bureau of Mines, Information Circular 8186, 1963.

64. Hughes, G. D. and Woodhouse, J. B., in "X-ray Optics and Microanalysis," (R. Castaing, P. Deschamps and J. Philibert, Eds.), Hermann, Paris, 1966, p. 202.

65. Deslattes, R. D., Air Force Office of Scientific Research Report AFOSR TN-58-784, 1958, 76 p. ASTIA Doc. 202-009.

66. Sweeney, W. R., Seal, R., and Birks, L., Spectrochimica Acta. 17, 1961, p. 365.

67. Wrede, W., Ann. Phys. 36, Ser. 5, 1939, p. 681.

68. Hughes, G. D., Woodhouse, J. B., and Bucklow, I. A., Brit. J. Appl. Phys. Ser. 2, 1, 1968, p. 695.

69. Ershov, O. A., Brytov, I. A., and Lukirskii, A. P., Optics and Spect. (U.S.A.) 22, 1967, p. 66.

70. Lukirskii, A. P., Savinov, E. P., Ershov, O. A., and Shepelev, Y. F., Optics and Spect. (U.S.A.) 16, 1964, p. 168.

71. Jaegle, P., Combet Farnoux, F., Dhez, P., Cremonese, M., and Onori, G., Phys. Letters 26A, 1968, p. 364.

72. Singer, S., J. Appl. Phys. 38, 1967, p. 2897.

73. Jaegle, P., Missoni, G., and Dhez, P., Phys. Rev. Let. 18, 1967, p. 887.

74. Jaegle, P., and Missoni, G., Comp. Rend. Acad. Sci., Paris 262B, 1966, p. 71.

75. Haensel, R., Kunz, C., and Sonntag, B., Phys. Let. 25A, 1967, p. 205.

76. Haensel, R., Kunz, C., Sasaki, T., and Sonntag, B., Appl. Optics 7, 1968, p. 301.

77. Fomichev, V. A. and Lukirskii, A. P., Optics and Spect. (U.S.A.) 22, 1967, p. 432.

78. Lukirskii, A. P. and Zimkina, T. M., Bull. Acad. Sci., U.S.S.R., Phys. Ser. 27, 1963, p. 808.

79. Ederer, D. L., Phys. Rev. Let. 13, 1964, p. 760.

80. Bearden, J. A., Rev. Mod. Phys. 39, 1967, p. 78.

81. Bearden, J. A., "X-ray Wavelengths," N.Y.O. 10586, Fed. Sci. and Tech. Inf. Center, U. S. Department of Commerce, Springfield, Virginia, 1963.

82. Bearden, J. A. and Burr, A. F., Rev. Mod. Phys. 39, 1967, p. 125.

83. Dewey, R. D., "Computed X-ray Wavelengths" and Dewey, R. D., Mapes, R. S. and Reynolds, T. W., "Wavelength Tables," report under Research Project Code 36 XMB-220, Reynolds Metals Co., Richmond, Virginia, 1966.

84. Kemp, J. W., "X-ray Wavelength Tables," Applied Research Laboratories, Inc., Glendale, California, 1963.

85. Moore, Charlotte E., "Atomic Energy Levels" NBS Circ. No. 467, I, 1949, II, 1952, III, 1958, U. S. Government Printing Office.

86. Biermann, H. H., Ann. Physik 26, 1936, p. 740.

87. Dersheim, E. and Schein, M., Phys. Rev. 37, 1931, p. 1238.

88. Tomboulian, D. H., Bedo, D. E. and Neupert, W. M., J. Phys. Chem. Sol. 3, 1957, p. 282.

89. Lukirskii, A. P., Zimkina, T. M. and Brytov, I. A., Opt. and Spect. (U.S.A.) 16, 1964, p. 372.

90. Lukirskii, A. P., Savinov, E. P. and Shepelev, Y. F., Opt. and Spect. (U.S.A.) 15, 1963, p. 290.

91. Bezdenezhnykh, G. V., Zapysov, A. L., Israilev, I. M. and Saprykin, V. N., Opt. and Spect. (U.S.A.) 23, 1967, p. 553.

92. Fomichev, V. A. and Zhukova, I. I., Opt. and Spect. (U.S.A.) 24, 1968, p. 147.

93. Hopkins, J. I., J. Appl. Phys. 30, 1959, p. 185.

94. Ogier, W. T., Lucas, G. J. and Park, B. J., Appl. Phys. Let. 5, 1964, p. 146.

95. Cooke, B. A. and Stewardson, E. A., Brit. J. Appl. Phys. 15, 1964, p. 1315.

96. Tomboulian, D. H. and Pell, E. M., Phys. Rev. 83, 1951, p. 1196.

97. McCrary, J. H., Plassmann, E. H., Puckett, J. M., Conner, A. L. and Zimmermann, G. W., Phys. Rev. 153, 1967, p. 307.

98. Andrews, C. L., Phys. Rev. 54, 1938, p. 994.

99. Woernle, B., Ann. Physik 5, 1930, p. 475.

100. Schmickley, R. D. and Pratt, R. H., Phys. Rev. 164, 1967, p. 104.

101. Cooper, J. W., Phys. Rev. 128, 1962, p. 681.

102. Cooper, J. W., Phys. Rev. Let. 13, 1964, p. 762.

103. Manson, S. T. and Cooper, J. W., Phys. Rev. 165, 1968, p. 126.

104. Herman, F. and Skillman, S., "Atomic Structure Calculations," Prentice-Hall Inc., Englewood Cliffs, New Jersey, 1963.

105. Rau, A. R. P. and Fano, U., Phys. Rev. 167, 1968, p. 7.

106. Colby, J. W., in "Advances in X-ray Analysis," (G. R. Mallett, M. Fay and W. M. Mueller, Eds.), XII. To be published in 1968.

107. Reed, S. J. B. and Long, J. V. P., in "X-ray Optics and X-ray Microanalysis," (H. H. Pattee, V. E. Cosslett and A. Engstrom, Eds.), Academic Press, New York, 1963, p. 317.

108. Birks, L. S., J. Appl. Phys. 29, 1961, p. 387.

109. Reed, S. J. B., Brit. J. Appl. Phys. 16, 1965, p. 913.

110. Duncumb, P. and Shields, P. K., in "X-ray Optics and X-ray Microanalysis," (H. H. Pattee, V. E. Cosslett and A. Engstrom, Eds.), Academic Press, New York, 1963, p. 329.

111. Colby, J. W., Report NLCO-969, National Lead Co. of Ohio, Cincinnati, Ohio, 1964.

112. Fink, R. W., Jopson, R. C., Mark, H., and Swift, C. D., Rev. Mod. Phys. 38, 1966, p. 513.

113. Burhop, E. H. S., J. Phys. Radium 16, 1955, p. 625.

114. Laberrigue, J. and Radvanyi, P., J. Phys. Radium 17, 1956, p. 944.

115. Hagedoorn, H. L. and Wapstra, A. H., Nucl. Phys. 15, 1960, p. 146.

116. Bailey, L. E. and Swedlund, J. B., Phys. Rev. 158, 1967, p. 6.

117. Green, M. and Cosslett, V. E., Proc. Phys. Soc. 78, 1961, 1206.

118. Henoc, J., Thesis, University of Paris. Publication CNET Etude No. 655 PCM, 1963.

119. Henoc, J., Maurice, F., and Kirianenko, A., Rapport CEA-R 2421, 1964.

120. Everhart, T. E., J. Appl. Phys. 31, 1960, p. 1483.

121. Archard, G. D., J. Appl. Phys. 32, 1961, p. 1505.

122. Nakhodkin, N. G., Ostroukhov, A. A., and Romanovskii, V. A., Soviet Physics, Solid State Physics 4, 1962, p. 1112.

123. Cosslett, V. E. and Thomas, R. N., Brit. J. Appl. Phys. 15, 1964, p. 235.

124. Cosslett, V. E. and Thomas, R. N., Brit. J. Appl. Phys. 15, 1964, p. 883.

125. Cosslett, V. E. and Thomas, R. N., Brit. J. Appl. Phys. 15, 1964, p. 1283.

126. Cosslett, V. E. and Thomas, R. N., Brit. J. Appl. Phys. 16, 1965, p. 779.

127. Worthington, C. R. and Tomlin, S. G., Proc. Phys. Soc. A69, 1956, p. 401.

128. Archard, G. D., in "X-ray Optics and Microanalysis," (A. Engstrom, V. Cosslett and H. Pattee, Eds.), Elsevier, Amsterdam, 1960, p. 331.

129. Green, M., Proc. Phys. Soc. 82, 1963, p. 204.

130. Bishop, H. E., Proc. Phys. Soc. 85, 1965, p. 855.

131. Bishop, H. E., Brit. J. Appl. Phys. 18, 1967, p. 703.

132. Webster, D. L., Clark, H., and Hansen, W. W., Phys. Rev. 37, 1931, p. 115.

133. Bethe, H. A., Ann. Phys., Lpz. 5, 1930, p. 325.

134. Mott, N. F. and Massey, H. S. W., "The Theory of Atomic Collisions," Clarendon Press, Oxford University, 1949.

135. Webster, D. L., Hansen, W. W., and Duveneck, F. B., Phys. Rev. 44, 1933, p. 258.

136. Moiseiwitsch, B. L. and Smith, S. J., Rev. Mod. Phys. 40, 1968, p. 238.

137. Glupe, G. and Mehlhorn, W., Phys. Letters 25A, 1967, p. 274.

138. Drawin, H. W., Zeit. fur Phys. 164, 1961, p. 512.

139. Bloch, F., Zeit. fur Phys. 81, 1933, p. 363.

140. Jensen, H., Zeit. fur Phys. 106, 1937, p. 620.

141. Wilson, R. R., Phys. Rev. 60, 1941, p. 749.

142. Duncumb, P. and DaCasa, C., Proc. Second Nat. Conf. on Electron Probe Microanalysis, Boston, Massachusetts, June, 1967.

143. Kulenkampff, H. and Spyra, W., Zeit. fur Phys. 137, 1954, p. 416.

144. Sternglass, E. J., Phys. Rev. 95, 1954, p. 345.

145. Kanter, H., Ann. Phys., Lpz. 20, 1957, p. 144.

146. Bishop, H. E., in "X-ray Optics and Microanalysis," (R. Castaing, P. Deschamps and J. Philibert, Eds.) Hermann, Paris, 1966, p. 153.

147. Weinryb, E. and Philibert, J., Comp. Rend. 258, 1964, p. 4535.

148. Thomas, P. M., U. K. Atomic Energy Research Establishment Report A.E.R.E. No. 4593, Harwell, Berks., England, 1964.

149. Tomlin, S. G., Australian J. of Phys. 17, 1964, p. 452.

150. Duncumb, P. and Shields, P., Brit. J. Appl. Phys. 14, 1963, p. 617.

151. Hansen, M., "Constitution of Binary Alloys," 2nd Edition, McGraw-Hill Book Co., Inc., 1958, p. 704.

152. Brown, J. D., in "The Electron Microprobe," (T. D. McKinley, K. F. J. Heinrich and D. B. Wittry, Eds.) John Wiley and Sons, New York, p. 189.

153. Frazer, J., in Proc. of the First Nat. Conf. on Electron Probe Microanalysis, College Park, Maryland

154. Frazer, J. Z., Fitzgerald, B. W., and Reid, A. M., University of California, LaJolla, California, Report SIO 66, June, 1966.

155. Hobby, M. G. and Wood, G. C., Acta. Met. 75, 1967, p. 143.

156. Lifshin, E. and Hanneman, R. E., General Electric Report No. 66-C-250, Part II, General Electric Co., Schnectady, New York, September, 1966.

157. Beaman, D. R., Proc. Sec. Nat. Conf. on Electron Probe Microanalysis, Boston, Massachusetts, June, 1967.

APPENDIX A

COMPUTER PROGRAM FOR CALCULATION OF DETECTOR SYSTEM DEADTIME

A computer program for the computation of a detector system deadtime is given. The program language is FORTRAN II. The listing is as follows:

```
      DIMENSION XN(100),XMA(100),TITLE(8),R(100)
 1000 READ 1, TITLE
    1 FORMAT (8A4)
      DO 43 J=1,100
      READ 40,XMA(J),XN(J)
   40 FORMAT (F6.5,2X,F6.1)
      IF (XMA(J))99,42,43
   43 CONTINUE
   42 M=J-1
      SXN=0.0
      SR=0.0
      SXNR=0.0
      SXN2=0.0
      DO 30 I=1,M
      SXN=SXN+XN(I)
      R(I)=XN(I)/XMA(I)
      SXNR=SXNR+XN(I)*R(I)
      SXN2=SXN2+XN(I)*XN(I)
   30 SR=SR+R(I)
      C=M
      B=(SXN2*SR-SXNR*SXN)/(C*SXN2-SXN*SXN)
      A=(SXNR-B*SXN)/SXN2
      TAU=A/B
      PRINT 20, TITLE
   20 FORMAT (1H1, 10X, 13HDEADTIME FOR , 8A4///11X, 51HNO.  COUNTS/SEC.
     1   MICROAMPS   COUNTS/MICROAMP SEC. /)
      DO 26 I=1,M
   21 FORMAT (11X,I2,3X,F10.2,3X,F10.6,7X,E12.5)
   26 PRINT 21, I, XN(I), XMA(I), R(I)
      PRINT 22, A, B, TAU
   22 FORMAT (/// 18X,1HA,14X,1HB,10X,8HDEADTIME// 12X,3(E12.5,3X))
      PRINT 23
   23 FORMAT (1H1)
   99 CONTINUE
      GO TO 1000
      END
```

APPENDIX B

COMPUTER PROGRAM FOR NUMERICAL INTEGRATION OF RELATION FOR STOPPING POWER FACTOR

A computer program in FORTRAN II is given for the calculation of numerical values of the Stopping Power factor. The program integrates by numerical methods the relation:

$$K = C \frac{R_u}{R_s} \frac{\int_{E_c}^{E_o} \frac{Q}{S_u} \, d\,E}{\int_{E_c}^{E_o} \frac{Q}{S_s} \, d\,E}$$

The listing is as follows:

```
      COMMON AA,AZ,EO,EC
      DIMENSION TITLE (10)
F     VOLT ,PW17
      RIT7,5, TITLE
 1001 RIT7, 2,Z,ZAV
      RIT7,2, A, AAV
      RIT7,2,EO,EC
      RIT7,2, RA,RAB
      RIT7,2, C
    2 FORMAT (2F10.0)
    5 FORMAT (10A6)
      AZ=Z
      AA=A
      CA1=QUA1(VOLT ,PW17)
      AZ=ZAV
      AA=AAV
      CA2=QUA1(VOLT ,PW17)
      CA=C*RA*CA1/(RAB*CA2)
      WCT6,6,TITLE
      WCT 6,3,Z,ZAV,A,AAV,EO,EC,RA,RAB,C
    6 FORMAT(30H1 ATOMIC NUMBER CORRECTION FOR  ,10A6)
    3 FORMAT(110H      Z            ZAV           A            AAV
     1C          EC           RA           RAB          C          /9E12.6//)
      WCT6,4,CA1,CA2,CA
    4 FORMAT(37H      CA1          CA2          CA       / 3E12.6)
      GO TO 1001
      END


      FUNCTION VOLT(E)
      COMMON AA,AZ,EO, EC
      ER=EO/E
      VOLT     =(AZ*ELOG(EO/(ER+(EO-ER)*E)))/(AA*EO**0.837*(ER+(EO-ER)*E)
     1**0.163*ELOG(2.0*(ER+(EO-ER)*E)/(11.5*AZ)))
      RETURN
      END
```

APPENDIX C

COMPUTER PROGRAM FOR REDUCTION OF RAW MICROPROBE DATA TO COMPOSITION

The complexity of the correction procedures and the necessity for performing the calculations in an iterative manner suggest the use of a digital computer for reduction of raw microprobe data to composition. Several computer programs are available in the literature.[106, 152-157] However, each method either has an extensive input requirement or is limited in application. Brown's[152] program necessitates much looking up of constants in tables, uses a questionable atomic number correction, and by virtue of containing many subroutines, lets the user choose the correction procedure to give him the answer desired. Frazer's program[153,154] and the program of Hobby and Wood[155] do not contain an atomic number correction. Lifshin and Hanneman's program[156] requires much input and is primarily useful only for binary systems. Colby's program,[106] similar in some respects to the present one, uses an inadequate background correction and does not provide for output in the case of an inhomogeneous sample, such as a diffusion couple. Beaman's program[157] is relatively difficult to use, lets the user choose the correction procedure and is applicable particularly to intermediate weight elements.

The goal in writing the present program was to generate a computational method that was most general in character, simple to use and easily adaptable to a time-sharing system when coupled to the now available automatic readout systems for electron microprobes. A minimum of input data is required. All constants necessary for the various calculations are either stored internally or calculated in the program.

In the listing of the program that follows, comment statements can be used to follow the course of the calculation. The constants stored internally are given in Appendix D. The input requirements are outlined in detail in Appendix E and a typical output is given in Appendix F. The program is written in the FORTRAN IV language.

```
C
C
C                    UI MRL MAGIC II PROGRAM
C
C       UI - UNIVERSITY OF ILLINOIS
C
C       MRL - MATERIALS RESEARCH LABORATORY
C
C    MAGIC - MICROPROBE ANALYSIS GENERAL INTENSITY CORRECTION - PROGRAM
C
C                         VERSION II
C
C       PROGRAM CORRECTS RAW MICROPROBE X-RAY INTENSITY DATA FOR DEAD-
C       TIME LOSSES (FIXED-TIME OR FIXED-COUNT), BACKGROUND AS A
C       FUNCTION OF COMPOSITION, ABSORPTION (DUNCUMB-SHIELDS-PHILIBERT),
C       CHARACTERISTIC LINE FLUORESCENCE (REED), ATOMIC NUMBER EFFECTS
C       (DUNCUMB-DUNCUMB & DA CASA), AND INSTRUMENT DRIFT BASED ON BEAM
C       CURRENT. ALL PARAMETERS ARE STORED OR CALCULATED INTERNALLY.
C       AS MANY AS 8 ELEMENTS (AND ONE BY DIFFERENCE) MAY BE ANALYZED.
C       ONLY REQUIRED INPUT ARE ACCELERATING POTENTIAL, CHEMICAL
C       SYMBOLS OF ELEMENTS ANALYZED, AND CHARACTERISTIC LINES USED FOR
C       ANALYSIS. IF DENSITY IS INPUT, MEAN DEPTH OF PENETRATION IS
C       CALCULATED.
C
C
0001        DIMENSION AVR(8),RDEV(8)
0002        DIMENSION AVWP(9),AVAP(9)
0003        DIMENSION WPDEV(9),APDEV(9)
0004        DIMENSION C1(8),ATOM(9)
0005        DIMENSION CO(8),C3(8)
0006        DIMENSION SR(8),FAL(8)
0007        DIMENSION SRSQ(8),ACAL(8)
0008        DIMENSION EC(9),E(8)
0009        DIMENSION Z(9),A(9)
0010        DIMENSION VAL(8),SIGMA(8)
0011        DIMENSION HS(8),US(8)
0012        DIMENSION FS(8),WS(9)
0013        DIMENSION R(9),FACT(8)
0014        DIMENSION FL(9),AP(9)
0015        DIMENSION WP(9),SAP(9)
0016        DIMENSION SWP(9),SAPSQ(9)
0017        DIMENSION SWPSQ(9),SSI(8)
0018        DIMENSION RINT(8)
0019        REAL LIMIT(8)
0020        DIMENSION ASI(8) ,ABGD(8)
0021        DIMENSION XI(8),SI(8)
0022        DIMENSION C(9),PEAK(8)
0023        DIMENSION MPEAK(8),UAL(8)
0024        DIMENSION NAB(8),LINE(9)
0025        DIMENSION ELO(8),STD(8,2)
0026        DIMENSION U(9),TITLE(7)
0027        DIMENSION DATE(4),NAME(5)
0028        DIMENSION LOOP(300),EDGE(9)
0029        DIMENSION WAVE(9),MM(3)
0030        DIMENSION ABET(26),ALPHA(8)
0031        DIMENSION FIDI(8),TAU(8)
0032        DIMENSION TAUM(8),AJR(9)
0033        DIMENSION FYR(9),PF(8)
```

```
0034                DIMENSION BCSUM(8), STDSUM(8)
0035                DIMENSION BCAVG(8), BKUD(8)
0036                DIMENSION XXI(8), BEAM(300)
0037                DIMENSION BC(8,99), STDIT(8,99)
0038                DIMENSION BKSUM(8,8), ABK(8,8)
0039                DIMENSION BR(8,99,8)
0040                DIMENSION AC(8,9),B(8,9)
0041                DIMENSION ROUT(8,300),P(100,36)
0042                DIMENSION NXI(8,300),NSI(8,300)
0043                DIMENSION WPC(9,300),APC(9,300)
                C
                C
                C       INITIALIZATION AND INPUT OF BASIC PARAMETERS
                C
                C
0044                READ 81 ,   ((P(I,J),J=1,11),I=1,100)
0045             81 FORMAT (F7.3,A3,3F6.3,6F7.3)
0046                READ 82,    ((P(I,J),J=12,22),I=1,100)
0047             82 FORMAT (7F7.3,4F5.3)
0048                READ 7, ((P(I,J),J=23,29),I=1,100)
0049              7 FORMAT (F5.3,4F7.3,F10.3,5X,E14.8)
0050                READ 8, ((P(I,J),J=30,36),I=1,100)
0051              8 FORMAT (5E14.8)
0052                READ 5,     (NN(I),I=1,3)
0053              5 FORMAT (3A2)
0054                READ 530,     ST2,LT2
0055            530 FORMAT (A3,A2)
0056                READ 500,     (ABET(I),I=1,26)
0057            500 FORMAT (26A1)
0058                READ 501,     PRFX,NMBR
0059            501 FORMAT (A1,I4)
                C
                C
                C       INPUT PROBLEM DATA
                C
                C
0060              1 READ 2,TAG,NPROB,DATE,NAME,TITLE
0061              2 FORMAT (A1,I4,2X,3A4,A3,2X,5A4,2X,6A4,A1)
0062                READ 88,EQ,NB,TIME,RHO,TI,TMETA,TAUM
0063             88 FORMAT (F4.1,2X,I2,2X,F5.1,2X,2(F5.2,2X),F4.1,2X,8F3.1)
0064                READ 6,(EL(I),LINE(I),I=1,9)
0065              6 FORMAT (9(A3,A2,2X))
                C
                C
                C       DETERMINE NUMBER OF ELEMENTS IN SYSTEM, AND NUMBER ANALYZED
                C
                C
0066                DO 509 I=1,9
0067                IF (EL(I).EQ.ST2) GO TO 518
0068                IF (LINE(I).EQ.LT2) GO TO 510
0069            509 CONTINUE
0070            518 NEL=I-1
0071                NA=I-1
0072                GO TO 511
0073            510 NEL=I
0074                NA=I-1
                C
                C
```

```
                C       ASSIGN PROBLEM NUMBER AND PUNCH CARDS FOR GENERATING CROSS INDEX
                C
                C
CC75              511 IF (NPROB.NE.0) GO TO 502
CC76                  NMBR=NMBR+1
CC77                  IF (NMBR.LE.9999) GO TO 504
CC78                  DO 506 L=1,25
CC79                  IF (ABET(L).EQ.PRFX) GO TO 507
CC80              506 CONTINUE
CC81              507 PRFX=ABET(L+1)
CC82                  NMBR=100
CC83              504 NPROB=NMBR
CC84                  TAG=PRFX
CC85              502 DO 508 M=1,2
CC86             1001 FORMAT (     A1,I4,2X,3A4,A3,2X,5A4,2X,6A4,A1)
CC87              508 WRITE (7,1001)TAG,NPROB,DATE,NAME,TITLE
                C
                C
                C       CHECK FOR X-RAY EMERGENCE ANGLE. IF NONE FURNISHED, ASSUME 52.5
                C       DEGREES
                C
                C
CC88                  IF (THETA.EQ.0.) THETA = 52.5
CC89                  CSC=1./SIN(THETA*3.14159/180.)
                C
                C
                C       DETERMINE OR CALCULATE, FOR EACH ELEMENT ANALYZED, ALL PARAMETERS
                C       NECESSARY FOR CORRECTIONS
                C
                C
CC90                  PRINT 615, TAG, NPROB, DATE
CC91                  PRINT 2000
CC92             2000 FORMAT (//4X,7HELEMENT,3X,7HAT. NO.,5X,7HAT. WT.,4X,2HPF,7X,4HEDGE
                    1,6X,2HEC,7X,4HWAVE,5X,1HU,8X,1HR/)
CC93                  DO 95 K=1,NA
CC94                  DO 102 I=1,100
CC95                  IF (P(I,2).EQ.EL(K)) GO TO 103
CC96              102 CONTINUE
                C
                C
                C       DETERMINE ATOMIC NUMBER AND ATOMIC WEIGHT, AND CALCULATE
                C       FACTOR FOR ATOMIC NUMBER CORRECTION
                C
                C
CC97              103 Z(K)=I
CC98                  A(K)=P(I,1)
CC99                  PF(K)=Z(K)*(14.*(1.-EXP(-.1*Z(K)))+75.5/(Z(K)**(Z(K)/7.5))-Z(K)/(
                    1100.+Z(K)))
C1CC                  NL=3
                C
                C
                C       DETERMINE ANALYTICAL LINE ABSORPTION EDGE, CRITICAL EXCITATION
                C       POTENTIAL AND WAVELENGTH, AND CALCULATE OVERVOLTAGE
                C
                C
C1C1                  DO 4 M=1,2
C1C2                  IF (LINE(K).EQ.MM(M)) GO TO 3
C1C3              4   NL=NL+1
```

```
0104                EDGE(K)=P(I,17)
0105                GO TO 96
0106              3 EDGE(K)=P(I,3*NL)
0107             96 EC(K)=P(I,NL)
0108                WAVE(K)=P(I,NL+3)
0109                U(K)=E0/EC(K)
0110                IF (U(K).GT.20.) U(K)=20.
0111                R(K)=0.
0112                KK=34
                C
                C
                C       DETERMINE OVERVOLTAGE DEPENDENT BACKSCATTER LOSS FACTOR
                C
                C
0113                DO 107 J=1,6
0114                R(K)=U(K)*R(K)+P(I,KK)
0115             107 KK=KK-1
0116                PRINT 2001,EL(K),I    ,A(K),PF(K),EDGE(K),EC(K),WAVE(K),U(K),R(K)
0117            2001 FORMAT (6X,A3,7X,I2,6X,F8.3,2X,F8.3,2X,F7.3,3X,F6.3,3X,F7.3,3X,F5
                   1.2,3X,F8.6)
0118              95 CONTINUE
0119                IF (NEL.EQ.NA) GO TO 98
                C
                C
                C       IF AN ELEMENT IS TO BE DETERMINED BY DIFFERENCE, DETERMINE EXTRA
                C       ELEMENT ATOMIC NUMBER, ATOMIC WEIGHT, CHARACTERISTIC LINE
                C       ABSORPTION EDGE, CRITICAL EXCITATION POTENTIAL AND WAVELENGTH,
                C       AND CALCULATE OVERVOLTAGE AND BACKSCATTER LOSS FACTOR
                C
                C
0120                DO 104 I=1,100
0121                IF (P(I,2).EQ.EL(NEL)) GO TO 105
0122             104 CONTINUE
0123             105 Z(NEL)=I
0124                A(NEL)=P(I,1)
0125                NL=3
0126                DO 100 J=1,2
0127                IF (P(I,NL).LT.E0) GO TO 99
0128             100 NL=NL+1
0129                EDGE(NEL)=P(I,17)
0130                GO TO 101
0131              99 EDGE(NEL)=P(I,3*NL)
0132             101 EC(NEL)=P(I,NL)
0133                WAVE(NEL)=P(I,NL+3)
0134                LINE(NEL)=MM(NL-2)
0135                U(NEL)=E0/EC(NEL)
0136                IF (U(NEL).GT.20.) U(NEL)=20.
0137                R(NEL)=0.
0138                KK=34
0139                DO 108 J=1,6
0140                R(NEL)=U(NEL)*R(NEL)+P(I,KK)
0141             108 KK=KK-1
0142                PF(NEL)=0.
0143                PRINT 2001,EL(NEL),I      ,A(NEL),PF(NEL),EDGE(NEL),EC(NEL),WAVE(NE
                   1L),U(NEL),R(NEL)
                C
                C
                C       CALCULATE ABSORPTION COEFFICIENT MATRIX
```

```
C
0144      98 DO 200 I=1,NEL
C145         DO 200 J=1,NEL
C146         NZ=Z(J)
C147         F=1.0
C148         DO 202 M=9,18
0149         IF (WAVE(I).LT.P(NZ,M))GO TO 203
0150       202 CONTINUE
C151         CON=P(NZ,28)
C152         EX=P(NZ,23)
C153         GO TO 201
C154       203 INTER=M-8
C155         GO TO (204,205,206,207,208,209,210,211,212,213),INTER
0156       204 CON=P(NZ,24)
C157         EX=P(NZ,19)
C158         GO TO 201
C159       205 CON=P(NZ,25)
C16C         EX=P(NZ,20)
0161         GO TO 201
0162       206 F=0.961
C163         GO TO 205
0164       207 F=C.917
C165         GO TO 205
0166       208 CON=P(NZ,26)
0167         EX=P(NZ,21)
0168         GO TO 201
0169       209 F=C.984
C170         GO TO 208
C171       210 F=C.972
C172         GO TO 208
C173       211 F=0.946
C174         GO TO 208
C175       212 F=0.894
C176         GO TO 208
C177       213 CON=P(NZ,27)
C178         EX=P(NZ,22)
           C
           C
           C     CALCULATE ABSORPTION COEFFICIENT OF ELEMENT J FOR I RADIATION
           C
           C
C179       201 AC(I,J)=(CON*WAVE(I)**EX)**F
0180       200 CONTINUE
C181         PRINT 52
0182         IF (NA.LE.3) GO TO 2060
0183         PRINT 648, (EL(I), LINE(I), I=1,NA)
C184         PRINT 646
C185         DO 2050 J=1,NEL
C186         PRINT 668, EL(J), (AC(I,J),I=1,NA)
C187      2C50 CONTINUE
C188         GO TO 2065
0189      2C60 PRINT 647, (EL(I), LINE(I),I=1,NA)
C19C         PRINT 645
C191         DO 2065 J=1,NEL
0192         PRINT 667, EL(J), (AC(I,J),I=1,NA)
C193      2C65 CONTINUE
           C
```

```
C
C       CALCULATE COMMON EXPRESSIONS
C
C
C194          DO 30 I=1,NEL
0195       30 WS(I)=Z(I)/A(I)
C196          PRINT 2002
C197    2002 FORMAT ( //13X,2HWS,8X,3HE,8X,3HVAL,7X,5HSIGMA,6X,2HHS,8X,2HUS,8X,
             12HFS,7X,4HFACT/)
C198          DO 11 I=1,NA
0199          ALPHA(I)=1.
0200          E(I)=(EC(I)+EO)/2.
C201          VAL(I)=7.061+ALOG(E(I))
0202          SIGMA(I)=2.54E+05/(EO**1.5-EC(I)**1.5)
0203          HS(I)=4.5*A(I)/(Z(I)*Z(I))
0204          US(I)=1.+CSC*AC(I,1)/SIGMA(I)
0205          FS(I)=((1.+HS(I))*(1.+1.1*HS(I)/(4.+1.1*HS(I))*CSC*AC(I,1)/SIGMA(I
             1)))/(US(I)*(1.+HS(I)*US(I)))
0206          FACT(I)=FS(I)*R(I)/(HS(I)*(VAL(I)-ALOG(PF(I))))
0207    2003 FORMAT ( 6X,A3,1X,F7.4,3X,F7.4,3X,F7.4,3X,F7.4,3X,F8.2,2X,F7.4,3X,F7.4,3X,
             1F7.4,3X,F8.5)
0208       11 PRINT 2003,EL(I),WS(I),E(I),VAL(I),SIGMA(I),HS(I),US(I),FS(I),FACT
             1(I)
C209          DO 900 I=1,9
0210          FYR(I)=0.
0211          AJR(I)=0.
0212          DO 900 J=1,8
0213      900 B(J,I)=0.
C
C
C       CALCULATE PHILIBERT-LENARD ELECTRON STOPPING POWER
C
C
0214          ESP=.25049E+05-EO*(.24640E+04-EO*(.10164E+03-EO*(.20072E+01-EO*
             1.15447E-01)))
0215          PRINT 2004,ESP
C216    2004 FORMAT (//4X,6HESP = ,E14.8//)
C
C
C       CHECK FOR FLUORESCENCE AND CALCULATE APPROPRIATE FLUORESCENCE
C       YIELDS AND ABSORPTION JUMP RATIOS
C
C
0217          DO 878 K=1,NEL
0218          N=Z(K)
0219          IF (LINE(K).EQ.MM(3)) GO TO 878
0220          IF (LINE(K).EQ.MM(1)) GO TO 876
C221          AJR(K)=P(N,25)*P(N,10)**P(N,20)/(P(N,26)*P(N,12)**P(N,21))
0222          D=-.111065+Z(K)*(.013680-Z(K)*Z(K)*.217720E-06)
0223          GO TO 879
C224      876 AJR(K)=P(N,24)*P(N,9)**P(N,19)/(P(N,25)*P(N,9)**P(N,20))
0225          D=-.037948+Z(K)*(.034256-Z(K)*Z(K)*.116342E-05)
C226      879 D=D*D*D*D
0227          FYR(K)=D/(1.+D)
0228      878 CONTINUE
C229          DO 873 K=1,NA
0230          IF (LINE(K).EQ.MM(3)) GO TO 873
0231          DO 852 I=1,NEL
```

```
0232              IF ((EDGE(K).LE.WAVE(I)).OR.(LINE(I).EQ.MM(3))) GO TO 852
0233              IF (LINE(I).EQ.LINE(K)) GO TO 855
0234              IF (LINE(I).EQ.MM(1)) GO TO 859
0235              GO TO 860
C236          855 FF=.5
C237              GO TO 856
0238          859 FF=.21
0239              GO TO 856
0240          860 FF=1.2
C241          856 FY=FYR(I)
0242              RJ=AJR(K)
                  C
                  C
                  C       CALCULATE FACTOR FOR FLUORESCENCE CORRECTION
                  C
                  C
0243              B(K,I)=FF*FY*(RJ-1.)*A(K)*AC(I,K)/(RJ*A(I))*((U(I)-1.)/(U(K)-1.))*
                 1*1.67
0244              PRINT 2005,EL(I),EL(K),B(K,I)
0245          2005 FORMAT (  4X,24HFLUORESCENCE FACTOR FOR ,A3,13H FLUORESCING ,A3,3H
                 1IS ,F9.6)
C246          852 CONTINUE
0247          873 CONTINUE
0248              DO 901 I=1,8
0249              SAP(I)=0.
C25C              SWP(I)=0.
0251              SAPSQ(I)=0.
C252              SWPSQ(I)=0.
0253              SSI(I)=0.
0254              SR(I)=0.
0255          901 SRSQ(I)=0.
C256              SAP(9)=0.
C257              SAPSQ(9)=0.
C258              SWP(9)=0.
0259              SWPSQ(9)=0.
                  C
                  C
                  C       IF COMPOUND STANDARDS ARE USED INSTEAD OF PURE ELEMENTAL
                  C       STANDARDS, INPUT NECESSARY DATA AND CALCULATE APPROPRIATE
                  C       PARAMETERS TO CORRECT STANDARD DATA USING THE SAME GENERAL
                  C       METHODS OUTLINED
                  C
                  C
0260              IF (N8.EQ.0) GO TO 53
0261              DO 603 K=1,N8
C262              READ 13,ID,STD(K,1),STD(K,2),CS,EL2
C263          13 FORMAT (I2,A6,A1,F6.4,A3)
0264              DO 106 I=1,100
C265              IF (P(I,2).EQ.EL2) GO TO 109
0266          106 CONTINUE
                  C
                  C
                  C       DETERMINE ATOMIC NUMBER AND ATOMIC WEIGHT OF SECOND ELEMENT IN
                  C       COMPOUND STANDARD
                  C
                  C
0267          109 I2=I
C268              A2=P(I,1)
```

```
C269                NL=3
                C
                C
                C       DETERMINE CRITICAL EXCITATION POTENTIAL AND CALCULATE OVER-
                C       VOLTAGE AND BACKSCATTER LOSS FACTOR FOR SECOND ELEMENT IN
                C       COMPOUND STANDARD
                C
                C
C270                DO 110 J=1,2
C271                IF (P(I,NL).LT.EC) GO TO 94
C272            110 NL=NL+1
C273             94 EC2=P(I,NL)
C274                U2=E0/EC2
C275                IF (U2.GT.20.) U2=2C.
C276                R2=C.
C277                KK=34
C278                DO 112 J=1,6
C279                R2=U2*R2+P(I,KK)
C28C            112 KK=KK-1
                C
                C
                C       CALCULATE SECOND ELEMENT ABSORPTION COEFFICIENT
                C
                C
C281                F=1.0
C282                DO 3C2 M=9,18
C283                IF (WAVE(ID).LT.P(I,M)) GO TO 303
C284            302 CONTINUE
C285                CON= P(I,28)
C286                EX= P(I,23)
C287                GO TO 301
C288            303 INTER=M-8
0289                GO TO (304,305,306,307,308,309,310,311,312,3131,INTER
C29C            304 CON= P(I,24)
C291                EX=P(I,19)
C292                GO TC 301
C293            305 CON=P(I,25)
C294                EX=P(I,20)
C295                GO TO 301
C296            306 F=C.961
C297                GC TO 305
C298            307 F=C.917
C299                GO TO 305
C300            308 CON=P(I,26)
03C1                EX=P(I,21)
C3C2                GO TO 301
C3C3            309 F=C.984
C3C4                GO TO 308
C3C5            310 F=C.972
C3C6                GO TO 308
C3C7            311 F=0.946
03C8                GO TO 308
C3C9            312 F=C.894
031C                GO TO 308
0311            313 CON=P(I,27)
0312                EX=P(I,22)
0313            301 AC2=(CON*WAVE(ID)**EX)**F
0314                C2=1.-CS
```

```
0315            WAB=CS*WS(ID)+C2*Z2/A2
                C
                C
                C       CALCULATE OTHER PARAMETERS FOR COMPOUND STANDARD
                C
                C
0316            ZAB=CS*Z(ID)+C2*Z2
0317            PFAB=ZAB*(14.*(1.-EXP(-.1*ZAB))+75.5/(ZAB**(ZAB/7.5))-ZAB/(100.+
               1ZAB))
0318            RAB=CS*R(ID)+C2*R2
0319            ACAB=CS*AC(ID,ID)+C2*AC2
0320            UAB=1.+CSC*ACAB/SIGMA(ID)
0321            HAB=4.5/(ZAB*WAB)
0322            FAB=((1.+HAB)*(1.+1.1*HAB/(4.+1.1*HAB)*CSC*ACAB/SIGMA(ID)))/(UAB*(
               11.+HAB*UAB))
0323            ALPHA(ID)=CS*FAB*RAB/(FACT(ID)*WAB*(VALL(ID)-ALOG(PFAB)))
0324          603 ELO(K)=EL(ID)
                C
                C
                C       CHECK FOR TYPE OF DATA (FIXED-TIME OR FIXED-COUNT) AND
                C       ESTABLISH DEAD-TIME CORRECTION
                C
                C
0325           53 IF (TAG.EQ.ABET(26)) GO TO 331
0326              IF (TIME.EQ.0.) TIME=1.
0327              DO 10 J=1,NA
0328              IF (TAUM(J).EQ.0.) TAUM(J)=1.
0329           10 TAU(J)=1.0E-06*TAUM(J)
                C
                C
                C       READ BEAM CURRENTS AND STANDARD INTENSITIES
                C
                C
0330              DO 5005 J=1,NA
0331              BCSUM(J)=0.
0332              STDSUM(J)=0.
0333              READ 5002,N
0334         5002 FORMAT (I2)
0335              NN=N
0336              DO 5003 K=1,N
0337              READ 5004,BC(J,K),STDI(J,K)
0338         5004 FORMAT (F6.0,2X,F6.0)
0339              IF (BC(J,K).EQ.0.) BC(J,K)=1.
0340              BCSUM(J)=BCSUM(J)+BC(J,K)
                C
                C
                C       DEADTIME CORRECT STANDARD INTENSITIES AND AVERAGE DRIFT
                C       CORRECTED INTENSITIES
                C
                C
0341              STDI(J,K)=STDI(J,K)*TIME/(TIME-TAU(J)*STDI(J,K))
0342         5003 STDSUM(J)=STDSUM(J)+STDI(J,K)
0343              BCAVG(J)=BCSUM(J)/NN
0344              IF (J.EQ.1) BCREF=BCAVG(1)
0345              SI(J)=STDSUM(J)/NN*BCREF/BCAVG(J)
0346         5005 ASI(J)=SI(J)
0347              PRINT 2008
0348         2008 FORMAT (//15X,53HSTANDARD INTENSITIES CORRECTED FOR DEADTIME AND D
```

```
     1RIFT)
C349      PRINT 2009,(EL(J),J=1,NA)
C350 2009 FORMAT (/4X,12HBEAM CURRENT,9(5X,A3,3X))
C351      PRINT 2010,BCREF,(SI(J),J=1,NA)
C352 2010 FORMAT (/7X,F8.1,3X,9(F9.2,2X))
C353      DO 5008 J=1,8
C354      DO 5008 K=1,8
C355 5008 BKSUM(J,K)=0.
C
C
C       READ BEAM CURRENTS AND BACKGROUNDS
C
C
C356      DO 5009 J=1,NA
C357      BCSUM(J)=0.
C358      READ 5002,N
C359      NN=N
C360      DO 5010 K=1,N
C361      READ 5011,BC(J,K),(BK(J,K,L),L=1,NA)
C362 5011 FORMAT (9(F6.0,2X))
C363      IF (BC(J,K).EQ.0.) BC(J,K)=1.
C364      BCSUM(J)=BCSUM(J)+BC(J,K)
C
C
C       DEADTIME CORRECT BACKGROUNDS AND AVERAGE DRIFT-CORRECTED
C       BACKGROUNDS
C
C
C365      DO 5010 L=1,NA
C366      BK(J,K,L)=BK(J,K,L)*TIME/(TIME-TAU(L)*BK(J,K,L))
C367 5010 BKSUM(J,L)=BKSUM(J,L)+BK(J,K,L)
C368      BCAVG(J)=BCSUM(J)/NN
C369      DO 5014 L=1,NA
C370 5014 ABK(J,L)=BKSUM(J,L)/NN*BCREF/BCAVG(J)
C371      BKGD(J)=ABK(J,J)
C372 5009 NAB(J)=ABK(J,J)+.5
C373      PRINT 5100, TIME
C374      IF (NA.LE.3) GO TO 2080
C375      PRINT 5201, (EL(I), LINE(I), I=1,NA)
C376      PRINT 5202
C377      DO 2070 J=1,NA
C378      PRINT 5204, EL(J), (ABK(J,L), L=1,NA)
C379 2070 CONTINUE
C380      GO TO 331
C381 2080 PRINT 5101, (EL(I), LINE(I), I=1,NA)
C382      PRINT 5102
C383      DO 2085 J=1,NA
C384      PRINT 5104, EL(J), (ABK(J,L),L=1,NA)
C385 2085 CONTINUE
C
C
C       READ BEAM CURRENTS AND RAW INTENSITIES FROM UNKNOWN, AND
C       COMPUTE CONCENTRATIONS
C
C
C386  331 SUMSAL=0.
C387      DO 40 I=1,300
C388      ITER=0
```

```
C389                READ 5015, BEAM(I),(XI(J),J=1,NA)
C390          5015 FORMAT (9(F6.0,2X))
C391                IF (BEAM(I).LE.999997.) GO TO 5016
C392                KODE=BEAM(I)-999997.
C393                GO TO 78
C394          5016 IF (TAG.NE.ABET(26)) GO TO 5017
C395                DO 5018 J=1,NA
C396          5018 SI(J)=1.
C397                GO TO 5019
C398          5017 IF (BEAM(I).EQ.0.) BEAM(I)=1.
0399          5019 DO 75 J=1,NA
C4CC                IF (TAG.NE.ABET(26)) GO TO 5020
C4C1                IF (ITER.NE.0) GO TO 22
04C2                GO TO 333
C4C3          5020 IF (ITER.NE.0) GO TO 5023
0404                NSI(J,I)=ASI(J)
                C
                C
                C       DEADTIME AND DRIFT CORRECT UNKNOWN INTENSITIES
                C
                C
C405                XXI(J)=XI(J)*TIME/(TIME-TAU(J)*XI(J))*BCREF/BEAM(I)
C4C6                NXI(J,I)=XXI(J)
                C
                C
                C       CORRECT FOR STANDARD BACKGROUNDS
                C
                C
C4C7                XI(J)=XXI(J)-BKGD(J)
C408                IF (I.EQ.1) SI(J)=SI(J)-BKGD(J)
C4C9                SSI(J)=SSI(J)+SI(J)
C41C                GO TO 333
C411          5023 ABGD(J)=0.
                C
                C
                C       CORRECT FOR CONCENTRATION DEPENDENT BACKGROUNDS
                C
                C
C412                DO 5024 K=1,NA
C413          5024 ABGD(J)=ABGD(J)+C(K)*ABK(K,J)
C414                XI(J)=XXI(J)-ABGD(J)
                C
                C
                C       FORM K-RATIOS
                C
                C
C415           333 RINT(J)=XI(J)/SI(J)
C416                IF (RINT(J).GT..9999) RINT(J)=.9999
C417                IF (RINT(J).LT.0.) RINT(J)=0.
C418                IF (ITER.EQ.0) ROUT(J,I)=RINT(J)+.0005
C419            75 CONTINUE
C42C                IF (ITER.NE.2) GO TO 5030
C421                DO 41 J=1,NA
C422                SR(J)=SR(J)+RINT(J)
C423            41 SRSQ(J)=SRSQ(J)+RINT(J)*RINT(J)
C424          5030 DO 5040 J=1,NA
C425                RINT(J)=ALPHA(J)*RINT(J)
C426                IF (ITER.EQ.0) C(J)=RINT(J)
```

```
C427          5040 CONTINUE
C428            22 ITER=ITER+1
C429               IF (ITER.NE.1) GO TO 5060
C430               DO 5050 J=1,NA
C431               CO(J)=RINT(J)
C432          5050 CONTINUE
C433               GO TO 5070
C434          5060 IF (ITER.LE.2) GO TO 5070
C435               DO 5080 J=1,NA
C436          5080 CO(J)=C(J)
C437          5070 IF (NEL.EQ.NA) GO TO 25
C438               C(NEL)=1.
C439               DO 24 J=1,NA
C440            24 C(NEL)=C(NEL)-C(J)
C441               IF (C(NEL).LT.0.) C(NEL)=0.0
C442            25 RAL=0.
C443               ZAL=0.
C444               WSAL=0.
C445               DO 902 J=1,8
C446               FIDI(J)=0.
C447           902 ACAL(J)=0.
                C
                C
                C       CALCULATE ABSORPTION COEFFICIENTS FOR UNKNOWN
                C
                C
C448               DO 26 K=1,NEL
C449               DO 26 J=1,NEL
C450               ACAL(K)=ACAL(K)+C(J)*AC(K,J)
C451               IF (ACAL(K).LE.0.) ACAL(K)=.0000001
C452               IF(ACAL(K).GT.100000.) ACAL(K)=100000.0
C453            26 CONTINUE
                C
                C
                C       CALCULATE BACKSCATTER LOSS FACTOR, MEAN ATOMIC NUMBER AND MEAN
                C       Z / A FOR UNKNOWN
                C
                C
C454               DO 27 J=1,NEL
C455               RAL=RAL+R(J)*C(J)
C456               ZAL=ZAL+Z(J)*C(J)
C457            27 WSAL=WSAL+WS(J)*C(J)
C458               HAL=4.5/(ZAL*WSAL)
C459               PAL=ZAL*(14.*(1.-EXP(-.1*ZAL))+75.5/(ZAL**(ZAL/7.5))-ZAL/(100.+ZAL
                  1))
                C
                C
                C       CALCULATE CONCENTRATIONS
                C
                C
C460               DO 28 K=1,NA
C461               UAL(K)=1.+CSC*ACAL(K)/SIGMA(K)
C462               YP=CSC*ACAL(K)
C463               DO 880 J=1,NEL
C464               Y=YP/ACAL(J)
C465               V=ESP/ACAL(J)
C466           880 FIDI(K)=FIDI(K)+C(J)*B(K,J)/ACAL(J)*(ALOG(1.+Y)/Y+ALOG(1.+V)/V)
C467               FAL(K)=((1.+HAL)*(1.+FIDI(K))*(1.+1.1*HAL/(4.+1.1*HAL))*CSC*ACAL(K)
```

```
                1/SIGMA(K)))/(UAL(K)*(1.+HAL*UAL(K)))
 046E           C(K)=RINT(K)*WSAL*(VAL(K)-ALOG(PAL))*FACT(K)/(FAL(K)*RAL)
 0469           IF (C(K).LT.0.) C(K)=0.0
 C47C           IF(C(K).GT..9999) C(K)=.9999
 C471           IF (ITER.NE.1) GO TO 5090
 0472           C1(K)=C(K)
 C473           GO TO 28
 0474      5C90 IF (ITER.GT.2) C1(K)=C3(K)
 C475           C3(K)=C(K)
 0476           CDEN=CO(K)-2.*C1(K)+C3(K)
 0477           IF (CDEN.LE.0.) CDEN=.0000001
 047E           C(K)=(CO(K)*C3(K)-C1(K)*C1(K))/CDEN
 C479           IF(C(K).GT..9999) C(K)=.9999
 C48C           IF (C(K).LE.0.) C(K)=C3(K)
 0481        28 CONTINUE
             C
             C
             C      TEST FOR CONVERGENCE AND CHECK NUMBER OF ITERATIONS
             C
             C
 C482           IF (ITER.LT.3) GO TO 5019
 C483           DO 85 M=1,NA
 0484           DEL=ABS(C3(M)-C(M))
 0485           IF (DEL.GE..0005) GO TO 86
 C486        85 CONTINUE
 C487           GO TO 87
 C488        86 IF (ITER.LT.20) GO TO 5019
 C489        87 LCOP(I)=ITER
             C
             C
             C      SUM CONCENTRATIONS FOR AVERAGING
             C
             C
 C49C           SWSAL=SWSAL+WSAL
 C491           PRINT 615,TAG,NPROB,DATE
 C492           PRINT 2011,I
 C493     2011 FORMAT (  4X,12HOBSERVATION ,I3)
 C494           DO 31 K=1,NA
 0495           IF (SR(K).LT..0001) SR(K)=.0001
 0496           IF(SRSQ(K).LT..00000001) SRSQ(K)=.00000001
 0497           PRINT 2014,ITER,EL(K),XXI(K),ABGD(K),XI(K),SI(K),SSI(K)
 049E     2014 FORMAT(4X,13HON ITERATION ,I2,6H, FOR ,A3,8H  XXI = ,F9.2,3X,7HABG
                1D = ,F8.2,3X,5HXI = ,F9.2,3X,5HSI = ,F9.2,3X,6HSSI = ,F12.2)
 0499           PRINT 2016,ITER,EL(K),SR(K),SRSQ(K),RINT(K)
 0500     2016 FORMAT ( /4X,13HON ITERATION ,I2,5H FOR ,A3,2X,5HSR = ,F9.6,3X,7HS
                1RSQ = ,F9.6,3X,19HC = RINT X ALPHA = ,F8.6)
 0501           PRINT 2017,EL(K),ACAL(K)
 0502     2017 FORMAT (/4X,38HABSORPTION COEFFICIENT OF UNKNOWN FOR ,A3,12HRADIAT
                1ION = ,F9.1)
 0503           PRINT 2018,RAL,ZAL,WSAL,HAL,PAL
 0504     2018 FORMAT (//4X,19HFOR UNKNOWN, RAL = ,F9.5 ,3X,6HZAL = ,F9.5 ,3X,7HW
                1SAL = ,F9.5 ,3X,6HHAL = ,F9.5 ,3X,6HPAL = ,E14.6/)
 0505           PRINT 2019,EL(K),UAL(K),YP,FIDI(K),FAL(K),C(K)
 0506     2019 FORMAT ( 4X,4HFOR ,A3,11HIN UNKNOWN ,3X,6HUAL = ,F7.4,3X,5HYP = ,F
                112.4,3X,7HFIDI = ,F9.5 ,3X,6HFAL = ,F9.5 ,3X,4HC = ,F8.6)
 C5C7           PRINT 2021,ITER,EL(K),CO(K),C1(K),C3(K),C(K)
 C5C8     2021 FORMAT (4X,13HON ITERATION ,I2,5H FOR ,A3,6H CO = ,F8.6,3X,5HC1 =
                1,F8.6,3X,5HC3 = ,F8.6,3X,8HC-BAR = ,F8.6/)
```

```
0509            WP(K)=100.*C(K)
0510         31 WPC(K,I)=WP(K)
0511            IF (NEL.EQ.NA) GO TO 34
0512            WP(NEL)=100.
0513            DO 33 K=1,NA
0514         33 WP(NEL)=WP(NEL)-WP(K)
0515            IF (WP(NEL).LT.0.) WP(NEL)=0.
0516         34 WPC(NEL,I)=WP(NEL)
0517            DO 35 K=1,NEL
0518         35 ATOM(K)=WP(K)/A(K)
0519            DEN=0.
0520            DO 36 K=1,NEL
0521         36 DEN=DEN+ATOM(K)
0522            DO 40 K=1,NEL
0523            AP(K)=100.*ATOM(K)/DEN
0524            APC(K,I)=AP(K)
0525            SAP(K)=SAP(K)+AP(K)
0526            SAPSQ(K)=SAPSQ(K)+AP(K)*AP(K)
0527            SWP(K)=SWP(K)+WP(K)
0528            SWPSQ(K)=SWPSQ(K)+WP(K)*WP(K)
0529         40 CONTINUE
0530         78 NS=I-1
0531            OBS=NS
0532            IF (NS.GT.1) GO TO 760
0533            DIV=1.
0534            GO TO 765
0535        760 DIV=OBS*OBS*(OBS-1.)
                C
                C
                C     CALCULATE AVERAGE K-RATIOS AND RMS DEVIATIONS
                C
                C
0536        765 DO 42 K=1,NA
0537            AVR(K)=SR(K)/OBS+.00005
0538         42 RDEV(K)=2.*SQRT((OBS*SRSQ(K)-SR(K)*SR(K))/DIV)+.00005
                C
                C
                C     CALCULATE PEAK-TO-BACKGROUND RATIOS AND MINIMUM DETECTABILITY
                C     LIMITS
                C
                C
0539            IF (TAG.EQ.ABET(26)) GO TO 334
0540            DO 730 K=1,NA
0541            PEAK(K)=SI(K)/(ALPHA(K)*BKGD(K))
0542            MPEAK(K)=PEAK(K)
0543            LIMIT (K)= 329./SQRT(SI(K)*PEAK(K))
0544        730 CONTINUE
                C
                C
                C     CALCULATE AVERAGE CONCENTRATIONS
                C
                C
0545        334 DO 43 K=1,NEL
0546            AVWP(K)=SWP(K)/OBS+.005
0547            AVAP(K)=SAP(K)/OBS+.005
0548            WPDEV(K)=2.*SQRT((OBS*SWPSQ(K)-SWP(K)*SWP(K))/DIV)+.005
0549         43 APDEV(K)=2.*SQRT((OBS*SAPSQ(K)-SAP(K)*SAP(K))/DIV)+.005
0550            IF (NEL.EQ.NA) GO TO 76
```

```
C551            AVWP(NEL)=100.0
C552            AVAP(NEL)=100.0
C553            DO 77 K=1,NA
C554            AVWP(NEL)=AVWP(NEL)-AVWP(K)
C555         77 AVAP(NEL)=AVAP(NEL)-AVAP(K)
C556            IF (AVWP(NEL).GE.0.) GO TO 78
C557            AVWP(NEL)=0.
C558            AVAP(NEL)=0.
C
C
C       START OUTPUT OF ALL DATA INCLUDING CONSTANTS CALCULATED
C
C
C559         76 PRINT 615,TAG,NPRCB,DATE
C560        615 FORMAT (1H1,//40X,15HPROBLEM NUMBER ,A1,I4//68X,3A6,A3//)
C561            PRINT 29
C562         29 FORMAT (/17X,6HATOMIC,5X,6HATOMIC,5X,11HBACKSCATTER,5X, 10HEXCITAT
               1ION,5X,10HABSORPTION,5X,11HFLUORESCENT/5X,7HELEMENT,5X,6HNUMBER,5X
               2,6HWEIGHT,7X,6HFACTOR,8X,9HPOTENTIAL,6X,10HJUMP RATIO,8X,5HYIELD//
               3)
C563            DO 39 I=1,NEL
C564            NZ=Z(I)
C565            AJR(I)=AJR(I)+.005
C566            FYR(I)=FYR(I)+.0005
C567            PRINT 38,EL(I),NZ,A(I),R(I),EC(I),AJR(I),FYR(I)
C568         38 FORMAT (7X,A3,8X,I3,5X,F8.3,7X,F5.3,10X,F7.3,8X,F6.2,11X,F5.3)
C569         39 CONTINUE
C570            PRINT 52
C571         52 FORMAT (///33X,28HMASS ABSORPTION COEFFICIENTS)
C572            IF (NA.LE.3) GO TO 637
C573            PRINT 648,(EL(I),LINE(I),I=1,NA)
C574        648 FORMAT (/3X,9HRADIATION,5X,8(A3,A2,6X))
C575            PRINT 646
C576        646 FORMAT (/,4X,8HABSORBER//)
C577            DO 658 J=1,NEL
C578            PRINT 668,EL(J),(AC(I,J),I=1,NA)
C579        668 FORMAT (9X,A3,3X,8(F8.0,4X))
C580        658 CONTINUE
C581            PRINT 5100, TIME
C582            PRINT 5201,(EL(I),LINE(I),I=1,NA)
C583       5201 FORMAT (/ 41X,11HBACKGROUNDS//1X,14HCONTRIBUTED TO,2X,8(A3,A2,6X))
C584            PRINT 5202
C585       5202 FORMAT (/2X,11HBY ICO & CF//)
C586            DO 5203 J=1,NA
C587       5204 FORMAT (9X,A3,3X,8(F6.1,4X))
C588       5203 PRINT 5204,EL(J),(ABK(J,L),L=1,NA)
C589            IF (NS.LE.1) GO TO 73
C590            PRINT 615,TAG,NPRCB,DATE
C591            IF (TIME.EQ.1.) GO TO 626
C592            PRINT 617,(EL(I),I=1,NA)
C593        617 FORMAT (///33X,37HINTENSITIES (CPS X COUNTING INTERVAL)/35X,33HCOR
               1RECTED FOR DEAD-TIME AND DRIFT//6X,8(A3,10X)//)
C594            GO TO 610
C595        626 PRINT 627,(EL(I),I=1,NA)
C596        627 FORMAT (///43X,17HINTENSITIES (CPS)/35X,33HCORRECTED FOR DEAD-TIME
               1 AND DRIFT//6X,8(A3,10X)//)
C597        610 DO 688 I=1,NS
C598            PRINT 698,(NXI(J,I),NSI(J,I),J=1,NA)
```

```
C599          698 FORMAT (1X,8(I7,2H /,I7,1X))
C600          600 CONTINUE
C601              IF (TIME.EQ.1.) GO TO 619
C602              PRINT 620,(NAB(I),I=1,NA)
C603          620 FORMAT(//29X,46HSTANDARD BACKGROUNDS (CPS X COUNTING INTERVAL)//5X
                 1,8(I4,9X))
C604              GO TO 621
C605          619 PRINT 622,(NAB(I),I=1,NA)
C606          622 FORMAT (//39X,26HSTANDARD BACKGROUNDS (CPS)//5X,8(I4,9X))
C607          621 PRINT 623,(TAUN(I),I=1,NA)
C608          623 FORMAT (//40X,24HDEAD-TIME (MICROSECONDS)//6X,8(F3.1,10X))
C609              IF (TIME.EQ.1.) GO TO 625
C610              PRINT 695,TIME
C611          695 FORMAT (//36X,18HCOUNTING INTERVAL ,,F6.1,8H SECONDS)
C612          625 PRINT 15,TAG,NPROB,DATE
C613              PRINT 694,(EL(I),I=1,NA)
C614          694 FORMAT (18X,33HINDIVIDUAL K-RATIOS CORRECTED FOR/17X, 36HDEAD-TIME
                 1, DRIFT AND BACKGROUND ONLY//5X,3HN,4X,8(A3,5X))
C615              DO 568 I=1,NS
C616              PRINT 578,LOOP(I),(ROUT(J,I),J=1,NA)
C617          578 FORMAT (3X,I3,2X,8(F6.4,2X))
C618          568 CONTINUE
C619              IF (NB.EQ.0) GO TO 1000
C620              PRINT 74
C621              PRINT 674,(ELO(K),STD(K,1),STD(K,2),K=1,NB)
C622          674 FORMAT (//17X,A3,37HDETERMINED RELATIVE TO A STANDARD OF ,A4,A1)
C623              GO TO 1000
C624          637 PRINT 647,(EL(I),LINE(I),I=1,NA)
C625          647 FORMAT (/25X,9HRADIATION,5X,3(A3,A2,8X))
C626              PRINT 645
C627          645 FORMAT (/,26X,8HABSORBER//)
C628              DO 657 J=1,NEL
C629              PRINT 667,EL(J),(AC(I,J),I=1,NA)
C630          667 FORMAT (31X,A3,3X,3(F8.0,6X))
C631          657 CONTINUE
C632              PRINT 5100, TIME
C633         5100 FORMAT (////36X,10HCOUNTING INTERVAL ,,F6.1,10H SECONDS)
C634              PRINT 5101,(EL(I),LINE(I),I=1,NA)
C635         5101 FORMAT ( /41X,11HBACKGROUNDS//19X,14HCONTRIBUTED TO,5X,3(A3,A2,8X
                 1))
C636              PRINT 5102
C637         5102 FORMAT (/23X,11HBY 100 X OF//)
C638              DO 5103 J=1,NA
C639         5104 FORMAT (31X,A3,3X,3(F6.1,6X))
C640         5103 PRINT 5104,EL(J),(A0K(J,L),L=1,NA)
C641              IF (NS.LE.1) GO TO 73
C642              PRINT 15,TAG,NPROB,DATE
C643           15 FORMAT (1H1,24X,15HPROBLEM NUMBER ,A1,I4//52X,3A4,A3//)
C644              IF (TIME.EQ.1.) GO TO 643
C645              PRINT 655,(EL(I),I=1,NA)
C646          655 FORMAT (///16X,37HINTENSITIES (CPS X COUNTING INTERVAL)/18X,33HCOR
                 1RECTED FOR DEAD-TIME AND DRIFT//14X,3(A3,16X)///)
C647              GO TO 642
C648          643 PRINT 654,(EL(I),I=1,NA)
C649          654 FORMAT (///26X,17HINTENSITIES (CPS)/18X,33HCORRECTED FOR DEAD-TIME
                 1 AND DRIFT//14X,3(A3,16X)///)
C650          642 DO 697 I=1,NS
C651              PRINT 697,(NXI(J,I),NSI(J,I),J=1,NA)
```

```
0652          697 FORMAT (2X,3(7X,I7,2H /,I7))
C653          687 CONTINUE
C654              IF (TIME.EQ.1.) GO TO 652
C655              PRINT 651,(NAB(I),I=1,NA)
C656          651 FORMAT (//12X,46HSTANDARD BACKGROUNDS (CPS X COUNTING INTERVAL)//1
                 13X,3(I4,15X))
C657              GO TO 665
C658          652 PRINT 537,(NAB(I),I=1,NA)
C659          537 FORMAT (//22X,26HSTANDARD BACKGROUNDS (CPS)//13X,3(I4,15X))
C66C          665 PRINT 664,(TAUM(I),I=1,NA)
C661          664 FORMAT (//23X,24HDEAD-TIME (MICROSECONDS)//14X,3(F3.1,17X))
C662              IF (TIME.EQ.1.) GO TO 663
C663              PRINT 662,TIME
C664          662 FORMAT (//19X,18HCOUNTING INTERVAL=,F6.1,8H SECONDS)
C665          663 PRINT 15,TAG,NPROB,DATE
C666              PRINT 70,(EL(J),J=1,NA)
0667           70 FORMAT (18X,33HINDIVIDUAL K-RATIOS CORRECTED FOR/17X, 36HDEAD-TIME
                1, DRIFT AND BACKGROUND ONLY//9X,1HN,7X,3(A3,13X))
C668              DO 702 I=1,NS
C669              PRINT 71,LOOP(I),(ROUT(J,I),J=1,NA)
C67C           71 FORMAT (7X,I3,5X,3(F6.4,1CX))
C671          7C2 CONTINUE
C672              IF (NB.EQ.0) GO TO 10C8
C673              PRINT 74
C674           74 FORMAT (//30X,10H***NCTE***)
0675              PRINT 51,(ELO(K),STD(K,1),STD(K,2),K=1,NB)
C676           51 FORMAT (//24X,A3,19HDETERMINED RELATIVE/24X,17HTO A STANDARD OF ,
                1A4,A1)
C677         1008 IF (NS.LE.1) GO TO 73
C678              DO 1270 L=1,2
C679              IF (NA.GT.3) GO TO 1200
C68C              PRINT 15,TAG,NPROB,DATE
C681              GO TO 1110
C682         1200 PRINT 615,TAG,NPROB,DATE
0683         1110 PRINT 89,NAME,TITLE
C684              PRINT 66,EO,THETA
C685              IF (TAG.EQ.ABET(26)) GO TO 1130
0686              PRINT 67
0687              DO 1130 K=1,NA
0688              PRINT 68,EL(K),MPEAK(K),LIMIT(K)
C689         1130 CONTINUE
C69C              IF (NA.GT.3) GO TO 1240
C691              PRINT 1150
0692         1150 FORMAT (//23X,20HCHEMICAL COMPOSITION/26X,14HWEIGHT PERCENT/26X,14
                1HATOMIC PERCENT/)
C693              IF (NEL.EQ.NA) GO TO 1152
C694              PRINT 1153,EL(NEL)
C695         1153 FORMAT (19X,A3,24HDETERMINED BY DIFFERENCE/)
C696         1152 PRINT 1154,(EL(K),K=1,NEL)
0697         1154 FORMAT (/3X,3HOBS,9X,4(A3,13X)/)
C698              DO 1170 I=1,NS
C699              PRINT 1160,I,(WPC(K,I),K=1,NEL)
C7CC         1160 FORMAT (/3X,I3,5X,4(F8.3,8X))
C7C1              PRINT 1165,(APC(K,I),K=1,NEL)
C7C2         1165 FORMAT (11X,4(F8.3,8X))
C7C3         1170 CONTINUE
C7C4              GO TO 1270
C7C5         1240 PRINT 1250
```

```
C706          1250 FORMAT (//46X,20HCHEMICAL COMPOSITION/49X,14HWEIGHT PERCENT/49X,14
                  1HATOMIC PERCENT/)
C707                IF (NEL.EQ.NA) GO TO  1252
C708                PRINT 1253,EL(NEL)
C709          1253 FORMAT (42X,A3,24HDETERMINED BY DIFFERENCE/)
C710          1252 PRINT 1254,(EL(K),K=1,NEL)
0711          1254 FORMAT (13X,3HOBS,7X,9(A3,8X)/)
C712                DO 1270 I=1,NS
C713                PRINT 1260,I,(WPC(K,I),K=1,NEL)
0714          1260 FORMAT (/3X,I3,4X,9(F8.3,4X))
C715                PRINT 1265,(APC(K,I),K=1,NEL)
C716          1265 FORMAT (10X,9(F8.3,4X))
C717          1270 CONTINUE
0718            73 DO 69 L=1,2
C719                PRINT 15,TAG,NPROB,DATE
C720                PRINT 89,NAME,TITLE
0721            89 FORMAT (5X,13HSUBMITTED BY ,5A4//5X,14HDESCRIPTION - ,6A4,A1//)
C722                PRINT 49,NS
C723            49 FORMAT (/18X,33HMEAN CHEMICAL COMPOSITION AND TWO/18X, 21HSIGMA LI
                  1MITS BASED ON,I4,9H ANALYSES,///29X,6HWEIGHT,12X,6HATOMIC/16X,7HEL
                  2EMENT,6X,7HPERCENT,11X,7HPERCENT//)
0724                DO 45 K=1,NA
0725                PRINT 44,EL(K),AVWP(K),WPDEV(K),AVAP(K),APDEV(K)
0726            44 FORMAT (18X,A3,2X,F8.3,2H -,F6.3,2X,F8.3,2H -,F6.3/)
C727            45 CONTINUE
0728                IF (NEL.EQ.NA) GO TO 47
0729                PRINT 48,EL(NEL),AVWP(NEL),WPDEV(NEL),AVAP(NEL),APDEV(NEL)
C730            48 FORMAT (18X,A3,1H*,1X,F8.3,2H -,F6.3,2X,F8.3,2H -,F6.3///21X, 26H*
                  1 DETERMINED BY DIFFERENCE)
0731            47 PRINT 64
0732            64 FORMAT  (//5X,65H----------------------------------------------
                  1---------///13X,42HMEAN INTENSITY RATIOS AND TWO SIGMA LIMI
                  2TS//21X,7HELEMENT, 12X,1HK//)
C733                DO 63 K=1,NA
0734                PRINT 65,EL(K),AVR(K),RDEV(K)
C735            65 FORMAT (23X,A3,7X,F6.4,2H -,F7.4)
0736            63 CONTINUE
0737                PRINT 66,EO,THETA
C738            66 FORMAT (///13X,20HACCELERATING VOLTAGE,13X,F5.1,4H KEV//13X, 21HX-
                  1RAY EMERGENCE ANGLE,12X,F5.1,8H DEGREES)
0739                IF (T1.EQ.0.) GO TO 83
C740                PRINT 84,T1
C741            84 FORMAT (/13X,14HFILM THICKNESS,19X,F6.2,8H MICRONS)
                C
                C
                C       CALCULATE DEPTH OF ANALYZED REGION
                C
                C
C742            83 IF (RHO.EQ.0.) GO TO 92
0743                DM=.033*08S/(SWSAL*RHC)*SCRT(EO*EO*EO)+.005
                C
                C
                C       CONTINUE OUTPUTTING OF DATA
                C
                C
C744                PRINT 93,RHC,DM
0745            93 FORMAT (/13X,7HDENSITY,26X,F6.2//13X,24HDEPTH OF ANALYZED REGION,9
                  1X,F6.2,8H MICRONS)
```

```
C746          92 IF (TAG.EQ.ABET(26)) GO TO 69
C747             IF (NA.GT.3) PRINT 15,TAG,NPROB,DATE
C748          747 PRINT 67
C749          67 FORMAT (//13X,44HSTANDARD PEAK-TO-BACKGROUND RATIOS (P/B) AND/17X,
                 134HMINIMUM DETECTABILITY LIMITS (MDL)//16X,7HELEMENT,6X,3HP/B,13X,
                 23HMDL//)
C75C             DO 341 K=1,NA
C751             PRINT 68,EL(K),MPEAK(K),LIMIT(K)
C752          68 FORMAT (18X,A3,5X,I5,2H/1,8X,F7.4,5H WT %//)
C753          341 CONTINUE
C754          69 CONTINUE
                C
                C
                C     CHECK FOR MORE DATA. IF LAST PROBLEM STORE LAST PROBLEM NUMBER
                C     ASSIGNED ON PUNCHED CARD FOR NEXT RUN INPUT
                C
                C
C755             GO TO (1,80), KCDE
C756          80 PRINT 1002,TAG,NPROB
C757          1002 FORMAT (1H1,//10X,27HLAST PROBLEM NUMBER USED IS,1X,A1,I4)
C758             WRITE (7,1003)TAG,NPROB
C759          1003 FORMAT (    A1,I4)
C76C             STOP
C761             END
```

APPENDIX D

INITIALIZATION CONSTANTS

The constants to be stored internally in the computer for use in the program given in Appendix C are given. These data are inserted as part of the input data, immediately following the main program. The list of the data is as follows:

1.008 H	.014						999.	999.	999.
4.003HE	.025						499.	999.	999.
6.939LI	.055			228.			226.5	999.	999.
9.012BE	.111			114.			111.	999.	999.
10.811 B	.188	.005		67.6			65.6	999.	999.
12.011 C	.284	.006		44.7			43.68	999.	999.
14.007 N	.400	.009		31.60			30.99	999.	999.
15.999 O	.532	.007		23.62			23.32	524.	999.
18.998 F	.685	.009		18.32			18.09	398.	999.
20.183NE	.867	.018		14.610			14.302	275.	677.
22.990NA	1.072	.031		11.910			11.569	247.3	398.8
24.312MG	1.303	.049		9.890			9.512	197.3	249.3
26.982AL	1.560	.073		8.339			7.948	142.5	169.49
28.086SI	1.840	.101		7.125			6.738	105.0	123.
30.974 P	2.144	.132		6.157			5.784	81.0	93.7
32.064 S	2.470	.165		5.372			5.019	64.1	75.2
35.453CL	2.820	.200		4.728			4.397	52.1	61.8
39.948AR	3.203	.245		4.192			3.871	43.2	50.2
39.102 K	3.608	.295		3.741			3.437	36.4	41.8
40.080CA	4.038	.346		3.358	36.33		3.070	30.7	35.13
44.956SC	4.489	.402	.007	3.031	31.35		2.762	26.8	30.6
47.900TI	4.965	.455	.004	2.749	27.42		2.497	23.4	26.94
50.942 V	5.464	.513	.002	2.504	24.25		2.269	19.72	23.8
51.996CR	5.989	.575	.002	2.290	21.64		2.070	17.84	21.24
54.938MN	6.538	.640	.003	2.102	19.45		1.896	16.15	19.05
55.847FE	7.111	.707	.004	1.936	17.59		1.743	14.65	17.202
58.933CO	7.710	.779	.003	1.789	15.972		1.608	13.38	15.618
58.710NI	8.332	.854	.004	1.658	14.561		1.488	12.3	14.242
63.540CU	8.980	.933	.002	1.541	13.336		1.381	11.27	13.014
65.370ZN	9.661	1.022	.008	1.435	12.254		1.283	10.06	11.862
69.720GA	10.368	1.117	.017	1.340	11.292		1.196	9.517	10.828
72.590GE	11.104	1.217	.029	1.254	10.436		1.117	8.773	9.924
74.922AS	11.865	1.323	.041	1.176	9.671		1.045	8.107	9.125
78.960SE	12.655	1.434	.054	1.105	8.990		.980	7.503	8.407
79.909BR	13.470	1.553	.069	1.040	8.375		.920	6.959	7.753
83.800KR	14.324	1.677	.089	.980	7.817		.866	6.47	7.168
85.470RB	15.202	1.807	.110	.926	7.318		.816	6.008	6.644
87.620SR	16.107	1.941	.133	.875	6.863		.770	5.592	6.173
88.905 Y	17.038	2.079	.157	.829	6.449		.728	5.217	5.756
91.220ZR	17.999	2.223	.180	.786	6.071		.689	4.879	5.378
92.906NB	18.987	2.371	.205	.746	5.724		.653	4.575	5.031
95.940MO	20.004	2.523	.227	.709	5.407		.620	4.304	4.719
99.000TC	21.047	2.678	.253	.675	5.115		.589	4.058	4.436
101.070RU	22.119	2.838	.279	.643	4.846		.561	3.835	4.180
102.905RH	23.220	3.002	.307	.613	4.597		.534	3.629	3.943
106.400PD	24.348	3.173	.335	.585	4.368		.509	3.437	3.723
107.870AG	25.517	3.351	.398	.559	4.154		.486	3.256	3.516
112.400CD	26.716	3.538	.440	.535	3.956		.464	3.085	3.326
114.82 IN	27.942	3.730	.443	.512	3.772		.444	2.926	3.147
118.690SN	29.195	3.929	.511	.491	3.600		.425	2.777	2.982
121.750SB	30.486	4.132	.528	.470	3.439		.407	2.639	2.830
127.600TE	31.811	4.342	.572	.451	3.289		.309	2.510	2.688
126.904 I	33.167	4.559	.631	.433	3.149		.374	2.388	2.554
131.300XE	34.590	4.782	.672	.416	3.017		.358	2.274	2.429
132.905CS	35.987	5.011	.726	.400	2.892		.345	2.167	2.314
137.340BA	37.452	5.247	.780	.385	2.776		.331	2.068	2.205
138.910LA	38.934	5.484	.832	.371	2.666	14.88	.318	1.978	2.105

140.120CE	40.453	5.723	.883	.357	2.562	14.04	.306	1.893	2.012
140.907PR	42.002	5.963	.926	.344	2.463	13.343	.295	1.814	1.926
144.240ND	43.574	6.209	.973	.332	2.370	12.68	.285	1.739	1.844
147. PM	45.198	6.461	1.027	.320	2.282	12.	.274	1.667	1.768
150.35 SM	46.849	6.717	1.073	.309	2.200	11.47	.265	1.600	1.695
151.96 EU	48.519	6.981	1.126	.298	2.121	10.96	.256	1.538	1.627
157.250GD	50.233	7.243	1.185	.288	2.047	10.46	.247	1.478	1.563
158.924TB	52.002	7.515	1.241	.279	1.977	10.00	.238	1.422	1.502
162.500DY	53.793	7.790	1.295	.270	1.909	9.59	.230	1.369	1.445
164.93 HO	55.619	8.068	1.351	.261	1.845	9.20	.223	1.319	1.391
167.26 ER	57.487	8.358	1.401	.252	1.784	8.82	.216	1.271	1.339
168.934TM	59.380	8.650	1.461	.244	1.727	8.48	.209	1.225	1.289
173.04 YB	61.300	8.944	1.528	.237	1.672	8.149	.202	1.182	1.243
174.97 LU	63.310	9.249	1.589	.229	1.620	7.840	.196	1.140	1.199
178.49 HF	65.310	9.558	1.662	.222	1.570	7.539	.190	1.100	1.155
180.948TA	67.403	9.877	1.743	.215	1.522	7.252	.184	1.061	1.114
183.85 W	69.508	10.200	1.814	.209	1.476	6.983	.178	1.025	1.075
186.20 RE	71.658	10.531	1.890	.203	1.433	6.729	.173	.989	1.037
190.2 OS	73.856	10.868	1.967	.197	1.391	6.490	.168	.956	1.001
192.2 IR	76.101	11.212	2.048	.191	1.351	6.262	.163	.924	.967
195.09 PT	78.381	11.562	2.133	.186	1.313	6.047	.158	.893	.934
196.967AU	80.720	11.921	2.220	.180	1.276	5.840	.154	.864	.903
200.590HG	83.109	12.286	2.313	.175	1.241	5.648	.149	.835	.872
204.37 TL	85.533	12.660	2.408	.170	1.207	5.460	.145	.808	.843
207.19 PB	88.005	13.041	2.502	.165	1.175	5.286	.141	.782	.815
208.980BI	90.534	13.426	2.603	.161	1.144	5.118	.137	.757	.789
210. PO	93.105	13.814	2.683	.156	1.114		.133	.732	.763
210. AT	95.730	14.214	2.787	.152	1.085		.129	.709	.739
222. RN	98.404	14.619	2.892	.148	1.057		.126	.687	.715
223. FR	99.999	15.031	3.000	.144	1.030		.123	.665	.692
226. RA	99.999	15.444	3.105	.140	1.005		.119	.645	.671
227. AC	99.999	15.871	3.219	.136	.980		.116	.625	.650
232.038TH	99.999	16.300	3.325	.133	.956	4.138	.115	.606	.630
231. PA	99.999	16.733	3.436	.129	.933	4.022	.110	.587	.610
238.030 U	99.999	17.165	3.545	.126	.911	3.910	.107	.570	.592
237. NP	99.999	17.610	3.666		.889		.104	.553	.574
244. PU	99.999	18.054	3.778		.868		.102	.537	.557
243. AM	99.999	18.504	3.887		.848		.099	.521	.540
247. CM	99.999	18.930	3.971				.097	.507	.521
247. BK	99.999	19.452	4.132				.091		
251. CF	99.999	19.930	4.253				.091	.475	.491
254. ES	99.999	20.410	4.374				.089	.461	.476
253. FM	99.999	20.900	4.498				.087	.448	.462

			2.335	
			2.786	
			2.652	
			2.852	
			2.661	
999.			2.921	2.365
999.			2.889	2.370
999.			2.850	2.346
999.			2.813	2.390
999.			2.803	2.452
677.491	999.		2.784	2.59
405.	999.		2.851	2.670
250.700	999.		2.780	2.770 1.309
170.490	999.		2.780	2.68 1.34
124.960	999.			

94.000999.								2.773	2.61	1.38	
75.800999.								2.748	2.592	1.42	
61.990	708.462999.							2.847	2.652	1.46	
50.563	490.043999.	846999.846						2.796	2.581	1.520	
42.278	365.572	696.522	696.522999.					2.802	2.54	1.522	
35.491	283.709	488.114	488.114999.					2.810	2.52	1.524	
30.826	230.447	383.842	383.842999.					2.795	2.495	1.526	
27.290	205.606	358.326	358.326999.					2.821	2.478	1.529	
24.172	186.437	327.992	327.992999.					2.847	2.308	2.453	
21.581	167.315	291.720	291.720999.					2.847	2.389	1.926	
19.380	147.772	255.104	255.104999.					2.864	2.660	1.94	
17.525	133.456	229.594	230.000999.					2.836	2.644	1.965	
15.915	123.119	202.000	208.371999.					2.841	2.688	1.98	
14.525	110.895	182.057	188.400999.					2.734	2.693	1.991	
13.288	110.600	159.500	166.000999.					2.734	2.749	1.820	
12.131	91.230	137.000	143.900999.					2.771	2.656	1.85	
11.100	78.419	116.087	120.487	712.534	712.534999.			2.560	2.636	1.88	
10.187	68.878	96.936	102.633	431.989	431.989999.			2.769	2.471	1.915	
9.367	60.924	84.686	88.243	300.924	300.924999.			2.589	2.650	1.97	
8.646	53.556	73.710	76.579	218.661	227.800999.			2.782	2.672	2.05	
7.984	48.336	65.494	68.309	176.863	179.682	399.000	2	2.771	2.647	2.14	
7.392	43.07	55.672	57.989	129.500	139.461	421.000	2	2.626	2.633	2.242	
6.862	38.491	50.114	51.984	110.895	112.403	388.000	2	2.593	2.606	2.34	
6.387	34.680	44.310	46.072	91.838	93.149	317.000	2	2.668	2.791	2.44	
5.962	31.499	39.687	41.286	77.682	78.768	275.600	2	2.578	2.594	2.53	
5.579	28.475	35.565	36.972	66.137	67.185	240.000	2	2.752	2.728	2.583	.40
5.230	26.469	32.709	34.154	59.779	60.597	214.100	2	2.661	2.734	1.923	.48
4.913	24.413	30.084	31.402	53.278	54.201	186.900	2	2.751	2.712	1.99	.70
4.630	22.5	27.578	28.853	47.508	48.140	162.	2.70	2.675	2.19	1.2	
4.369	20.945	25.461	26.511	42.660	43.039	145.500	2	2.613	2.657	2.46	1.46
4.130	19.454	23.342	24.492	38.561	39.286	136.800	2	2.426	2.682	2.55	1.56
3.907	18.109	21.603	22.699	34.941	35.494	122.600	2	2.674	2.701	2.604	1.59
3.700	16.878	20.119	21.061	30.82	31.14	110.500	2	2.427	2.700	2.393	.385
3.505	15.874	18.603	19.614	28.13	29.50	101.000	2	2.469	2.703	2.574	1.60
3.324	14.764	17.314	18.285	26.718	27.166	91.100	2	2.396	2.701	2.55	1.60
3.156	13.867	16.050	17.200	24.28	24.90	85.800	2	2.656	2.702	2.500	1.593
3.000	13.020	15.072	16.014	22.699	23.114	76.600	2	2.475	2.618	2.37	1.48
2.856	12.275	14.186	15.080	21.124	21.528	72.000	2	2.526	2.644	2.16	1.26
2.720	11.575	13.345	14.193	19.660	20.050	66.900	2	2.453	2.648	1.94	.92
2.593	10.8	12.410	13.232	17.8	18.441	60.1	2.44	2.616	1.880	.757	
2.474	10.186	11.641	12.428	16.766	17.089	53.718	2	2.435	2.609	1.92	.83
2.363	9.590	10.907	11.672	15.560	15.890	49.004	2	2.415	2.657	1.96	.90
2.261	9.108	10.294	11.036	14.612	14.907	45.851	2	2.375	2.606	2.04	1.24
2.166	8.642	9.741	10.459	13.756	14.036	42.811	2	2.326	2.615	2.13	1.44
2.079	8.205	9.270	9.975	13.122	13.394	40.716		2.617	2.28	1.72	
1.997	7.870	8.838	9.556	12.459	12.737	39.334		2.611	2.43	1.95	
1.919	7.55	8.426	9.137	11.791	12.073	37.6		2.61	2.58	2.12	
1.846	7.196	8.047	8.732	11.288	11.552	35.864		2.623	2.722	2.26	
1.776	6.888	7.682	8.374	10.711	11.013	34.420		2.674	2.746	2.36	
1.712	6.592	7.344	8.030	10.186	10.461	32.991		2.711	2.755	2.4	
1.650	6.301	7.014	7.694	9.724	9.989	31.159		2.740	2.685	2.39	
1.592	6.057	6.732	7.399	9.304	9.574	29.782		2.755	2.664	2.38	
1.537	5.825	6.448	7.120	8.910	9.174	28.456		2.760	2.632	2.37	
1.484	5.619	6.181	6.843	8.601	8.847	27.606		2.768	2.601	2.36	
1.433	5.374	5.933	6.579	8.186	8.487	26.284		2.769	2.600	2.35	
1.386	5.170	5.706	6.359	7.865	8.115	25.448		2.763	2.568	2.34	
1.341	4.977	5.477	6.127	7.562	7.805	24.492		2.764	2.558	2.32	

1.297	4.767	5.241	5.882	7.223	7.461	23.040	2.7442.5332.31
1.255	4.585	5.020	5.650	6.870	7.110	21.9242.5172.6132.5892.30	
1.216	4.407	4.815	5.435	6.590	6.830	20.8372.0432.6682.5412.28	
1.177	4.236	4.620	5.234	6.330	6.560	19.837	2.7252.51 2.25
1.141	4.071	4.433	5.043	6.073	6.300	18.949	2.7622.4922.22
1.106	3.915	4.260	4.861	5.830	6.050	17.966	2.7032.4682.17
1.072	3.762	4.093	4.686	5.590	5.810	17.172	2.6532.5202.06
1.040	3.616	3.936	4.518	5.374	5.584	16.339	2.5112.5282.068
1.009	3.478	3.783	4.355	5.157	5.360	15.492	2.5952.4742.12
.979	3.346	3.634	4.198	4.952	5.153	14.664	2.6992.3332.19
.951	3.217	3.492	4.047	4.757	4.955	13.874	2.6012.4562.280
.923	3.094	3.359	3.904	4.572	4.764	13.2152.2282.5872.5272.313	
.898	2.988	3.217	3.755	4.431	4.621	12.457	2.60 2.36 2.24
.872	2.872	3.093	3.619	4.262	4.449	11.898	2.82 2.18 2.09
.848	2.766	2.981	3.504	4.103	4.286	11.301	2.6532.1471.92
.825	2.665	2.865	3.385	3.953	4.133	10.753	2.6852.15 1.82
.803	2.571	2.762	3.270	3.817	3.993	10.260	2.7272.1541.76
.781	2.479	2.663	3.172	3.679	3.852	9.770	2.7152.28 1.73
.761	2.392	2.567	3.068	3.557	3.729	9.325	2.6892.6471.74
.741	2.310	2.479	2.970	3.433	3.602	8.938	2.66 1.81
.722	2.235	2.392	2.884	3.333	3.497	8.605	3.1472.6761.888
.704	2.166	2.310	2.796	3.220	3.382	8.262	2.74 1.95
.687	2.090	2.237	2.721	3.121	3.282	7.955	2.8192.03
.670	2.026	2.171	2.656	3.030	3.190	7.667	2.82 2.08
.655	1.972	2.103	2.584	2.933	3.122	7.546	2.83 2.13
.637	1.891	2.017	2.491	2.840	3.000	7.064	2.84 2.17
.622	1.836	1.950	2.427	2.757	2.915	6.892	2.85 2.22
.607	1.777	1.886	2.361	2.678	2.834	6.637	2.86 2.25
.593	1.721	1.825	2.297	2.601	2.756	6.401	2.87 2.27

.084			.10059716E+01
.250			.10085924E+01
.404			.10119003E+01
.889			.10153530E+01
1.350	.295		.10194915E+01
2.311	.471		.10240062E+01
3.529	.818		.10284504E+01
4.943	.904		.10335616E+01
7.322	1.098		.10390856E+01
9.322	.80		.10442539E+01
11.601	.700		.10499690E+01
14.87	1.110	7.338	.10555707E+01
18.122	1.88	8.5	.10614998E+01
22.020	2.6	10.0	.10669828E+01
27.626	3.330	11.2	.10730918E+01
27.864	3.548	12.5	.10785874E+01
35.312	4.567	13.715	.10843181E+01
42.038	5.8	15.	.10905935E+01
48.678	7.3	16.8	.10957055E+01
54.052	8.8	18.1	.11017059E+01
60.083	10.927	19.593	.11071056E+01
64.977	12.056	.742	.11122901E+01
77.899	12.661	6.095	.11173825E+01
83.305	10.979	6.4	.11228172E+01
97.144	12.734	6.8	.11276960E+01
108.210	14.322	7.2	.11322652E+01
117.098	15.520	7.839	.11371081E+01

	123.080	15.783	18.830			.11413858E+01
	146.550	19.124	18.2			.11459289E+01
	142.035	20.238	17.0			.11499011E+01
	169.094	24.425	16.246			.11536316E+01
	156.083	24.434	14.6			.11573735E+01
	188.918	26.852	13.5			.11614852E+01
	207.363	29.204	12.0			.11647602E+01
	209.178	32.008	10.150			.11681141E+01
	217.375	35.425	9.2			.11709942E+01
	238.313	34.296	8.6			.11741591E+01
	261.398	42.122	7.8			.11770344E+01
	277.847	41.921	7.356	6.		.11796616E+01
	291.277	44.976	22.304	8.		.11822350E+01
	325.568	49.133	20.0	14.		.11845544E+01
	332.	53.	18.4	18.		.11865519E+01
	338.246	57.048	15.0	28.		.11891662E+01
	266.121	60.395	13.0	66.		.11910259E+01
	380.209	62.906	11.593	155.		.11927648E+01
	278.270	66.473	18.157	1478.19		.11947537E+01
	325.561	70.806	14.947	108.		.11963426E+01
	291.804	75.185	16.8	44.		.11979680E+01
	429.243	79.510	20.595	34.465		.11993455E+01
	360.505	87.573	30.1	51.8		.12009454E+01
	428.535	90.994	57.0	86.		.12018723E+01
	391.501	94.983	74.0	156.		.12033243E+01
	393.	102.108	83.443	403.675		.12043491E+01
	396.	107.580	76.	340.		.12050691E+01
	400.642	108.976	64.	259.		.12067255E+01
	406.	117.488	52.	210.		.12073447E+01
	415.658	128.292	42.	155.		.12081746E+01
		133.322	36.	120.		.12092015E+01
		138.475	31.8	81.		.12099530E+01
		143.5	30.8	57.		.12105282E+01
		150.262	30.254	34.		.12112746E+01
		164.053	31.414	19.5		.12120670E+01
		171.439	32.195	9.0		.12127263E+01
		182.478	35.891	5.0		.12127321E+01
		191.747	37.859	4.0		.12133597E+01
		203.031	40.695	6.0		.12139165E+01
		210.729	42.976	8.8		.12146045E+01
		222.047	45.248	9.9		.12148826E+01
		227.861	47.589	11.8		.12153547E+01
		239.732	50.412	14.5		.12156483E+01
	.018	247.226	53.018	16.2	19900.	.12154626E+01
	.018	785.744	221.796	53.096	18.4	19011.799	.12159731E+01
	.018	344.007	244.065	55.507	21.0	18100.	.12160668E+01
	.067		271.	60.5	23.0	17300.	.12162942E+01
	.017		290.700	63.573	25.5	16500.	.12164937E+01
	.016		291.982	67.423	27.6	15700.	.12164491E+01
	.016		277.059	66.215	27.8	14935.4	.12166268E+01
	.043		241.237	70.331	27.626	10444.5	.12165546E+01
	.058		290.	75.655	24.6	9100.	.12168429E+01
	.073		342.330	85.413	21.0	7800.	.12163713E+01
	.088		311.716	81.287	20.128	6500.	.12165291E+01
	.106	631.182	325.828	82.053	20.591	5216.8	.12163066E+01
			348.	82.	23.0		.12162152E+01
			371.	96.	27.5		.12159503E+01

	394.339112.607	36.0	.12157646E+01
	420. 117.	47.0	.12154985E+01
	440.969121.092	57.0	.12152714E+01
	441. 114.	62.0	.12147656E+01
	441.914108.024	58.0	.12144476E+01
	108.	51.0	.12141881E+01
	649.224108.019	46.169	.12136381E+01
	122.	47.0	.12132737E+01
	144.388	48.	.12129561E+01
	155.	51.	.12121884E+01
	164.	56.	.12120564E+01
	166.	63.	.12119586E+01
	169.5	67.	.12116752E+01
	173.	74.	.12112705E+01
	175.	80.	.12111340E+01
-.51088316E-02	.11210435E-02	-.11886647E-03	.58783242E-05	-.10814593E-06
-.72186773E-02	.14225237E-02	-.14111194E-03	.66914334E-05	-.11980721E-06
-.10267103E-01	.19859984E-02	-.19498321E-03	.91950086E-05	-.16415866E-06
-.14245915E-01	.28139927E-02	-.28115056E-03	.13437614E-04	-.24230877E-06
-.18509077E-01	.36845955E-02	-.36908566E-03	.17648433E-04	-.31814958E-06
-.23691260E-01	.48299260E-02	-.49167519E-03	.23763519E-04	-.43147057E-06
-.29437536E-01	.61336917E-02	-.63336010E-03	.30898163E-04	-.56450902E-06
-.35199645E-01	.74029719E-02	-.76721501E-03	.37474758E-04	-.68485599E-06
-.41864668E-01	.89623354E-02	-.93928950E-03	.46210926E-04	-.84851560E-06
-.49116674E-01	.10703541E-01	-.11347223E-02	.56245418E-04	-.10379369E-05
-.56049932E-01	.12310884E-01	-.13096993E-02	.65021871E-04	-.12007774E-05
-.63725327E-01	.14165786E-01	-.15179592E-02	.75701781E-04	-.14020896E-05
-.71366790E-01	.15998293E-01	-.17221066E-02	.86106469E-04	-.15973207E-05
-.79481274E-01	.17990243E-01	-.19476971E-02	.97735780E-04	-.18172649E-05
-.87160478E-01	.19826558E-01	-.21511784E-02	.10805634E-03	-.20101768E-05
-.95653455E-01	.21945888E-01	-.23934259E-02	.12061385E-03	-.22485051E-05
-.10350848E+00	.23847385E-01	-.26056661E-02	.13142934E-03	-.24513122E-05
-.11171634E+00	.25877884E-01	-.28357954E-02	.14327977E-03	-.26751226E-05
-.12063543E+00	.28167495E-01	-.31023590E-02	.15726737E-03	-.29428023E-05
-.12824497E+00	.30004786E-01	-.33062601E-02	.16760104E-03	-.31357012E-05
-.13696853E+00	.32247548E-01	-.35671998E-02	.18128080E-03	-.33972816E-05
-.14503823E+00	.34273003E-01	-.37984821E-02	.19324300E-03	-.36238338E-05
-.15291678E+00	.36249918E-01	-.40240545E-02	.20490146E-03	-.38444980E-05
-.16072637E+00	.38216675E-01	-.42489089E-02	.21653708E-03	-.40649144E-05
-.16898749E+00	.40360370E-01	-.44993224E-02	.22969026E-03	-.43166779E-05
-.17663502E+00	.42308407E-01	-.47236572E-02	.24135446E-03	-.45383465E-05
-.18395179E+00	.44157222E-01	-.49350727E-02	.25228900E-03	-.47453615E-05
-.19162687E+00	.46154730E-01	-.51685157E-02	.26454822E-03	-.49799279E-05
-.19865794E+00	.47943894E-01	-.53739211E-02	.27519705E-03	-.51818324E-05
-.20602707E+00	.49873145E-01	-.56000292E-02	.28708913E-03	-.54095794E-05
-.21274769E+00	.51595238E-01	-.57985500E-02	.29740763E-03	-.56055462E-05
-.21919369E+00	.53240969E-01	-.59875816E-02	.30720443E-03	-.57912005E-05
-.22566990E+00	.54918897E-01	-.61823635E-02	.31737469E-03	-.59849446E-05
-.23259096E+00	.56772842E-01	-.64027040E-02	.32906669E-03	-.62101742E-05
-.23852883E+00	.58300778E-01	-.65788492E-02	.33821274E-03	-.63836742E-05
-.24456601E+00	.59884886E-01	-.67641096E-02	.34793033E-03	-.65693493E-05
-.25004521E+00	.61292189E-01	-.69259326E-02	.35631479E-03	-.67281488E-05
-.25585394E+00	.62832701E-01	-.71071974E-02	.36585778E-03	-.69109125E-05
-.26131735E+00	.64271190E-01	-.72754737E-02	.37467921E-03	-.70793358E-05
-.26647808E+00	.65619559E-01	-.74320953E-02	.38284496E-03	-.72346212E-05
-.27157351E+00	.66965836E-01	-.75897928E-02	.39111550E-03	-.73925414E-05
-.27634956E+00	.68213686E-01	-.77345390E-02	.39865139E-03	-.75356829E-05

-.28073135E+00	.69337986E-01	-.78629577E-02	.40525732E-03 -.76600255E-05
-.28582501E+00	.70728039E-01	-.80292836E-02	.41410562E-03 -.78306480E-05
-.29001167E+00	.71814000E-01	-.81541870E-02	.42055995E-03 -.79525070E-05
-.29403845E+00	.72858135E-01	-.82741686E-02	.42675539E-03 -.80694276E-05
-.29833832E+00	.74010390E-01	-.84098331E-02	.43388315E-03 -.82056114E-05
-.30214063E+00	.74997904E-01	-.85231436E-02	.43972127E-03 -.83155561E-05
-.30597373E+00	.76011294E-01	-.86410743E-02	.44586206E-03 -.84321089E-05
-.30948495E+00	.76919693E-01	-.87447947E-02	.45118255E-03 -.85319524E-05
-.31323346E+00	.77921045E-01	-.88619773E-02	.45730311E-03 -.86483225E-05
-.31616897E+00	.78646785E-01	-.89414513E-02	.46124204E-03 -.87202754E-05
-.31969356E+00	.79586642E-01	-.90510780E-02	.46695028E-03 -.88285401E-05
-.32269303E+00	.80351500E-01	-.91369988E-02	.47129456E-03 -.89091177E-05
-.32530877E+00	.80987026E-01	-.92051589E-02	.47460651E-03 -.89685980E-05
-.32900290E+00	.82008486E-01	-.93273969E-02	.48108620E-03 -.90930449E-05
-.33145460E+00	.82601088E-01	-.93905135E-02	.48413154E-03 -.91473912E-05
-.33412717E+00	.83274589E-01	-.94650044E-02	.48784260E-03 -.92153709E-05
-.33701012E+00	.84027757E-01	-.95508860E-02	.49222640E-03 -.92972007E-05
-.33954821E+00	.84664835E-01	-.96209508E-02	.49569756E-03 -.93604821E-05
-.34185234E+00	.85223639E-01	-.96803460E-02	.49855117E-03 -.94111708E-05
-.34432934E+00	.85842550E-01	-.97478971E-02	.50187197E-03 -.94713033E-05
-.34684918E+00	.86483371E-01	-.98189606E-02	.50541124E-03 -.95360534E-05
-.34919348E+00	.87066345E-01	-.98822445E-02	.50850526E-03 -.95918031E-05
-.35074655E+00	.87372330E-01	-.99069973E-02	.50934814E-03 -.96014296E-05
-.35301387E+00	.87932134E-01	-.99672026E-02	.51226411E-03 -.96535270E-05
-.35518044E+00	.88459059E-01	-.10022944E-01	.51492216E-03 -.97003808E-05
-.35747831E+00	.89032813E-01	-.10085205E-01	.51795940E-03 -.97549566E-05
-.35927929E+00	.89432565E-01	-.10123148E-01	.51957029E-03 -.97802358E-05
-.36129036E+00	.89909138E-01	-.10172039E-01	.52182953E-03 -.98188980E-05
-.36307709E+00	.90307205E-01	-.10209906E-01	.52343928E-03 -.98441771E-05
-.36428614E+00	.90505087E-01	-.10220125E-01	.52344112E-03 -.98366117E-05
-.36629296E+00	.90982954E-01	-.10269137E-01	.52570012E-03 -.98781434E-05
-.36780074E+00	.91288432E-01	-.10294398E-01	.52658101E-03 -.98855786E-05
-.36944046E+00	.91638452E-01	-.10325525E-01	.52778792E-03 -.99024313E-05
-.37103485E+00	.91975714E-01	-.10355106E-01	.52891343E-03 -.99177449E-05
-.37232571E+00	.92206793E-01	-.10369838E-01	.52916608E-03 -.99150840E-05
-.37385404E+00	.92521425E-01	-.10396121E-01	.53009035E-03 -.99261452E-05
-.37506964E+00	.92727292E-01	-.10407283E-01	.53013042E-03 -.99190754E-05
-.37668731E+00	.93074957E-01	-.10438065E-01	.53130967E-03 -.99352238E-05
-.37738192E+00	.93098117E-01	-.10423582E-01	.52983961E-03 -.98970312E-05
-.37879579E+00	.93375409E-01	-.10444441E-01	.53043021E-03 -.99009704E-05
-.37972521E+00	.93481251E-01	-.10441243E-01	.52960782E-03 -.98758739E-05
-.38078480E+00	.93635483E-01	-.10444841E-01	.52918176E-03 -.98588646E-05
-.38159628E+00	.93700760E-01	-.10435839E-01	.52801171E-03 -.98265157E-05
-.38245741E+00	.93781724E-01	-.10428664E-01	.52693158E-03 -.97957581E-05
-.38317627E+00	.93812360E-01	-.10414347E-01	.52542786E-03 -.97562349E-05
-.38389147E+00	.93841810E-01	-.10399708E-01	.52389703E-03 -.97160336E-05
-.38422579E+00	.93736706E-01	-.10366139E-01	.52125106E-03 -.96528487E-05
-.38470337E+00	.93676237E-01	-.10338166E-01	.51890823E-03 -.95955598E-05
-.38518653E+00	.93618256E-01	-.10310387E-01	.51656750E-03 -.95381665E-05
-.38523503E+00	.93400300E-01	-.10259642E-01	.51286035E-03 -.94524679E-05
-.38541494E+00	.93224969E-01	-.10214321E-01	.50944720E-03 -.93724564E-05
-.38554613E+00	.93025953E-01	-.10165031E-01	.50577736E-03 -.92868621E-05
-.38503845E+00	.92596007E-01	-.10082920E-01	.50016376E-03 -.91610925E-05
-.38515389E+00	.92377917E-01	-.10029531E-01	.49619830E-03 -.90686893E-05
-.38516918E+00	.92113527E-01	-.99686511E-02	.49175586E-03 -.89659814E-05
-.38481991E+00	.91711352E-01	-.98877062E-02	.48610989E-03 -.88382291E-05
-.38416494E+00	.91188823E-01	-.97887816E-02	.47936677E-03 -.86873630E-05
-.38363713E+00	.90693381E-01	-.96920228E-02	.47269105E-03 -.85370969E-05

KALAMA

ABCDEFGHIJKLMNOPQRSTUVWXYZ
A1129

APPENDIX E

SPECIFICATION FOR INPUT OF DATA

Specifications for input data for reduction of probe intensity ratios to composition are given. A minimum of four cards in addition to the data are used. The formats of the various cards are given below.

First Card

Column		Format
1- 5	Problem Number, or blank	A1, I4; if blank, assigned by computer
6- 7	Blank	2X
8-22	Date of Analysis	15A1 (3A4,A3)
23-24	Blank	2X
25-44	Name of Person Submitting Problem	5A4
45-46	Blank	2X
47-71	Description of Sample	25A1 (6A4,A1)

Second Card

1- 4	Accelerating Voltage (Kev)	F4.1
5- 6	Blank	2X
7- 8	Number of Compound Standards (If blank, elemental standards assumed)	I2 (Number is right justified)
9-10	Blank	2X
11-15	Counting Interval (seconds)	F5.1 (If blank, 1.0 sec. assumed)
16-17	Blank	2X
18-22	Density of Sample (g/cc)	F5.2 (May be left blank)
23-24	Blank	2X
25-29	Film Thickness in Micrometers, If Analysis of Thin Film	F5.2 (May be left blank)
30-31	Blank	2X
32-35	X-ray Emergence Angle (degrees)	F4.1 (If blank, 52.5° assumed)
36-37	Blank	2X
38-40	Deadtime for Element #1 (Microsec.)	F3.1 (If blank, 1.0 microsec. assumed)
41-43	Deadtime for Element #2 (Microsec.)	F3.1 " " "
44---	Above Deadtime Repeated for Each Element Analyzed	

Third Card

1- 2	First Element Analyzed, Chemical Symbol	A2
3	Blank	1X
4- 5	First Element Analytical Line (KA, LA, MA)	A2
6- 7	Blank	2X
8- 9	Second Element Analyzed, Chemical Symbol	A2
10	Blank	1X
11-12	Second Element Analytical Line	A2
13-14	Blank	2X

15--- Repetition of Above Cycle for All Elements

If one more element present than is analyzed, and that element is to be determined by difference, its chemical symbol is listed last without an analytical line.

Chemical symbols are right justified, in their field. Analytical lines are KA, LA or MA. A typical sequence follows: NB_LA__ZR_LA___N_KA___O

Fourth Card(s) if Required

1- 2	Number of Element in List on Third Card to Which Compound Standard Applies	I2 (Right justified)
3- 7	Standard Name	5A1 (A4,A1)
8-13	Weight Percent of Element in Binary Compound Standard	F6.4
14-15	Chemical Symbol of Other Element in Compound Standard	A2 (Right justified)

A separate card is required for each element for which a binary compound standard is used, the total number of cards being equal to "Number of compound standards" on second card.

Standards Data

Column		Format
	First Card	
1- 2	Number of Observations on Standard	I2
	Other Cards	
1- 6	Beam Current	F6.0
7- 8	Blank	2X
9-14	Standard Counts	F6.0

The above cycle is repeated for each element on the third card, in the order of elements listed on that card.

The total number of sets of standard data must be equal to the total number of elements analyzed.

Background Data

Column		Format
	Background Data from First Standard	
	First Card	
1- 2	Number of Background Observation Taken on First Standard	I2 (Right justified)
	Other Cards	
1- 6	Beam Current	F6.0
7- 8	Blank	2X
9-14	Background Taken on First Standard Contributed to First Analytical Line	F6.0
15-16	Blank	2X
17-22	Background Taken on First Standard Contributed to Second Analytical Line	F6.0
23-24	Blank	2X
25-30	Background Taken on First Standard Contributed to Third Analytical Line	F6.0
31-32	Blank	2X
33---	The Above Cycle Is Repeated for Contribution of First Standard to Other Analytical Lines	

The number of these cards must equal the number of observations for background on first standard.

Background Data from Second Standard

First Card

1- 2	Number of Background Observations Taken on Second Standard	I2 (Right justified)

Other Cards

1- 6	Beam Current	F6.0
7- 8	Blank	2X
9-14	Background Taken on Second Standard Contributed to First Analytical Line	F6.0
15-16	Blank	2X
17-22	Background Taken on Second Standard Contributed to Second Analytical Line	F6.0
23-24	Blank	2X
25-30	Background on Second Standard Contributed to Third Analytical Line	F6.0
31-32	Blank	2X
33---	The Above Cycle Is Repeated for Contribution of Second Standard to Other Analytical Lines	

The number of these cards must equal the number of observations for background on second standard.

The above sequence is repeated for data taken on each standard for contribution to other analytical lines.

The total number of sets of background data must be equal to the total number of elements analyzed.

Sample Data

1- 6	Beam Current	F6.0
7- 8	Blank	2X
9-14	Counts for First Element	F6.0
15-16	Blank	2X
17-22	Counts for Second Element	F6.0
23-24	Blank	2X
25-30	Counts for Third Element	F6.0
31-32	Blank	2X
33---	Counts, Blank, Blank Repeated for All Elements Measured	

This card is repeated for each observation. A maximum of 300 observations permitted.

Trailer Card

After the last analysis in a problem, a trailer card with routing information is required.

Column		Format
1- 6	999998 Is Inserted if More Data for New Problem Follows	F6.0
	999999 Is Inserted if Most Recent Data Is last Data	

APPENDIX F

TYPICAL OUTPUT FROM REDUCTION OF MICROPROBE DATA TO COMPOSITION

A typical output from the MAGIC II program is given. These output sheets are the summaries of the calculation. In addition, the numerical results for several variables are printed out at the end of the calculation for each observation. The typical summary sheets are as follows:

PROBLEM NUMBER A1122

JULY 17, 1968

ELEMENT	AT. NO.	AT. WT.	PF	EDGE	EC	WAVE	U	R
SN	50	118.690	678.617	3.156	3.929	3.600	3.82	0.741258
NI	28	58.710	362.046	1.488	8.332	1.658	1.80	0.914241

MASS ABSORPTION COEFFICIENTS

RADIATION	SN LA	NI KA
ABSORBER		
SN	506.	312.
NI	489.	61.

	WS	E	VAL	SIGMA	MS	US	FS	FACT
SN	0.4213	9.4645	9.3085	5472.30	0.0570	1.1166	0.8899	0.56157
NI	0.4769	11.6660	9.5177	7816.11	0.0899	1.0098	0.9895	0.52315

ESP = 0.586570ICE C4

FLUORESCENCE FACTOR FOR NI FLUORESCING SN IS 4.494869

STANDARD INTENSITIES CORRECTED FOR DEADTIME AND DRIFT

BEAM CURRENT	SN	NI
18187.4	52325.44	63393.88

COUNTING INTERVAL, 10.0 SECOND(S)

BACKGROUNDS

CONTRIBUTED TO BY 100 % OF	SN LA	NI KA
SN	1058.4	856.1
NI	946.8	649.6

PROBLEM NUMBER A1122

JULY 17, 1968

ELEMENT	ATOMIC NUMBER	ATOMIC WEIGHT	BACKSCATTER FACTOR	EXCITATION POTENTIAL	ABSORPTION JUMP RATIO	FLUORESCENT YIELD
SN	50	118.690	0.741	3.929	3.45	0.082
NI	28	58.710	0.914	8.332	7.67	0.392

MASS ABSORPTION COEFFICIENTS

RADIATION ABSORBER	SN LA	NI KA
SN	506.	312.
NI	489.	61.

COUNTING INTERVAL, 10.0 SECOND(S)

BACKGROUNDS

CONTRIBUTED TO BY 100 % OF	SN LA	NI KA
SN	1058.4	856.1
NI	546.8	649.6

PROBLEM NUMBER A1122

JULY 17, 1968

INTENSITIES (CPS X COUNTING INTERVAL)
CORRECTED FOR DEAD-TIME AND DRIFT

SN	NI
32343 /53335	23631 /63393
33050 /53335	23760 /63393
32931 /53335	23844 /63393
30871 /53335	22949 /63393
30868 /53335	23151 /63393
31415 /53335	23089 /63393
32230 /53335	22695 /63393
31995 /53335	22837 /63393
31755 /53335	23027 /63393
32126 /53335	22805 /63393
32040 /53335	22905 /63393
32378 /53335	22958 /63393
32277 /53335	22958 /63393
32873 /53335	22855 /63393
32151 /53335	22961 /63393
32384 /53335	23089 /63393
32328 /53335	22902 /63393
32589 /53335	23152 /63393
32503 /53335	22632 /63393
32448 /53335	22790 /63393
32558 /53335	22725 /63393
32511 /53335	22999 /63393
32150 /53335	22867 /63393
32367 /53335	22851 /63393
32298 /53335	22832 /63393
32227 /53335	23135 /63393
32516 /53335	22896 /63393
32447 /53335	22984 /63393
32111 /53335	22882 /63393
31843 /53335	22697 /63393
32351 /53335	22751 /63393
32665 /53335	22780 /63393

STANDARD BACKGROUNDS (CPS X COUNTING INTERVAL)

1058	650

DEAD-TIME (MICROSECONDS)

2.1	2.3

COUNTING INTERVAL, 10.0 SECONDS

PROBLEM NUMBER A1122

JULY 17, 1968

INDIVIDUAL K-RATIOS CORRECTED FOR
DEAD-TIME, DRIFT AND BACKGROUND ONLY

N	SN	NI
3	0.5989	0.3668
3	0.6125	0.3688
3	0.6102	0.3702
3	0.5708	0.3555
3	0.5707	0.3591
3	0.5812	0.3581
3	0.5968	0.3519
3	0.5923	0.3541
3	0.5877	0.3581
3	0.5948	0.3536
3	0.5932	0.3552
3	0.5996	0.3561
3	0.5977	0.3561
3	0.6051	0.3544
3	0.5953	0.3561
3	0.5957	0.3581
3	0.5987	0.3552
3	0.6036	0.3591
3	0.6020	0.3509
3	0.6010	0.3534
3	0.6031	0.3523
3	0.6022	0.3567
3	0.5953	0.3546
3	0.5994	0.3544
3	0.5981	0.3540
3	0.5967	0.3589
3	0.6022	0.3551
3	0.6009	0.3565
3	0.5945	0.3548
3	0.5894	0.3519
3	0.5991	0.3528
3	0.6051	0.3522

PROBLEM NUMBER A1122

JULY 17, 1968

SUBMITTED BY PC DANIEL

DESCRIPTION - NI-SN FROM SN+4 CL BATH

ACCELERATING VOLTAGE 15.0 KEV

X-RAY EMERGENCE ANGLE 52.5 DEGREES

STANDARD PEAK-TO-BACKGROUND RATIOS (P/B) AND MINIMUM DETECTABILITY LIMITS (MDL)

ELEMENT	P/B	MDL
SN	49/1	0.2047 WT %
NI	56/1	0.1336 WT %

CHEMICAL COMPOSITION
WEIGHT PERCENT
ATOMIC PERCENT

OBS	SN	NI
1	62.125 46.861	34.847 53.139
2	63.265 47.287	34.888 52.713
3	63.056 47.103	35.025 52.897
4	59.808 46.394	34.183 53.606
5	59.766 46.171	34.466 53.829
6	60.685 46.693	34.270 53.307
7	62.103 47.789	33.562 52.211
8	61.650 47.442	33.806 52.558
9	61.248 46.972	34.202 53.028

10	61.912	33.736
	47.583	52.417
11	61.753	33.852
	47.403	52.597
12	62.301	33.903
	47.616	52.384
13	62.135	33.920
	47.537	52.463
14	63.136	33.663
	48.125	51.875
15	61.926	33.949
	47.432	52.568
16	62.288	34.082
	47.479	52.521
17	62.228	33.834
	47.638	52.362
18	62.615	34.131
	47.574	52.426
19	62.569	33.423
	48.077	51.923
20	62.447	33.655
	47.858	52.142
21	62.640	33.540
	48.020	51.980
22	62.514	33.931
	47.680	52.320
23	61.941	33.817
	47.535	52.465
24	62.303	33.752
	47.727	52.273
25	62.192	33.740
	47.692	52.308
26	62.021	34.175
	47.301	52.699
27	62.540	33.790
	47.795	52.205
28	62.411	33.925
	47.643	52.357
29	61.875	33.848
	47.485	52.515
30	61.464	33.635
	47.474	52.526
31	62.294	33.618
	47.824	52.176
32	62.806	33.595
	48.043	51.958

PROBLEM NUMBER A1122

JULY 17, 1968

SUBMITTED BY MC CANIEL

DESCRIPTION - NI-SN FROM SN+4 CL BATH

MEAN CHEMICAL COMPOSITION AND TWO SIGMA LIMITS BASED ON 32 ANALYSES

ELEMENT	WEIGHT PERCENT	ATOMIC PERCENT
SN	62.065 - C.285	47.482 - 0.167
NI	37.568 - C.145	52.528 - 0.167

MEAN INTENSITY RATIOS AND TWO SIGMA LIMITS

ELEMENT	K
SN	C.6CC6 - 0.0033
NI	0.3544 - C.C016

ACCELERATING VOLTAGE	15.0 KEV
X-RAY EMERGENCE ANGLE	52.5 DEGREES

STANDARD PEAK-TO-BACKGROUND RATIOS (P/B) AND MINIMUM DETECTABILITY LIMITS (MDL)

ELEMENT	P/B	MDL
SN	49/1	C.2047 WT %
NI	56/1	0.1336 WT %